

The Petrography, Stratigraphy and Structure of the
Osborne Mine Sequence: Evidence for the origin of
Banded Iron-Formation-Hosted Cu-Au deposits in the
Soldiers Cap Group, Northwest Queensland.

by

James K. Williams

Submitted in fulfilment of the requirements for the degree of Master of
Science

School of Earth Sciences, Macquarie University, N.S.W. 2109, Australia.

February, 1995

Abstract

Two stratabound banded iron-formations (BIFs) host epigenetic Cu-Au mineralisation in multiply deformed metasediments of the Osborne mine, within the Cloncurry–Selwyn zone of the Mount Isa Eastern Succession. The Proterozoic host rocks have been subdivided into seven conformable units that are cut by amphibolites and pegmatites, affected by four phases of ductile deformation (D_x – D_3), amphibolite facies metamorphism and later alteration involving the formation of sulphide minerals.

Evidence for the first deformation, labelled " D_x " because of its uncertain age and extent, is restricted to straight inclusion trails (S_x) within some porphyroblasts of garnet, cordierite and tourmaline. D_1 is labelled to conform with existing nomenclature involving the regional 1595 Ma Isan Orogeny, which resulted in a lineation in amphibolites (L_1) and a widespread bedding-parallel foliation in metasediments (S_1), which is also parallel to the axial surfaces of small asymmetrical Group 1 folds. Peak metamorphic mineral assemblages, which developed during D_1 , include garnet-cordierite-sillimanite in metapelitic gneisses, suggesting metamorphic conditions of $T=746\pm136^\circ\text{C}$ and $P=5.1\pm1.0\text{ kbar}$. Refolding of S_0 and S_1 during D_2 resulted in the localized development of small symmetrical Group 2 folds, and D_3 produced sets of near-parallel Group 3 kink bands with curvi-planar S_2 axial surfaces.

Post folding Au-Cu minerals, quartz, pyrite and magnetite formed by late replacement (post D_3) of lenses of brecciated BIF. Brecciation is most intensely developed near contacts between BIFs and quartzo-feldspathic units, and formed as a result of strain incompatibility during post D_3 brittle deformation.

Narrow retrograde shear zones displace and thus postdate all metasedimentary units, intrusions and ore-bearing breccias. The relative displacements of marker units suggest that the net movement along the majority of shears was normal and non-rotational.

The BIFs are inferred to be metamorphosed syn-sedimentary units that were affected by all stages of deformation (D_x – D_3), and later Au-Cu mineralisation. A sedimentary origin for the BIFs is consistent with local and regional features, such as the stratigraphic restriction of BIFs to the Soldiers Cap Group, the conformable nature and lateral continuity of the BIF units, and the delicate bedding-parallel laminations of quartz-magnetite and quartz-magnetite-cummingtonite.

The material contained in this thesis is the work of the author and has not been submitted for a higher degree at any other university or institution.



.....
(James K. Williams)

Table of Contents

Abstract	i
List of figures	vii
List of Tables	ix
Acknowledgments	x
Introduction	1
Origin and aims of the project	2
Location	2
Exploration history	3
Methods	3
Mineral Abbreviations	4
Chapter 1. Regional Geology of the Mount Isa Inlier and the Cloncurry-Selwyn Zone	5
1.1 Regional Setting	6
1.11 Stratigraphic Framework	6
1.12 Igneous Intrusions	9
1.13 Deformation and Metamorphism	10
1.14 Tectonic Setting	10
1.15 Regional Geophysics	10
1.2 The Cloncurry-Selwyn Zone	12
1.21 Stratigraphic Framework	12
1.3 The Soldiers Cap Group	15
1.31 Deformation and Metamorphism	16
1.32 Folding	16
1.33 Faulting	17
1.34 Alteration	18
1.35 Economic Mineral Deposits	18

Chapter 2.	Stratigraphy and Geochemistry of the Osborne Deposit	20
2.1	Stratigraphic Framework	21
2.2	Metasedimentary Rocks	23
	2.21 Garnet-Cordierite-Sillimanite Layered Gneiss	23
	2.22 Plagioclase-Quartzite	23
	2.23 Upper BIF	25
	2.24 Layered Biotite-Albite-Quartzite	28
	2.25 Banded Quartz-Cummingtonite-Magnetite Schist	28
	2.26 Lower BIF	29
	2.27 Quartz-Plagioclase-Biotite Schist	29
2.3	Intrusives	29
	2.31 Amphibolite Dykes	29
	2.32 Pegmatites	31
2.4	Alteration and Economic Mineralisation	31
2.5	Veins	32
2.6	Oxidation	32
Chapter 3.	Petrology and Mineral Chemistry of the Osborne Mine Sequence	34
	Introduction	35
3.1	Garnet-Cordierite-Sillimanite Gneiss	35
	3.11 Cordierite	35
	3.12 Garnet	35
	3.13 Sillimanite	37
	3.14 Cummingtonite	37
	3.15 Plagioclase	37
	3.16 Biotite	37
	3.17 Quartz	37
	3.18 Tourmaline	38
	3.19 Petrogenesis	38

3.2	Plagioclase Quartzites	38
	3.21 Quartz	38
	3.22 Plagioclase	40
	3.23 Biotite	40
	3.24 Corundum	40
	3.25 Sillimanite	40
	3.26 Magnetite and Pyrite	40
	3.27 Petrogenesis	41
3.3	Banded Iron Formation—Oxide Facies	43
	3.31 Magnetite	43
	3.32 Quartz	43
	3.33 Apatite	45
	3.34 Plagioclase	45
	3.35 Petrogenesis	46
3.4	Banded Iron Formation—Silicate Facies	47
	3.41 Banded Quartz-Cummingtonite-Magnetite Schist	47
	3.42 Cummingtonite Schist	48
	3.43 Hornblende	48
	3.44 Petrogenesis	48
Chapter 4.	Structural Geology of the Osborne Deposit	52
	Introduction	53
4.1	Previous Structural Interpretations	55
4.2	Bedding (S_0)	57
4.3	Structures Related to Ductile Deformation	58
	4.31 Inclusion Fabrics Related to D_x	58
	4.32 Folds Related to D_1	58
	4.33 Folds Related to D_2	63
	4.34 Folds Related to D_3	63

4.4	Structures Related to Brittle-Ductile Deformation	65
	4.41 Brecciation and Economic Mineralisation	65
	4.42 Shear Zones	65
4.5	Structures Related to Brittle Deformation	67
	4.51 Joints	67
	4.52 Veins	67
 Chapter 5. An Overview of Ironstones and Precambrian		
	Iron Formations	69
	Introduction	70
5.1	Definition of Terms	70
5.2	Classification of Banded Iron Formations (BIFs)	70
	5.21 Classification According to Facies	71
	5.22 Classification According to Geologic Association	73
5.3	The Origin of Lake Superior-Type BIFs	74
5.4	The Origin of Algoma-Type BIFs	75
5.5	The Origin of "Ironstones"	76
5.6	BIF as Host to Base Metal Sulphides	79
5.7	BIF as Host to Au-Cu Sulphides	80
 Chapter 6. Massive Hematite Bodies North-North-East of the Osborne		
	Deposit—Examples of Metasomatic Ironstones	83
 Chapter 7. Synthesis		
	Introduction	90
7.1	Geological Summary	90
7.2	The Origin of the BIF units	91
7.3	Controls on Economic Minerals	94
7.5	Future Exploration	95

References	97
Appendix 1. Geological Cross Sections	I
Stratigraphic column	II
Section 21815N	III
Section 21745N	IV
Section 21675N	V
Section 21535N	VI
Section 21395N	VII
Section 21290N	VIII

List of Figures

1.1	Tectonic units of the Mount Isa Inlier	7
1.2	Stratigraphic Framework of the Mount Isa Inlier	8
1.3	Location and Geology of the Cloncurry-Selwyn zone	13
1.4	Tectono-stratigraphic correlation of the Soldiers Cap Group	14
2.1	(a) Proterozoic-Mesozoic angular unconformity	27
2.1	(b) Garnet-cordierite-sillimanite layered gneiss	27
2.1	(c) Quartz-magnetite BIF	27
2.1	(d) Albite mesobands in BIF	27
2.2	(a) Layered biotite-albite-quartzite	30
2.2	(b) Laminated albite-biotite±corundum±sillimanite marker horizon	30
2.2	(c) Banded quartz-cummingtonite-magnetite schist	30
2.2	(d) Kink banded cummingtonite schist	30
2.3	(a) Pyrite, chalcopyrite and magnetite overprinting pegmatite	33
2.3	(b) Calcite veins with "sericite" alteration haloes	33
3.1	(a) Photomicrograph of garnet-cordierite-sillimanite layered gneiss	39
3.1	(b) Simple twin in poikiloblastic cordierite	39
3.1	(c) Euhedral tourmaline	39
3.1	(d) Photomicrograph of plagioclase-quartzite	39
3.2	(a) Partially retrogressed corundum porphyroblast	44
3.2	(b) Magnetite with skeletal exsolution textures	44
3.2	(c) Delicate laminations in oxide facies BIF	44
3.2	(d) Incipient martitisation in magnetite from oxidized BIF	44
3.3	Stability of oxide facies BIF during high grade metamorphism	45
3.4	(a) Interbanded layers of cummingtonite-quartz and magnetite quartz	50
3.4	(b) S ₂ hinge line in cummingtonite schist	50
3.5	Relative stability fields of minerals in metamorphosed BIF	51

4.1	Block diagram of the Osborne deposit	54
4.2	Relationships between fabric elements in a transposed area	56
4.3	Profiles of the three groups of folds recognized in the mine sequence	61
4.4	(a) S_x inclusion fabric in poikiloblastic cordierite	62
4.4	(b) S_1 in layered biotite-albite-quartzite	62
4.4	(c) L_1 in amphibolite	62
4.4	(d) S_2 axial surface in Group 3 kink band	62
4.5	(a) Brecciated and altered BIF	64
4.5	(b) Rotated BIF clasts	64
4.6	(a) Biotite partially retrogressed to chlorite from within a shear zone	68
4.6	(b) Glide surface in plagioclase grain from within a shear zone	68
4.6	(c) Highly deformed plagioclase grain from within a shear zone	68
4.6	(d) Hematite, apatite and carbonate around fractured shear zone	68
5.1	Eh-Ph stability fields for sediment under normal seawater conditions	72
5.2	Depositional zones of iron-rich precipitates in a hypothetical basin	72
5.3	Cross section of the White Devil ironstone-hosted gold deposit	77
6.1	Outcrop map of hematite ironstones 80 km NNE of Osborne	86
6.2	(a) Brecciated quartz-hematite ironstone	87
6.2	(b) Foliated hematite ironstone	87
6.2	(c) Sandstone inclusion within ironstone	87
6.2	(d) Deformed pebble bearing polymictic conglomerate	87
6.3	(a) Irregular contact between ironstone and conglomerate	88
6.3	(b) Photomicrograph of quartz-muscovite metasedimentary rock	88
7.1	(a) Small oxide facies BIF from several kilometres north of Osborne	96
7.1	(b) Small oxide facies BIF from several kilometres north of Osborne	96

List of Tables

1.1	Deformation of the Mount Isa Inlier	11
1.2	BIF-hosted mines and prospects of the Soldiers Cap Group	19
2.1	Stratigraphy of the Osborne mine	22
2.2	Typical compositions of rocks from the Osborne mine sequence	24
2.3	Comparative chemistries of various oxide facies iron-formations	26
3.1	Averaged electron microprobe analyses from mine sequence rocks	36
4.1	Structural and metamorphic history of the Osborne mine	59
5.1	Comparative features of Superior- and Algoma-types of iron-formation	75

Acknowledgments

I thank the following people and organisations: Professor Ron Vernon for guidance, advice and proof reading of this thesis; Mr Richard White for proof reading and suggestions; Doctor Geoff Clarke for help in estimating P-T conditions using THERMOCALC; Doctor Mike Etheridge for initially proposing the project and for suggestions; Mr Neil Adshead for geochemical analyses and discussions of ideas; the Australian Post-Graduate Award scheme for financial support; Placer exploration for travel expenses, use of vehicles and access to drill core.

Introduction

Origin and Aims of the Project

It has been known for several decades that virtually all Ag-Pb-Zn deposits and a number of Cu-Au deposits in the Cloncurry-Selwyn zone occur within or adjacent to small banded iron formations (BIFs). However, only a small proportion of the outcropping BIFs contain large concentrations of economic minerals.

The origin of the BIFs, or "ironstones" as they are commonly referred to locally, has received renewed interest in recent years. Based largely on a detailed study of the BIFs around Selwyn, Davidson et al. (1989) concluded that they mostly formed early in the history of the sedimentary sequence (diagenesis, basin dewatering, early deformation), although they have been modified during subsequent deformation and metamorphism. In contrast, other workers (e.g. Switzer et al., 1988; Adshead, 1995) have suggested a syn-regional metamorphism to syn-Williams Batholith (1500 Ma) metasomatic origin for the "ironstones" and economic minerals.

This thesis is designed to describe and interpret the structure, petrology and stratigraphic relationships of BIFs and mine sequence rocks that host the Osborne Au-Cu ore body, and to provide a brief description of some small barren BIFs and "ironstones" that crop out in the surrounding district. The principal objectives are to (1) provide an improved understanding of the range of characteristics and genetic types of BIFs and "ironstones", (2) discuss the factors that control economic mineralisation, and (3) compare the BIFs at Osborne with other Precambrian gold-bearing BIFs and "ironstones" from Australia and overseas (Chapter 5).

Location

The Osborne deposit is located in remote country 195 km south east of Mt Isa, at latitude 22°04' South, longitude 140°34' East, on the Boullia 1:250 000 map sheet.

Exploration History

Exploration leading to the discovery of the Osborne deposit began in 1974, when Newmont first located a magnetic high, which they termed "Trough Tank", during an aeromagnetic survey as part of their search for "Pegmont-style" Pb-Ag-Zn deposits in the Cloncurry-Selwyn zone. No further work was conducted until 1976, when the company drilled a series of holes across the anomaly. Three holes intersected banded iron formation (BIF) containing minor traces of copper and gold. The tenement was subsequently relinquished by Newmont in 1976 (unpublished Placer report, 1993).

In 1985 Billiton and CSR formed a joint venture to search for BIF hosted Au-Cu deposits similar to the Selwyn deposit located approximately 70 km to the NNE. Exploration from 1985 to 1989 outlined two closely spaced magnetic horizons with a strike length of 20 km, including what were termed the North-East, Central and Southern anomalies. Drilling in the Central and Southern anomalies intersected thin and generally barren BIFs, whereas drilling in the North-East anomaly produced major intersections of BIF with weak to moderate concentrations of copper and gold. From 1988, Placer began to acquire an increasing interest in the Joint Venture, and by 1993 the company was the sole owner of the deposit and surrounding tenements (unpublished Placer report, 1993). Open-pit mining of the deposit is about to commence at the time of writing.

Methods

The analytical, mineralogical and structural descriptions in this thesis were obtained from diamond drill core selected from some of the 400 holes drilled through the deposit by Placer between 1989 and 1994. Each core was examined, logged, and where possible re-oriented on site, to provide the stratigraphic sequence (Chapter 2) and structural history (Chapter 4) of the mine sequence. The mineral assemblages, microstructures and mineral compositions of the Osborne host-rocks were obtained from representative core samples that were used to prepare thin and polished sections for optical microscopy and electron microprobe analysis (Chapter 3). Small outcropping bodies of Proterozoic BIF and "ironstone" located near Osborne were also sampled and mapped (Chapter 6).

Mineral Abbreviations

The use of mineral abbreviations in the main body of text has been avoided. However, the following abbreviations (after Kretz, 1983) have been used in figures:

Ab- Albite; Bt- Biotite; Cor- Corundum; Crd- Cordierite; Ctn- Cummingtonite; Grt- Garnet; Hbl- Hornblende; Mag- Magnetite; Mar- Martite; Mu- Muscovite; Sil- Sillimanite; T- Tourmaline; Qtz- Quartz.

Chapter 1

Regional Geology of the Mount Isa Inlier and the Cloncurry-Selwyn Zone.

1.1 Regional Setting

The Mount Isa Inlier is a 50 000 km² block of multiply deformed and metamorphosed early to mid-Proterozoic rocks, situated in northwestern Queensland between latitudes 18° and 22° S and longitudes 138° and 141°E.

As recognized by Carter et al. (1961), the Mount Isa Inlier is divided by major north-striking fault zones into three longitudinal belts, each of which has a characteristic Proterozoic stratigraphy (Fig. 1.1). The Western Fold Belt is subdivided by the Mount Isa Fault Zone into the Lawn Hill Platform and the Leichhardt River Fault Trough (Blake and Stewart, 1992). The Quilar Fault Zone is the boundary between the Western Fold Belt and the Kalkadoon-Leichhardt Belt, which is subdivided by Blake and Stewart (1992) into the Ewen Block, the Myally Shelf, and the Wonga Belt. The Eastern Fold Belt is composed of the Quamby-Malbon and Cloncurry-Selwyn Zones of Blake (1987), and is separated from the Kalkadoon-Leichhardt Belt by the Pilgrim Fault Zone, which has a probable displacement of several hundred kilometres, and is regarded as a terrane boundary (Blake and Stewart, 1992).

1.11 Stratigraphic Framework

Blake (1987) recognized four major cover sequences. The oldest exposed rocks, the *basement*, are sedimentary, volcanic and intrusive rocks that were deformed and metamorphosed during the 1900-1870 Ma Barramundi Orogeny.

The basement is overlain by three younger cover sequences that are major stratigraphic packages, with preserved thicknesses of several kilometres. They are separated by regional unconformities attributed to basin subsidence and tectonism. Sedimentary and volcanic structures indicate mainly fluvial to shallow marine or lacustrine depositional environments (Blake and Stewart, 1992). The relationships between the main stratigraphic units in the Mount Isa Inlier are summarized in Fig. 1.2.

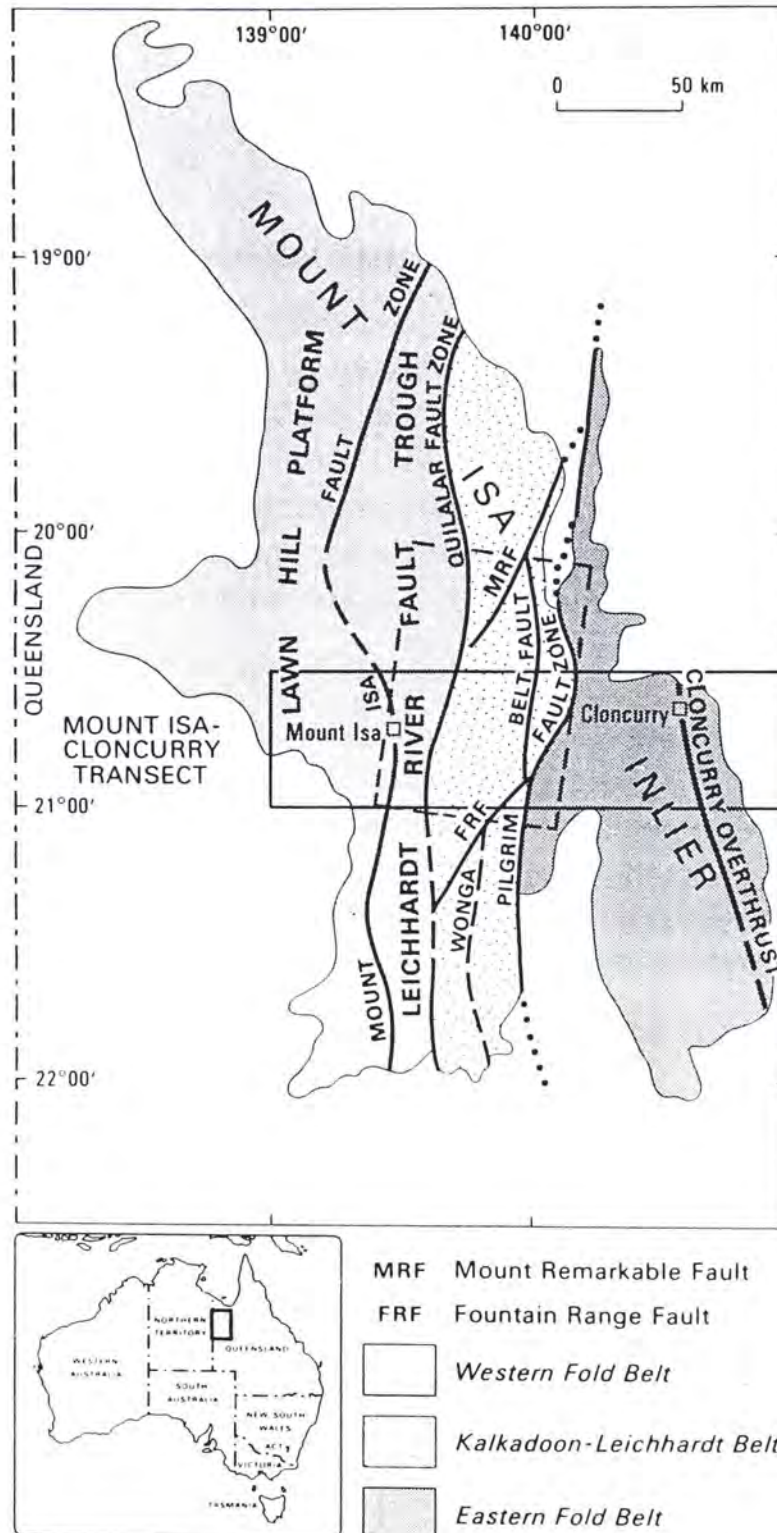


Fig. 1.1. Tectonic units of the Mount Isa Inlier.
From Blake and Stewart, 1992 (figure 1).

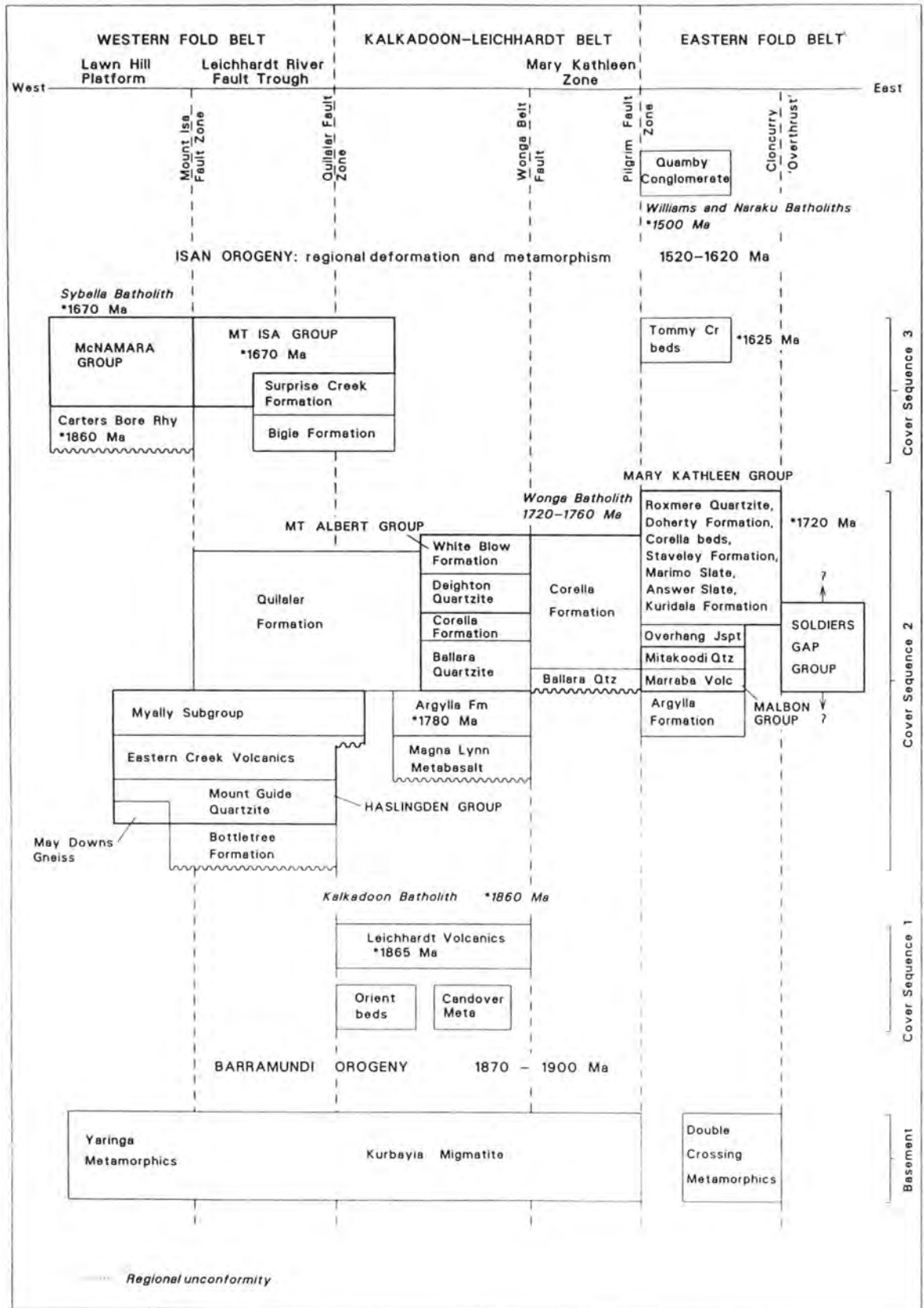


Fig. 1.2. Stratigraphic Framework of the Mount Isa Inlier.
From Blake and Stewart, 1992 (figure 2).

Cover sequence 1 predominantly consists of 1870-1850 Ma felsic volcanic rocks (Page 1988), and is confined to the Kalkadoon-Leichhardt Belt. *Cover sequence 2* ranges in age from about 1790 Ma to 1760 or 1720 Ma, and consists of sedimentary and bimodal volcanic rocks. Most of the rocks exposed in the Eastern Fold Belt are assigned to cover sequence 2 (Blake et al., 1990; Blake and Stewart 1992). *Cover sequence 3* is largely confined to the Western Fold Belt and the western part of the Kalkadoon-Leichhardt Belt, and consists mainly of finer grained sedimentary rocks and bimodal volcanic rocks, deposited between 1678 Ma and 1650 Ma ago (Page, 1978). Deposition of cover sequence 3 was terminated by the Isan Orogeny, a period of intense deformation and high temperature/low pressure metamorphism between 1620 Ma and about 1520 Ma ago. The Isan Orogeny postdates the 1670 Ma intrusion of the Sybella Batholith of the Western Fold Belt, and was closely followed by emplacement of the Naraku and Williams Batholiths at around 1500 Ma (Blake and Stewart 1992).

1.12 Igneous Intrusions

Igneous rocks of the Mount Isa Inlier include granitic plutons, mafic dykes and minor felsic intrusions, which were emplaced from before the 1870 Ma Barramundi Orogeny until around 1100 Ma ago (Blake, 1987).

Wyborn et al. (1988) identified seven major batholiths—the Williams, Naraku, Sybella, Wonga, Big Toby, Ewen and Kalkadoon, and two granitic plutons—the Weberra and the Yeldham. Granite outcrop has a combined surface area of 6711 km², or 14% by area of the Inlier. Geophysical evidence suggests the batholiths are part of a plutonic belt that extends under Phanerozoic cover for as much as 500 km, from Normanton on the Gulf of Carpentaria to well south of the Mount Isa Inlier (Wellman, 1992). The Kalkadoon, Ewen, Wonga and Sybella Batholiths are elongate north-south, and were deformed and metamorphosed between 1620 and 1550 Ma ago, whereas the Naraku and Williams batholiths were emplaced around 1500 Ma ago and are essentially undeformed. The Sybella, Wonga, Naraku and Williams Batholiths and the Weberra Pluton are predominantly anorogenic I-type granites, whereas the Big Toby Batholith and the Yeldham Pluton are predominantly S-types (Wyborn et al., 1988).

Blake (1987) inferred many separate ages for numerous minor mafic dykes and sills that intrude the Inlier, from older than 1870 Ma to around 1100 Ma. Most of the intrusions were subjected to metamorphism and deformation, and now consist of metadolerite, amphibolite or mafic schist. Several unmetamorphosed dykes post-date the 1620 to 1520 Ma Isan Orogeny (Blake et al., 1990). Minor felsic dykes are commonly found in close proximity to felsic volcanic rocks and granitic plutons, to which they are probably related (Blake et al., 1990).

1.13 Deformation and Metamorphism

Blake and Stewart (1992) recognized 7 episodes of deformation in the Mount Isa Inlier—four periods of extension, two periods of compression and a period of transcurrent faulting, as summarized in Table 1.1.

1.14 Tectonic Setting

Many workers (e.g. Plumb and Derrick, 1975; Dunnet, 1976; Glikson et al., 1976; Wilson, 1978; Plumb et al., 1980) have interpreted the Mount Isa Inlier as a mid-Proterozoic continental margin on the eastern side of the Australian Craton. More recently, an intracratonic rift environment has been suggested (e.g. Wyborn and Blake, 1982; Blake, 1987; Loosveld, 1989).

1.15 Regional Geophysics

Most of the Mount Isa Inlier lies within the 800 km long and 150 to 250 km wide Mount Isa Geophysical Domain (Wellman, 1992). Gravity and magnetic anomalies divide the Mount Isa Domain into six zones, which broadly coincide with most of the geological block boundaries identified by Blake and Stewart (1988), with boundaries of cover sequence 2 rocks, and with granitic batholiths. According to Wellman (1992), two major and widespread faulting sets occur in the Mount Isa Domain and surrounding crust, both younger than Cover Sequence 2: a northwest striking set of normal faults in the northern third of the region, and a northeast striking set of dextral faults with displacements of about 3 km in the central part.

Barramundi Orogeny~1870 Ma

A widespread event in northern Australia (Page, 1988) which produced tight folding and migmatisation in basement units of the Mount Isa Inlier.

Extension associated with cover sequences 1 and 2, 1870—1760 Ma

Extension which led to basin formation and deposition of cover sequence 2, felsic volcanism and plutonism, intrusion of dyke swarms and intrusion of the Yeldham Granite and Big Toby Batholith.

Extension between 1760 and 1700 Ma

Extension which led to emplacement of granites of the Wonga Batholith.

Extension associated with cover sequence 3, 1700—1660 Ma

Extension which led to deposition of basal rift and sag-phase sedimentation in the western part of the Inlier. Emplacement of the Weberra Granite and the Sybella Batholith may be related to this extension.

Isan Orogeny, 1620—1520 Ma

An orogenic event consisting of two main phases, a 1620 Ma phase of thrusting and folding resulting from north-south compression—D₁ of Bell (1983)—and a later, 1550 Ma phase of east-west compression, D₂, which resulted in the formation of the major north-trending upright folds characteristic of much of the Mount Isa Inlier. Regional metamorphism peaked during D₂.

Extension ~ 1500 Ma

The Williams and Naraku Batholiths were emplaced in the Eastern Fold Belt around 1500 Ma ago, implying crustal extension shortly after the Isan Orogeny.

Transcurrent Faulting

The main faults in the Mount Isa Inlier are mostly of Proterozoic age, although some were active during the Phanerozoic, and all have probably been reactivated several times. Movement was predominantly strike-slip, as the faults don't mark abrupt changes in metamorphic conditions. Horizontal displacements range up to many kilometres.

Table 1.1. Deformation of the Mount Isa Inlier (Blake and Stewart, 1992).

1.2 The Cloncurry-Selwyn Zone

The Cloncurry-Selwyn Zone contains rocks that have been extensively folded, faulted and metamorphosed up to regional amphibolite grade conditions, and economic deposit styles unique in the Mount Isa Inlier, such as the Banded Iron Formation (BIF) related Pegmont/Cannington-style of stratiform Ag-Pb-Zn deposits and the Cloncurry-style epigenetic Cu±Au deposits. The location and geology of the Cloncurry-Selwyn Zone is summarized in Fig. 1.3.

1.21 Stratigraphic Framework

The lack of reliable age control, the structural complexity and the effects of high-grade metamorphism mean that stratigraphic relationships in the Cloncurry-Selwyn Zone remain uncertain, despite over thirty years of study.

Early work by Carter et al. (1961) described the major units that dictate the Cloncurry-Selwyn Zone—the Soldiers Cap and Mary Kathleen Groups. Derrick et al. (1976, 1977) elevated the Soldiers Cap Formation of Carter et al. (1961) to group status, and defined three component formations in the Cloncurry region, from base to top: the Llewellyn Creek Formation, Mount Norna Quartzite and Toole Creek Volcanics. Further to the south in the Selwyn Region, the Soldiers Cap Group has been subdivided into lithologic units only (Blake et al., 1983). Beardsmore et al. (1988) defined two units underlying the Llewellyn Creek Formation, the Gandry Dam Gneiss and Glen Idol Schist, which together comprise the Fullarton River Group.

The Mary Kathleen Group (Fig. 1.2) consists of the Overhang Jaspilite, Answer Slate, Kuridala Formation, Doherty Formation, Stavely Formation, Agate Downs Siltstone, Marimo Slate and Roxmere Quartzite. However, the stratigraphic relationships between these units remains uncertain (Blake et al., 1984). The contact between the Mary Kathleen Group and the underlying Soldiers Cap Group is obscured by a brecciated carbonate, which was interpreted by Laing (1991) as representing a mylonitic terrane boundary. The carbonate was previously attributed to the Doherty Formation (Earlier known as the Corella formation, part of the Mary Kathleen Group, e.g. Glikson, 1972), but is now regarded as a much younger unit, the Gilded Rose Breccia, which postdates regional shearing (Loosveld, 1992).

Many workers have attempted to correlate the Soldiers Cap Group with units further to the west. Carter et al. (1961), Plumb and Derrick (1975), Derrick et al. (1976) and Loosveld (1989, 1992), correlated the Soldiers Cap Group with units of cover sequence 2—the Malbon Group, Haslingdon Group or Argylla Formation (Fig. 1.4), whereas Derrick (1991) subsequently proposed a correlation with the Tommy Creek beds of cover sequence 3. Others have suggested that the Soldiers Cap Group is the lateral facies equivalent of the lithologically similar Kuridala Formation, a member of the Mary Kathleen Group, (e.g. Donchak et al., 1983; Blake et al., 1983, 1984; Laing and Beardsmore, 1986; and Beardsmore et al., 1988). Beardsmore et al. (1988) proposed a major regional sequence, the "Maronan Supergroup", incorporating the Soldiers Cap Group (including the Kuridala Formation) and the Fullarton River Group.

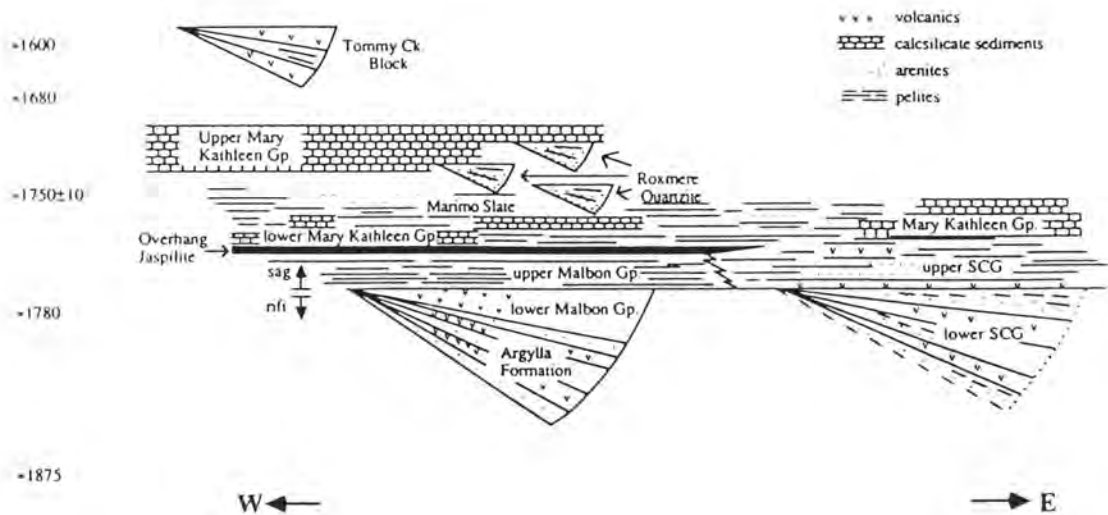


Fig. 1.4. Tectono-stratigraphic correlation of the Soldiers Cap Group with units to the west. From Loosveld 1992 (figure 2)

1.3 The Soldiers Cap Group

The Soldiers Cap Group is intruded by the Maramungee, Cowie, Mount Angelay, Saxby and Squirrel Hills Granites, as well as unnamed granite, pegmatite, amphibolite and dolerite, and is overlain unconformably by flat-lying Mesozoic sedimentary rocks. The group consists of three formations listed below, from oldest to youngest.

The *Llewellyn Creek Formation* consists of a 1 km-thick sequence of laterally continuous, thinly interbedded pelitic, psammopelitic and psammitic schists, commonly with garnet±andalusite±sillimanite, similar in style to the overlying Mount Norna Quartzite. Individual beds range from 0.1 m to 1 m thick for the metapelites and metapsammopelites, to 2 m for the metapsammitic horizons. Sedimentary structures include graded bedding, scour-and-fill structures, internal soft-sediment deformation and minor ripple cross-laminations. Precursor rocks have been interpreted as medium to coarse grained turbidites and minor shallow water sands, deposited as turbidites in a shelf to deep-basin environment (Newbery, 1991; Blake et al., 1984; Beardsmore et al., 1988).

The *Mount Norna Quartzite* conformably overlies the Llewellyn Creek Formation, and consists of a 1 km-thick sequence of medium to thickly bedded feldspathic metapsammite, quartzite, finely layered metasiltstone, commonly with garnet±andalusite±sillimanite, amphibolite, minor marble and calc silicates, and three (?) chemogenic BIF horizons, which are unique in the Mount Isa Inlier. An overall progressive coarsening of clastic material occurs up-sequence, from dominantly pelitic at the base to psammopelitic at the top. Sedimentary structures include minor graded bedding and ripple cross laminations. The parent rocks have been interpreted as turbidite sands and muds that were deposited in a moderate to low energy submarine fan, whereas distal exhalative BIFs and carbonates were deposited as chemogenic sediments (Newbery, 1991; Blake et al., 1984; Beardsmore et al., 1988; Jaques et al., 1982).

The *Toole Creek Volcanics* conformably overlie the Mount Norna Quartzite, and consist of amphibolite, mica schist, carbonaceous slate, blue quartzite, laminated scapolitic metasiltstone and metachert. Precursor rocks have been interpreted as subaqueous mafic volcanic rocks and related dolerite dykes, fine grained clastic sediments and minor evaporites, deposited by suspension or diffuse turbidity currents in an environment of intermediate water depth (Blake et al., 1984; Beardsmore et al., 1988; Loosveld, 1992).

1.31 Deformation and Metamorphism

Metamorphic assemblages of the Soldiers Cap Group typically include quartz + albite + microcline + biotite + muscovite \pm almandine \pm andalusite \pm sillimanite in pelitic and psammitic schist and gneiss; green and/or brown pargasitic hornblende + plagioclase (An₁₇₋₄₃) \pm salitic to diopsidic clinopyroxene \pm garnet in amphibolites; and edenitic to pargasitic hornblende + diopside + albite \pm grossular \pm scapolite in calc silicate rocks (Blake et al., 1983).

Jaques et al. (1982) recognized three main metamorphic zones (A, B and C), defined on the basis of mineral assemblages in metapelitic rocks. Unlike the weakly metamorphosed rocks in zone A, which have undergone upper greenschist facies metamorphism, rocks in zones B and C have been metamorphosed up to mid-amphibolite facies conditions, are strongly recrystallized, and cut by veins that may represent anatectic melt. Primary structures or textures in rocks of zones B and C are rarely preserved. Metamorphic zones are independent of granite intrusions, and isograds broadly follow regional foliation and dominant fold trends (Jaques et al., 1982).

Using the assemblage quartz + biotite + muscovite + garnet + plagioclase, Jaques et al. (1982) estimated pressures of 4 kbar (400 MPa) and temperatures of 680°C in the highest grade rocks of zone C. Evidence presented in this thesis (Chapter 3) suggests peak metamorphic conditions reached pressures of 5.1 kbar and temperatures of 746°C. Regional metamorphism was prograde during D₁, peaked during D₂ and was retrograde post D₂ (Jaques et al., 1982; Williams and Blake, 1993).

1.32 Folding

Beardsmore et al. (1988) recognized as many as six phases of deformation in the Cloncurry-Selwyn Zone, with D₁, D₂ and perhaps D₃ the dominant phases;

D₁—Extension (1760-1670 Ma) produced subhorizontal detachments with an upper plate towards true north sense of movement (Hill, 1987; Switzer, 1987; Holcombe et al., 1987). Evidence for an early extensional event comes from the abundance of metadolerite in the Mary Kathleen Group and the Maronan Supergroup (Loosveld, 1989; Holcombe et al., 1991; Oliver et al., 1991).

D₁—Compression (1620-1600 Ma) produced very tight to isoclinal overturned folds of crustal scale. A penetrative S₁ fabric is nearly everywhere parallel to bedding. Minor F₁ folds are only rarely observed (Williams and Blake, 1993).

D₂ involved compression (1544±12 Ma ago) and the development of upright to slightly inclined, tight to isoclinal folds with north-south (relative to true north) striking axial planes. F₂ folds have shallowly plunging axes and amplitudes of at least several kilometres. In schistose rocks, S₂ is a well developed differential crenulation cleavage (Williams and Blake, 1993; Beardsmore et al., 1988).

D₃ involved compression (1510±13 Ma ago) and is commonly only moderately developed. F₃ folds have upright to north-south to northwest-southeast (relative to true north) trending axial planes, and horizontal to vertical plunges. In schistose rock-types F₃ axial planes are defined by an open crenulation cleavage. D₂ and D₃ structures in the Cloncurry-Selwyn Zone have been assigned the same ages as Mount Isa D₁ and D₂ structures (Page and Bell, 1986), as both sets of structures have similar styles and orientations (Williams and Blake, 1993; Beardsmore et al., 1988). Post D₃ deformation events produced localized shearing, faulting, mesoscopic folding and kink banding.

1.33 Faulting

The fault pattern in the Cloncurry-Selwyn Belt is very complex. Many brittle faults are reactivated older ductile features in positions where large plutons of the Williams Batholith have provided mechanical influences on their development. Brittle deformation structures are commonly hosts for sulphide mineralisation (Williams and Blake, 1993).

Bedding-parallel strike-slip faults with minor displacements are common. They are represented by narrow shears, especially along contacts between different rock types, and are probably related to bedding-plane slip during the main folding event. The latest movements along these faults postdate folding and some postdate emplacement of the Williams Batholith (Blake et al., 1984).

1.34 Alteration

Williams and Blake (1993) recognized successive metasomatic events in the Cloncurry–Selwyn zone, each overprinting the other. They include albitisation, feldspathization, silicification ($\pm\text{Py}\pm\text{Cpy}\pm\text{Au}$) and epithermal alteration. Metasomatic alteration was focused in carbonate-bearing sequences of the Mary Kathleen Group, or in favourable sites such as brittle vein and breccia structures in the Maronan Supergroup. Most of the alteration post dates peak metamorphism and regional scale folding.

1.35 Economic Mineral Deposits

The Cloncurry-Selwyn Zone hosts the following two principal styles of economic mineralisation;

- (a) "Cloncurry style": structurally controlled, stratabound to transgressive $\text{Cu}\pm\text{Au}$ sulphides, hosted by a wide variety of rock types in a range of stratigraphic positions, and
- (b) "Pegmont style": stratigraphically controlled, stratiform $\pm\text{Zn}\pm\text{Ag}\pm\text{Pb}$ sulphides, hosted exclusively in BIFs of the Soldiers Cap Group.

Cloncurry style $\text{Cu}\pm\text{Au}$ mineralisation is hosted by faults and shear zones, e.g. the Kuridala and Mount Dore deposits (Williams and Blake, 1993), and in the brecciated contacts between rocks of different competencies, e.g. the Osborne and Selwyn deposits. $\text{Cu}\pm\text{Au}$ mineralisation was part of regional scale metasomatism in the Cloncurry-Selwyn zone, initiated soon after D_2 and peak metamorphic conditions, possibly related to emplacement of the post- D_2 Williams Batholith (Williams and Blake, 1993).

Pegmont style Zn-Pb-Ag mineralisation is invariably hosted by stratiform oxide and/or silicate facies BIFs, which have been folded by D_1 and subsequent deformations. Economic concentrations of Zn-Pb-Ag are thought to have formed at the same time as the BIFs and surrounding sediments, possibly as a result of submarine volcanic exhalations (Vaughan and Stanton, 1986; Newbery, 1991). Brief descriptions of BIF-hosted deposits of the Soldiers Cap Group are listed in Table 1.2.

Black Rock Prospect

Ore: Ag-Pb-Zn sulphides.

Associated Host Rocks: Tightly folded stratiform BIF and garnet quartzites.

References: Taylor and Scott, (1982).

Cannington Deposit

Ore: Stratiform Ag-Pb-Zn sulphides.

Associated Host rocks: Stratiform, laminated magnetite-pyroxene-garnet-amphibole-quartz BIF and garnet bearing quartzite, similar to Pegmont style. Expected to be the world's largest producer of Ag.

References: G. Davidson, Pers. Comm. (1994); Skrzeczynski, (1993).

Cowie Prospect

Ore: Stratiform Ag-Pb-Zn sulphides.

Associated Host Rocks: Highly folded stratiform BIF, 1 m thick, extends at least 2.5 km along strike.

References: Nisbet and Joyce, (1980); Taylor and Scott, (1982).

Fairmile Prospect

Ore: Disseminated Pb-Zn sulphides.

Associated Host Rocks: Tightly folded, mixed silicate/oxide facies BIF similar to Pegmont, with a strike length of several kilometres.

References: Taylor and Scott, (1982); Vaughan, (1980).

Maramungee Prospect

Ore: Zn Sulphides, minor Pb, Cu, Ag.

Associated Host Rocks: Stratiform BIF approximately 1 km strike length (Nisbet and Joyce, 1980; Taylor and Scott, 1982); gneiss, iron-rich metabasites and trondhjemitic granite (Williams and Heinemann, 1993).

Maronan Prospect

Ore: Primary disseminated Pb-Ag sulphides, with epigenetic Cu-Au sulphides associated with silicic alteration.

Associated Host Rocks: Oxide facies BIF, Mn-silicate-magnetite-garnet-quartz rocks and calcite-quartz-garnet-magnetite rocks

References: Williams and Blake, (1993); Randell, (1993).

Osborne Deposit

Ore: Epigenetic Cu-Au sulphides associated with silicic alteration.

Associated Host Rocks: Stratiform oxide facies BIF, feldspathic quartzite, cummingtonite schist.

References: Davidson et al. (1989); Adshead, (1995); Chapters 2, 3, and 4 of this thesis.

Pegmont Deposit

Ore: Stratiform Pb-Zn sulphides.

Associated Host Rocks: Complexly folded, laminated magnetite-pyroxene-garnet-amphibole-quartz BIF with garnet bearing quartzite, between 4 and 6 m thick, extending along strike for more than 2 km.

References: Locsei, (1977); Stanton and Vaughan, (1979); Orridge, (1980); Vaughan, (1980); Taylor and Scott, (1982); Vaughan and Stanton, (1986); Newbery, (1991).

Selwyn Deposit*

Ore: Cu-Au sulphides

Associated Host Rocks: Highly sheared, massive magnetite ironstones and magnetite rich schists of the Stavely Formation.

References: Laing et al. (1988); Davidson et al. (1989); Kary and Harley, (1990).

Table 1.2. The main BIF-hosted mines and prospects of the Soldiers Cap Group.

*Selwyn is hosted by magnetite-rich rocks of the Mary Kathleen Group, but is included in this table for completeness.

Chapter 2

Stratigraphy and Geochemistry of the Osborne Deposit

2.1 Stratigraphic Framework

The Osborne deposit is unconformably overlain by between 25 and 35 m of horizontal Mesozoic strata and a superficial layer of cemented silcrete (Table 2.1, Fig. 2.1a). The Mesozoic cover consists of marine siltstone and claystone of the Wilgunya Formation and underlying conglomerates and sandstones of the Longsite Sandstone (unpublished Placer report, 1993). Proterozoic rocks do not crop out in the immediate vicinity of the Osborne ore-body; thus stratigraphy is based on relationships observed in diamond drill core.

The Osborne deposit is divided into two distinct domains by a north-south trending discontinuity (termed the "Awesome Fault" by Placer geologists), which pre-dates the 1550 Ma Isan Orogeny. The Western Domain consists of seven Proterozoic metasedimentary units, two semi-continuous metasedimentary marker horizons, amphibolites, pegmatites, and various mineral assemblages related to metasomatic alteration, including gold and copper sulphides. Contacts between units dip at around 50° towards the east. The Eastern Domain is dominated by quartzose metasediments, amphibolites and pegmatites (Adshead, 1995), and is not discussed in this thesis.

The mine sequence has been informally subdivided into seven conformable units (Table 2.1), with a combined thickness of around 400 m. From base to top they are: quartz-plagioclase-biotite schist (including a cummingtonite schist marker horizon), lower BIF, banded quartz-cummingtonite-magnetite schist, layered albite-biotite-quartzite (including a laminated albite-biotite±corundum±sillimanite marker horizon), upper BIF, plagioclase-quartzite, and garnet-cordierite-sillimanite layered gneiss. Deposition of the mine sequence sediments probably took place between 1870 and 1760 Ma ago, during extension related to basin formation (Chapter 1).

Metasediments of the Osborne mine sequence are similar to descriptions by Blake et al., (1984); Beardsmore et al., (1988); Newbery, (1991) and Loosveld, (1992) of the Mount Norna Quartzite, the middle unit of the Soldiers Cap Group.

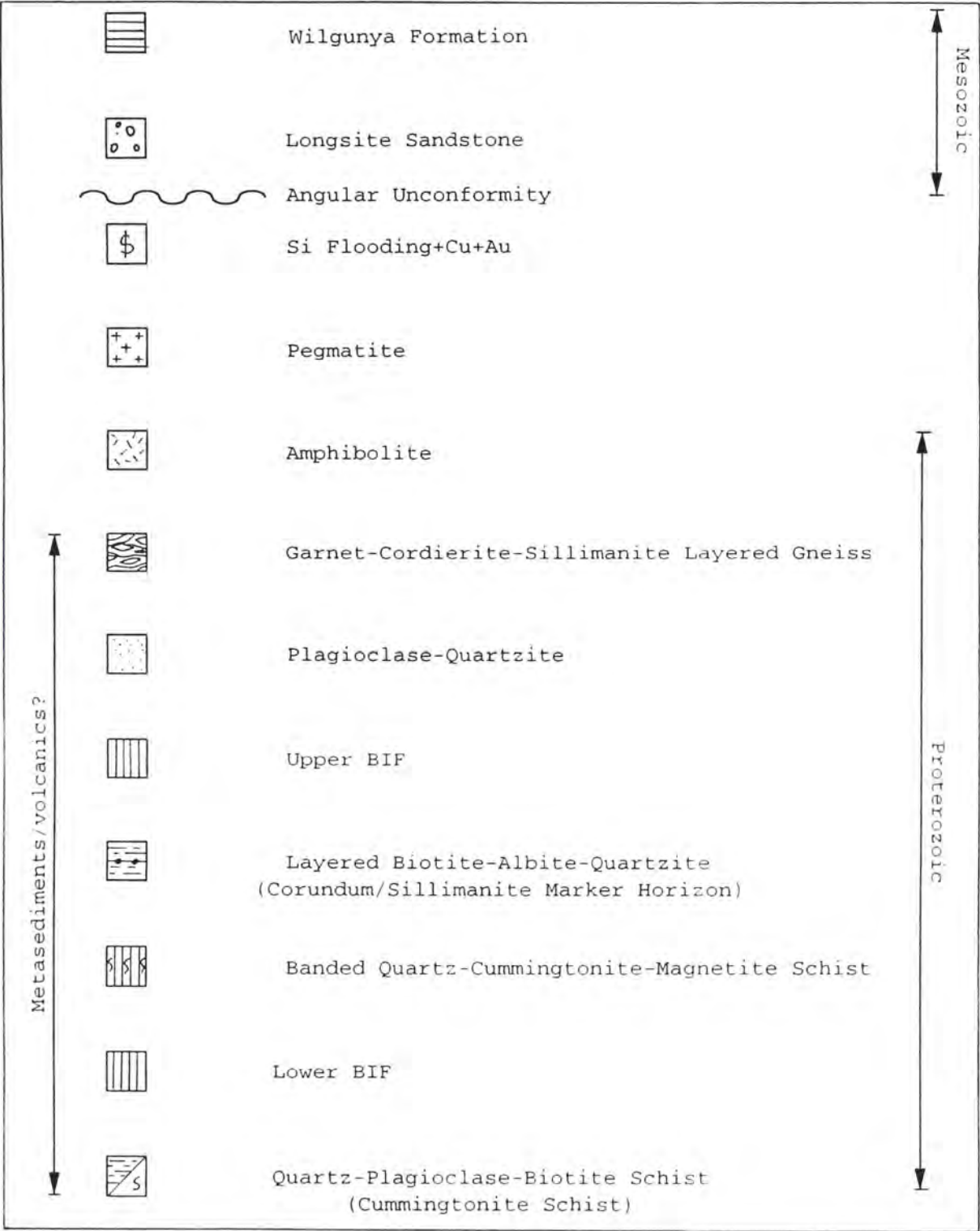


Table 2.1. Stratigraphy of the Osborne Mine.

2.2 Metasedimentary Rocks

2.21 Garnet-Cordierite-Sillimanite Layered Gneiss

The uppermost metasedimentary unit in the mine sequence, the garnet-cordierite-sillimanite layered gneiss, is a 200 m-thick, coarse-grained, layered gneissic unit. The unit is characterized by acicular sillimanite, cummingtonite and platy biotite that wrap around prominent porphyroblasts of cordierite (up to 15 mm in diameter) and almandine (up to 35 mm in diameter), quartz, albite and minor tourmaline. The layering is defined by alternating 5-20 mm-wide bands of pale quartz and albite, with darker bands rich in biotite, cordierite and almandine (Fig. 2.1b). Drill holes intersect the garnet-cordierite-sillimanite gneiss only at the southern end of the deposit, suggesting that the unit is truncated by the Awesome Fault.

2.22 Plagioclase-Quartzite

The plagioclase-quartzite is a 110 m-thick unit, typically consisting of massive light pink to pale grey feldspathic quartzite, massive white quartzite, and minor, strata-bound, 1–80 m-long lenses of laminated albite-biotite rock that locally contains sillimanite or corundum. Small flakes of disseminated biotite define a pervasive, bedding-parallel foliation (S_1), and narrow chloritic shear zones commonly obscure the basal contact with the underlying BIF unit. The chemical composition of a typical plagioclase-quartzite is presented in Table 2.2.

Previous workers have considered similar feldspathic quartzites of the Mount Norna Quartzite to be metamorphosed psammites (e.g. Beardsmore et al., 1988; Newbery, 1991; Loosveld, 1992). The petrogenesis of the plagioclase-quartzite and other units is discussed in Chapter 3.

Samples	1	2	3	4	5
Wt. %					
SiO ₂	33.33	66.09	56.6	62.26	73.73
TiO ₂	0.02	0.56	0.66	0.53	0.09
Al ₂ O ₃	0.48	18.52	20.4	18.3	12.34
Fe ₂ O ₃	65.78	1.92	6.3	2.52	2.3
MnO	0.03	0.00	0	0.03	0.02
MgO	0.42	0.40	3.6	1.01	3.72
CaO	0.50	0.90	0.82	1.08	0.43
Na ₂ O	0.22	9.83	7.33	9.64	6.64
K ₂ O	0.07	0.35	2.74	0.45	0.21
P ₂ O ₅	0.32	0.17	0.19	0.09	1.03
H ₂ O+	1.17	0.62	1.51	1.56	1.43
H ₂ O-	—	0.08	0.05	—	—
CO ₂	—	0.67	0.31	—	—
Total	102.31	100.10	101	97.47	101.9
Ppm					
Ba	0.00	161.40	700	NA*	NA
Cr	4.80	67.80	106	87	11
Cu	0.00	18.00	16.2	NA	NA
Ga	19.50	20.20	34	NA	20.5
Nb	2.74	14.40	18.2	15	50.7
Ni	41.80	11.20	58.6	11	20
Pb	1.74	11.80	14.8	10.3	7.9
Rb	10.70	15.40	176	22.4	18.6
Sr	3.66	44.00	47.6	33.3	16.6
Th	0.00	27.20	26.8	NA	NA
U	0.00	12.80	6.2	NA	NA
V	74.28	41.80	110	31	7.2
Y	8.78	52.40	34.6	16	29.1
Zn	12.40	13.00	13.8	16.6	17
Zr	9.74	106.80	164	146.4	168.2

*total iron as Fe₂O₃ **Note:** 0.00 = Below detection limit. Detection limits and

**NA=not analysed instrument specifications are listed on page IX, Appendix 2.

1: Adshead, (1995). Average oxide facies BIF (n=6).

2: Average leucosome, laminated albite-biotite marker horizon (n=5).

3: Average mesosome, laminated albite-biotite marker horizon (n=5).

4: Adshead, (1995). Representative plagioclase-quartzite (TT280 @ 300.5m).

5: Adshead, (1995). Representative cummingtonite schist (TT113 @ 169.3m).

Table 2.2. Typical compositions of rocks from the Osborne mine sequence.

2.23 Upper BIF

The upper BIF is a highly brecciated, sheared and folded unit that extends along strike for around 1 km. It is characterized by alternating mm- to cm-scale bands ("microbands" and "mesobands") of quartz and magnetite, with minor amounts of apatite and pyrite (Fig. 2.1c). The ratio of quartz to magnetite is approximately equal by volume, or about 1:2 by mass. Rare mesobands containing mostly pure albite with smaller amounts of magnetite and quartz are locally interbedded with mesobands of magnetite and quartz (Fig. 2.1d). Since apatite is the only phosphate bearing mineral in BIFs, the average wt. % of P_2O_5 (0.32%, Table 2.2) corresponds to a volume of around 0.5% apatite.

The chemical composition of the Osborne BIFs are similar to copper-gold bearing BIFs at the Selwyn mine, situated 150 km southeast of Mount Isa (Fig. 1.3, Chapter 1). The BIFs at the Osborne and Selwyn ore-bodies typically contain around 65 wt.% iron oxide, which is much higher than the sedimentary Algoman or Superior-type BIFs that seldom contain more than about 45 wt.% iron oxide (Table 2.3). Davidson et al. (1989) noted that both Osborne and Selwyn BIFs have some similarities with the exhalative Lahn-Dill-type iron ore deposits. The Lahn-Dill ores are atypical variants of volcanogenic Algoman iron-formations that overlie basic volcanic rocks in the European Paleozoic, and consist of more than 80 wt.% iron oxide (Quade, 1976).

The original thickness of the upper BIF was probably around 27 m. However, movement along normal and reverse shears has produced tectonic repetition, attenuation and thickness variations ranging from several metres to about 50 m (Appendix 1). Lenses of brecciated BIF host silicic alteration and related Cu-Au bearing sulphides (Figs 4.5a and 4.5b, Chapter 4). Brecciated zones locally destroy S_0 , S_x , S_1 and S_2 fabrics, but are broadly conformable with lithologic contacts (Appendix 1).

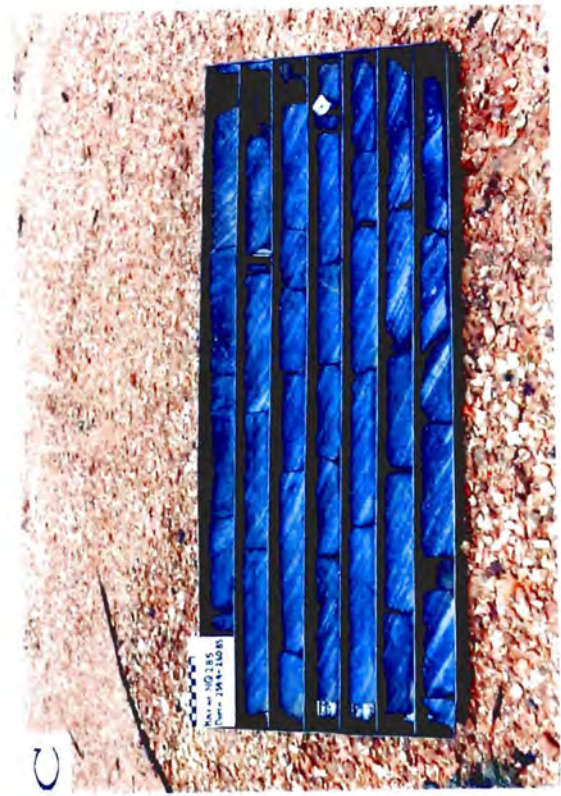
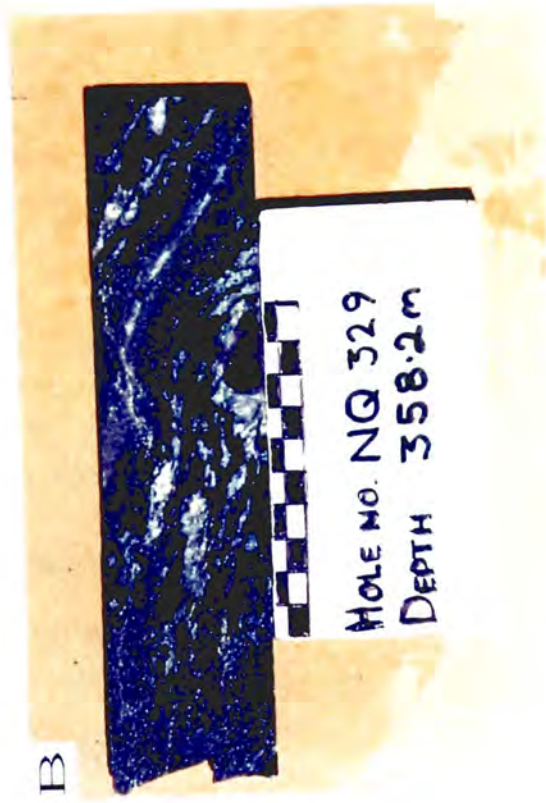
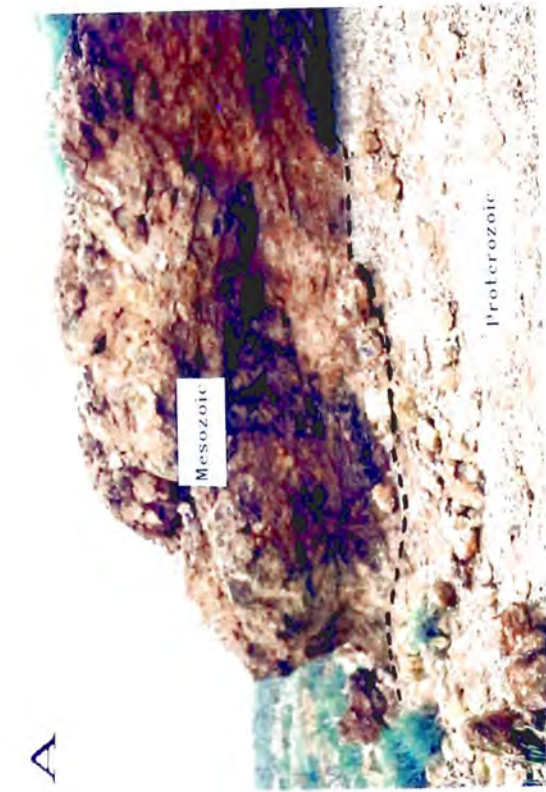
Samples	1	2	3	4	5	6	7	8	9	10	11
Wt. %											
SiO ₂	33.33	31.61	47.2	5.04	49.9	51.6	56.36	32.1	44.3	40.71	44.13
TiO ₂	0.02	0.18	0.02	—	0.01	0.36	0.01	0.6	0.27	0.12	—
Al ₂ O ₃	0.48	1.11	1.15	0.34	0.33	0.13	4.27	9.6	3.18	2.32	3.85
Fe ₂ O ₃ *	65.78	66.73	44.4	89.38	44.3	44.94	29.84	42	44.3	41.14	46.24
MnO	0.03	0.02	0.59	0.11	0.15	0.12	0.22	5.2	0.23	0.29	0.09
MgO	0.42	1.09	1.24	—	2.21	2.28	0.55	1.6	1.24	3.15	2.8
CaO	0.50	0.06	1.58	0.8	1.34	1.33	3.08	5.7	1.79	2.63	1.31
Na ₂ O	0.22	0.15	0.12	—	0.01	0.08	0.08	0.2	0.28	1.05	1.22
K ₂ O	0.07	0.07	0.14	—	0.21	0.03	0.08	0.3	0.45	0.57	0.36
P ₂ O ₅	0.32	0.03	0.06	—	0.22	0.04	0.23	3.2	0.35	0.25	—
Total**	101.15	101.05	96.5	95.67	98.68	100.91	94.72	100.5	96.39	92.23	100
Ppm											
Ba	0.00	12	180		<5						
Cr	4.80				6						
Cu	0.00	7,800	10		16.3		210				
Ga	19.50										
Nb	2.74				<0.4						
Ni	41.80	15			30.5	10	55				
Pb	1.74	<2	30		23.4		7				
Rb	10.70				<33						
Sr	3.66				4.3						
Th	0.00				0.09						
U	0.00				<0.8						
V	74.28				4.5	11					
Y	8.78				6.7						
Zn	12.40	<2	51		88.9	111	145				
Zr	9.74				1.7						

*total iron as Fe₂O₃**ignoring H₂O, CO₂, LOI

- 1: Adshead, (1995). Average oxide facies BIF, Osborne ore body (n=6).
- 2: Davidson et al., (1989). Average area 257 ironstone, Starra ore body (n=7).
- 3: Maynard, (1983). Average Hammersly BIF (n=148).
- 4: Quade, (1976). Average Lahn-Dill oxide facies ore, Fortuna mine (n=5).
- 5: Dymek and Klein, (1988). BIF from 3800 Ma Isua supracrustal belt (n=1).
- 6: Hall, (1985). Relict BIF, enclave within 3700 Ma granite (n=1).
- 7: Saager et al., (1987). Average BIF, Bar 20 ore body, Gwanda Greenstone Belt (n=6).
- 8: Johnson and Klinger, (1975). Broken Hill "mine sequence" BIF.
- 9: Yeo, (1986). Average Rapitan-type BIF (n=11).
- 10: Beukes, (1973). Kuruman Superior-type BIF, South Africa.
- 11: Bayley and James, (1973). Wind River Range Algoma-type BIF, Wyoming.

Table 2.3. Comparative composition of various oxide facies iron-formations.

- Fig. 2.1** (a) Angular unconformity between Mesozoic sandstone and Proterozoic metasediments, several kilometres NW of Osborne.
- 2.1 (b) Polished sample of the garnet-cordierite-sillimanite layered gneiss. From NQ329 @ 358.2m, scale bar=10 cm.
- 2.1 (c) Tray of split drill core, showing 6 m of well banded quartz-magnetite BIF. From NQ285 @ 254.4-260.85 m, scale bar=10 cm.
- 2.1 (d) Albite mesobands (marked with arrows) in quartz-magnetite BIF. From NQ304 @ 432.7 m, scale bar=10 cm.



2.24 Layered Biotite-Albite-Quartzite

The layered biotite-albite-quartzite ranges in thickness from 5 to 35 m, with an average of around 19 m, is continuous along strike for over a kilometre, and is conformable with the underlying banded quartz-cummingtonite-magnetite schist. It consists of well bedded biotite-rich metapelites, with minor layers rich in fine-grained magnetite or pyrite (Fig. 2.2a). Narrow shears sub-parallel to bedding are common in this unit, especially in and around biotite layers that are mechanically weaker than adjacent layers rich in quartz and plagioclase. A semi-continuous *laminated albite-biotite±corundum±sillimanite* marker horizon is a distinctive 1 m thick unit within the layered biotite-albite-quartzite. It is characterized by cm-scale monomineralic bands of pale pink albite, interbanded with dark biotite rich layers that commonly contain sillimanite or prominent porphyroblasts of corundum (Fig. 2.2b).

The averaged compositions of five samples of the laminated albite-biotite marker unit are presented in Table 2.2. The samples were collected several hundred metres apart, were split into biotite-rich (mesosome) and albite-rich (leucosome) bands, and were analysed by X-ray fluorescence. Corundum-bearing biotite-rich bands from HQ19 and NQ156 (Fig. 2.2b) have bulk compositions containing over 20 wt.% Al_2O_3 , and are therefore peraluminous.

2.25 Banded Quartz-Cummingtonite-Magnetite Schist

The banded quartz-cummingtonite-magnetite schist is a distinctive unit characterized by mm-scale interbanded laminations of quartz, cummingtonite and magnetite (Fig. 2.2c). The average unit thickness is 4 m, but ranges between 2 and 6 m. In places, intense silicic alteration has produced a white quartz rich rock with relic cummingtonite grains, which was interpreted as a "mylonitic shear zone" in unpublished Placer reports (e.g. Morrison 1991). However, the characteristic mineral assemblage, thin layering and lack of mylonitic deformation textures suggest this unit is the metamorphic equivalent of interbanded quartz, magnetite and a complex mixture of hydrous iron silicates and carbonates, i.e. original silicate facies iron-formation (Chapters 3 and 5). Banded quartz-cummingtonite-magnetite conformably overlies the lower BIF unit for at least 650 m.

2.26 Lower BIF

The lower BIF ranges in thickness from 7 to 17 m, has an average thickness of 13 m and is traceable as a planar magnetic anomaly for several kilometres (K. Logan, 1994; pers. comm.). It is texturally and mineralogically identical to the upper BIF, but is relatively unaffected by deformation or faulting. Cu-Au grades in this unit are low, compared with the upper BIF.

Since iron-formations in the Mount Isa Inlier are confined to the Mount Norna Quartzite, the upper and lower BIFs may be the stratigraphic equivalents of other BIF horizons in the Cloncurry-Selwyn zone.

2.27 Quartz-Plagioclase-Biotite Schist

The quartz-plagioclase-biotite schist is the lowermost unit in the mine sequence. It conformably underlies the lower BIF, and is distinguished from the plagioclase-quartzite by abundant coarse-grained biotite that strongly defines S_1 (Fig. 2.3b). The minimum thickness of the quartz-plagioclase-biotite schist is 15 m. However, the total thickness is unknown, due to a paucity of deep diamond drilling in the footwall of the deposit. The appearance of cummingtonite needles between 3 and 8 metres below the base of the lower BIF marks the beginning of a *cummingtonite schist*, a distinctive pale green marker horizon, usually about 7 m thick, that is commonly characterized by cm-scale kink folds (Fig. 2.2d).

2.3 Intrusives

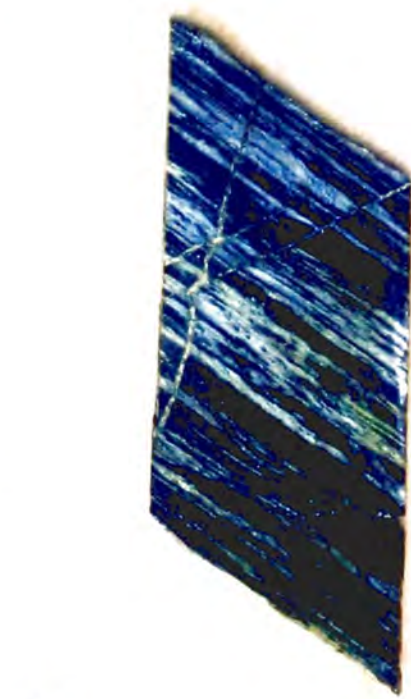
2.31 Amphibolite Dykes

The amphibolite dykes are dark, fine to medium-grained plagioclase-hornblende bearing rocks that cut metasedimentary units and the Awesome Fault, with an average orientation of $015^\circ/60^\circ/E$. They have been folded and have a well developed mineral lineation (L_1), defined by a preferred alignment of hornblende. The amphibolites probably predate the main 1595 Ma D_1 folding event and may have intruded the mine sequence during extension and basin formation between 1870 and 1760 Ma ago.

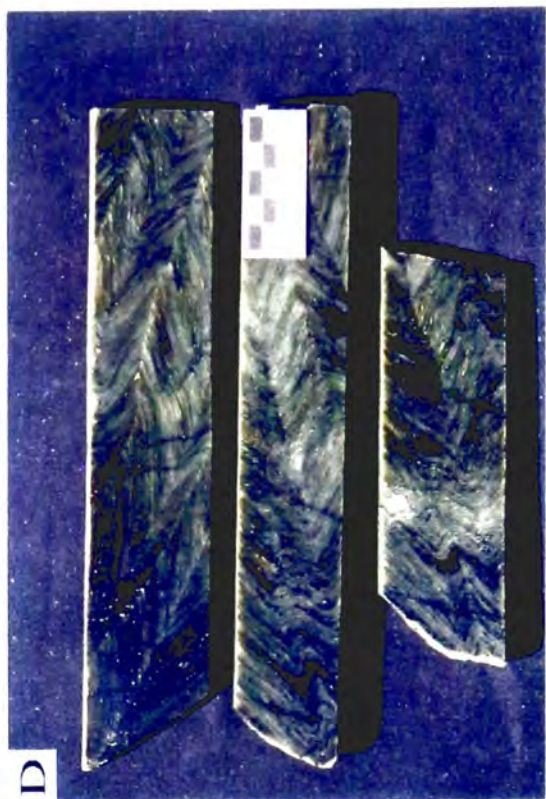
- Fig. 2.2 (a)** Layered biotite-albite-quartzite from between the upper and lower BIF. Scale bar=10 cm.
- 2.2 (b)** Polished samples of the laminated albite-biotite \pm corundum \pm sillimanite marker horizon, from left to right:
- HQ19 @ 209.0m
 - HQ185 @ 63.7m
 - HQ 63 @ 247.23m
 - HQ 183 @ 147.85m
 - NQ 173 @ 192.34m
 - NQ 156 @ 234.00m
- Scale bar=5 cm.
- 2.2 (c)** Banded quartz-cummingtonite-magnetite schist. Core dimensions approximately 6.2*12.7 cm. From HQ 92 @ 124.3m.
- 2.2 (d)** Kink-banded cummingtonite schist. From NQ173 @ 226.7m, scale bar=5 cm.



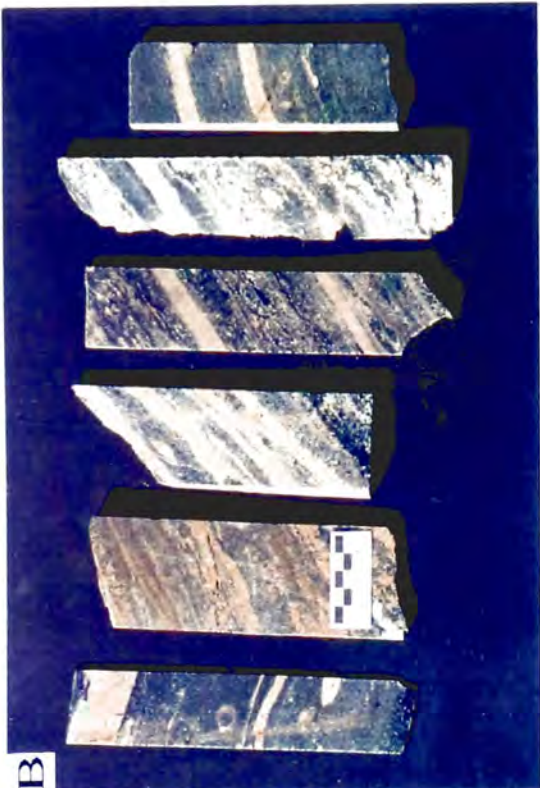
A



C



D



B

2.32 Pegmatites

Coarse-grained K-feldspar-quartz-plagioclase-biotite \pm tourmaline \pm apatite bearing pegmatites form thin, sheet-like swarms that cut all metasedimentary units and the "Awesome Fault" (Appendix 1). An average orientation of 033°/70°/W is inferred from drill-hole intersections and from magnetic susceptibility data that indicate pegmatites dip steeply to the west (Logan, 1995). The Pegmatites are probably related to the emplacement of the 1500 Ma old Williams Batholith. In places, the pegmatites are overprinted by secondary magnetite, sulphides and silicic alteration (Fig. 2.3a), suggesting that the economic mineralisation post-dates 1500 Ma ago.

2.4 Alteration and Economic Mineralisation

The main alteration style in the Western Domain is termed "silica-flooding" by Placer geologists, and is characterized by massive, transparent, grey or pale grey quartz, coarse-grained magnetite; and very fine-grained disseminated magnetite, pyrite and chalcopyrite. A second style of alteration is characterized by coarse-grained granular to massive magnetite, pyrite and chalcopyrite. The two styles of alteration are commonly closely associated and may be genetically related. Silica flooding and secondary magnetite cross-cut and hence post-date S_0 , amphibolites, pegmatites and all recognized deformation fabrics (S_x , S_1 , S_2) in metasedimentary units.

The upper BIF and, to a smaller extent the lower BIF, host all Cu-Au bearing sulphides in the Western Domain. Cu-Au minerals, pyrite and silicic alteration occur as breccia fill in lenses within BIF units, especially near contacts between BIFs and quartzo-feldspathic units. The pyrite, chalcopyrite and secondary magnetite grains are only weakly deformed, indicating that economic minerals post-date the 1620-1550 Ma Isan Orogeny.

2.5 Veins

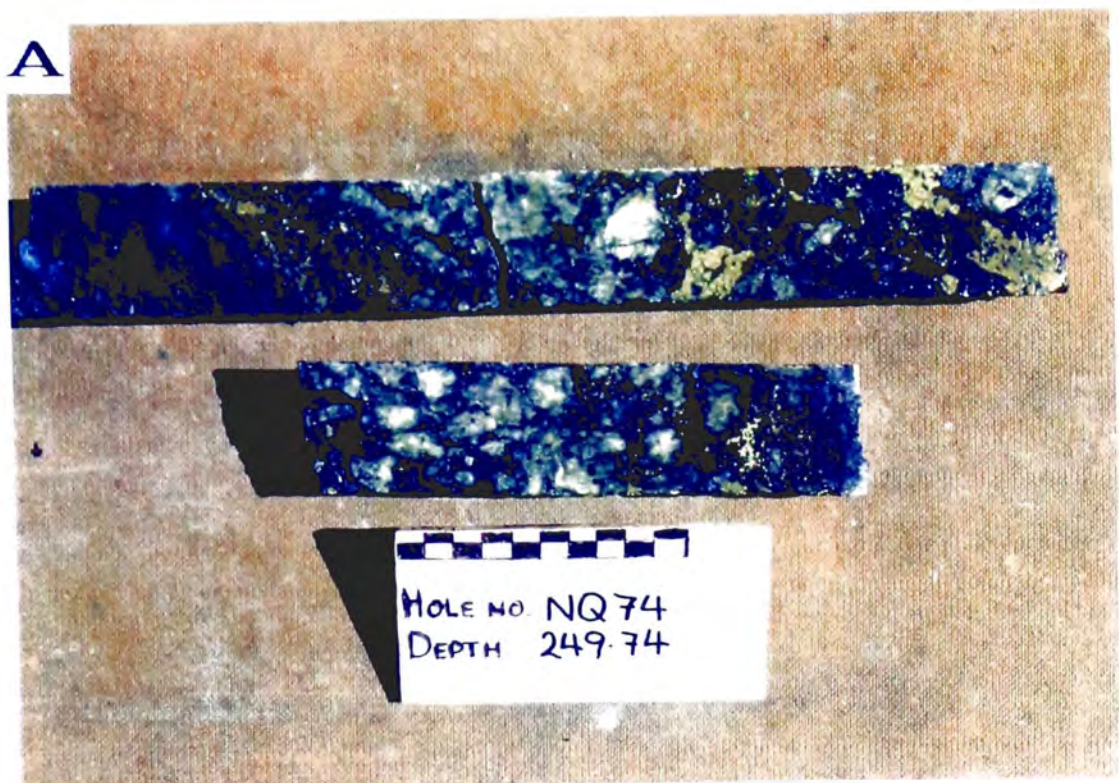
Numerous small uneconomic veins are characterized by blocky carbonate (calcite, dolomite or siderite) or quartz, with variable amounts of pyrite, chalcopyrite, apatite and hematite. The veins are parallel to the dominant 151°/46°/NE trending joint set, although locally they may mimic S_0/S_1 . Centimetre-scale alteration selvages are commonly developed around the veins, consisting of pale green "sericite" in quartzofeldspathic units (Fig. 2.3b) and hematite and red apatite in BIFs. Although most of the veins at Osborne appear to have formed as late-stage fill of open joints, others consist of several generations of incremental fibres that appear to have formed by the crack-seal process (e.g. Ramsay, 1980), whereas some contain angular fragments of wall rock and probably formed as a result of hydraulic fracturing.

2.6 Oxidation

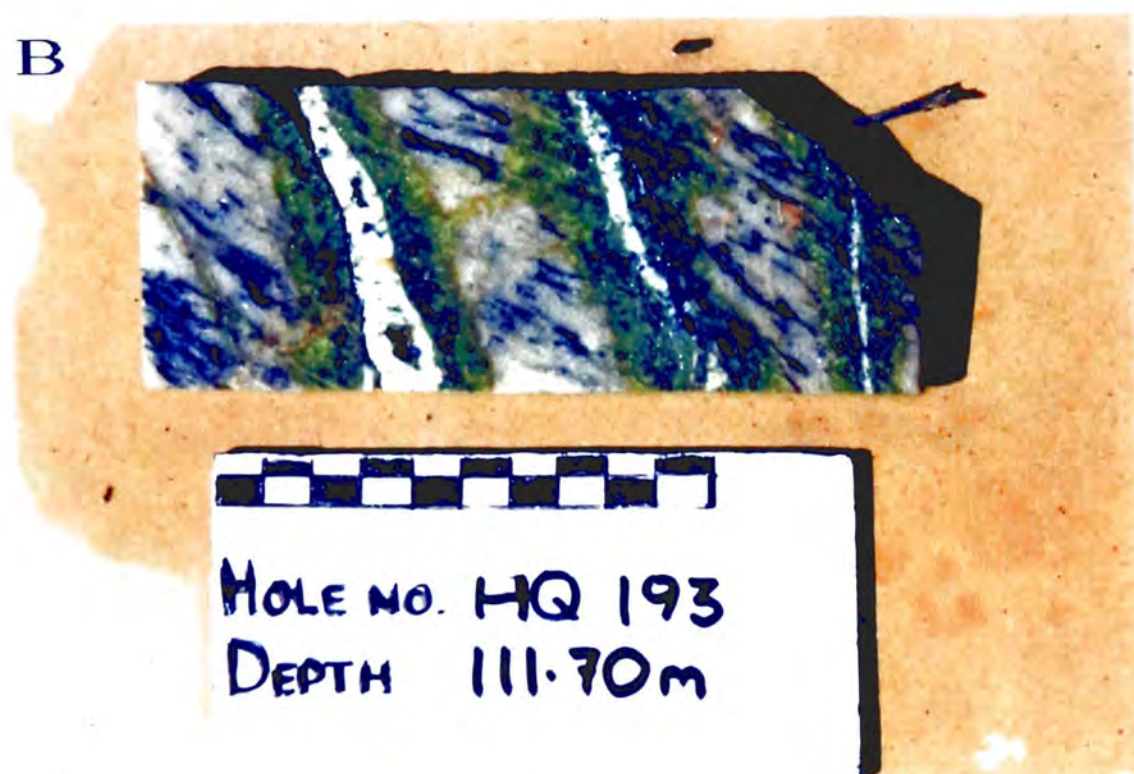
The oxidized zone extends to depths of around 30 to 50 m below the unconformity, and is characterized by abundant clay minerals, secondary hematite, "limonite" and muscovite in crumbly, iron-stained country rocks, and supergene malachite, cuprite, chrysocolla and small specks of native gold in vuggy mineralized zones. Box-work textures and goethite pseudomorphs, presumably after Fe-Cu sulphides, are common.

- Fig. 2.3 (a)** Pyrite, chalcopyrite and magnetite overprinting coarse-grained pegmatite. From NQ74 @ 249.74 m, scale bar=10 cm.
- 2.3 (b)** Blocky calcite veins with pale green "sericite" alteration haloes cross-cutting quartz-plagioclase-biotite schist. From HQ193 @ 111.70 m, scale bar=10 cm.

A



B



Chapter 3

Petrology and Mineral Chemistry of the Osborne Mine Sequence

Introduction

For the purposes of this chapter, the Osborne mine sequence is divided into three principal rock groups: garnet-cordierite-sillimanite bearing gneiss, plagioclase quartzite, and BIF (oxide and silicate facies). Although sedimentary bedding is preserved, deformation and high-grade metamorphism have erased relics of primary textures and minerals. Thus the petrogenesis is largely inferred from mineralogy and geochemistry. The gold and copper sulphide-bearing alteration assemblage that overprints and post-dates the mine sequence is described in detail by Adshead (1995).

3.1 Garnet-Cordierite-Sillimanite Gneiss

Acicular sillimanite, cummingtonite and platy biotite define a domainal schistosity (S_1), that wraps around lenticular porphyroblasts of cordierite and garnet in a quartz-albite matrix. Porphyroblasts are commonly poikiloblastic; a few grains contain straight inclusion trails (S_x) that lie at 90° to S_1 (Fig. 4.4a, Chapter 4).

3.11 Cordierite

Unaltered cordierite has an average composition ($\text{NaO}_{0.04}$) ($\text{Mg}_{1.3}$ $\text{Fe}_{0.73}$) [$\text{Si}_{5.04}\text{Al}_{3.89}$ O_{18}] (Table 3.1). Retrograde "pinite" is common along grain boundaries and fractures, and may pseudomorph entire grains. Abundant inclusions of plagioclase, quartz and biotite rarely define a straight S_x inclusion fabric that is sharply discordant with the external S_0/S_1 domainal schistosity (Chapter 4). Anhedral cordierite porphyroblasts may reach 20 mm in diameter, and commonly show both cyclic and simple twinning (Figs 3.1a, 3.1b).

3.12 Garnet

Poikiloblastic garnet (Fig. 3.1a), of average composition ($\text{Mg}_{1.27}\text{Fe}^{2+}_{4.63}\text{Mn}_{0.14}\text{Ca}_{0.02}$) ($\text{Al}_{3.90}\text{Fe}^{3+}_{0.1}$) [$\text{Si}_{5.96}\text{Al}_{0.04}$ O_{24}] (Table 3.1), may reach 30 mm in diameter. Subhedral garnet porphyroblasts are dominated by the almandine end-member (76.4%), with appreciable amounts of pyrope (20.96%), andradite (2.5%) and spessartine (2.3%). S_x inclusion fabrics are preserved in some garnet porphyroblasts.

Samples	1	2	3	4	5	6	7	8	9	10	11	12
Wt. %												
SiO ₂	37.11	47.63	36.66	35.55	67.44	54.75	57.28	0.03	66.94	34.94	36.49	44.87
TiO ₂	0.00	0.02	0.01	2.30	0.00	0.13	0.04	0.04	0.01	2.24	0.02	0.58
Al ₂ O ₃	20.79	31.18	60.52	17.92	19.19	3.09	0.32	99.15	20.45	18.17	61.77	34.42
Cr ₂ O ₃	0.02	0.03	0.01	0.06	0.00	0.04	0.03	0.05	0.00	0.04	0.05	0.01
FeO	35.16	8.27	0.25	17.65	0.03	18.83	12.79	0.90	0.06	17.35	0.86	2.75
MnO	1.05	0.06	0.01	0.00	0.01	0.00	0.07	0.00	0.02	0.02	0.00	0.00
MgO	5.30	8.26	0.01	10.92	0.00	21.17	26.53	0.00	0.00	11.48	0.01	0.53
CaO	0.09	0.01	0.01	0.00	0.53	0.05	0.27	0.00	1.22	0.00	0.01	0.00
Na ₂ O	0.01	0.19	0.02	0.35	11.26	0.29	0.05	0.00	10.99	0.11	0.00	0.72
K ₂ O	0.01	0.01	0.01	8.84	0.04	0.01	0.00	0.00	0.09	9.81	0.00	10.27
Total	99.54	95.66	97.51	93.59	98.5	98.36	97.38	100.17	99.78	94.16	99.21	94.15
no. oxygens	24	18	20	22	32	23	23	—	32	22	20	24
no. ions												
Si	5.96	5.04	4.06	5.46	11.97	7.73	7.94	—	11.76	5.36	3.99	6.65
Ti	0.00	0.00	0.00	0.27	0.00	0.01	0.00	—	0.00	0.26	0.00	0.06
Al	3.94	3.89	7.90	3.24	4.01	0.51	0.05	—	4.24	3.29	7.96	6.01
Cr	0.00	0.00	0.00	0.01	0.00	0.01	0.00	—	0.00	0.01	0.00	0.00
Fe	4.73	0.73	0.02	2.27	0.00	2.22	1.48	—	0.01	2.23	0.09	0.34
Mn	0.14	0.01	0.00	0.00	0.00	0.00	0.01	—	0.00	0.00	0.00	0.00
Mg	1.27	1.30	0.00	2.50	0.00	4.46	5.48	—	0.00	2.62	0.00	0.12
Ca	0.02	0.00	0.00	0.00	0.10	0.01	0.04	—	0.23	0.00	0.00	0.00
Na	0.00	0.04	0.00	0.10	3.87	0.08	0.01	—	3.74	0.03	0.00	0.21
K	0.00	0.00	0.00	1.73	0.01	0.00	0.00	—	0.02	1.92	0.00	1.94
Total	16.06	11.01	11.98	15.58	19.96	15.03	15.02	—	20.00	15.72	12.04	15.33

- 1: Average garnet from the garnet-cordierite-sillimanite layered gneiss, (n=21).
- 2: Average cordierite from the garnet-cordierite-sillimanite layered gneiss, (n=19).
- 3: Average sillimanite from the garnet-cordierite-sillimanite layered gneiss, (n=3).
- 4: Average biotite from the garnet-cordierite-sillimanite layered gneiss, (n=8).
- 5: Average albite from the garnet-cordierite-sillimanite layered gneiss, (n=11).
- 6: Average cummingtonite from the garnet-cordierite-sillimanite layered gneiss, (n=10).
- 7: Average cummingtonite from the cummingtonite schist, (n=14).
- 8: Average corundum from the layered biotite-albite-quartzite, (n=13).
- 9: Average albite from the layered biotite-albite-quartzite, (n=23).
- 10: Average biotite from the layered biotite-albite-quartzite, (n=12).
- 11: Average sillimanite from the layered biotite-albite-quartzite, (n=2).
- 12: Average retrograde muscovite replacing corundum from the layered biotite-albite-quartzite, (n=4).

Note: 0.00 = Below detection limit. Detection limits and instrument specifications are listed on page IX, Appendix 2.

Table 3.1. Averaged electron microprobe analyses from mine sequence rocks.

3.13 Sillimanite

Sillimanite closely approximates the ideal Al_2SiO_5 composition, with a limited amount of iron present (Table 3.1). Together with cummingtonite and biotite, the sillimanite defines a bedding-parallel domainal schistosity (S_1). It forms bundles of "fibrolite", as well as individual needles that commonly reach 5 mm in length (Fig. 3.1a).

3.14 Cummingtonite

Cummingtonite has an average composition of $(\text{Al}_{0.25}\text{Fe}_{2.22}\text{Mg}_{4.46}\text{Na}_{0.08}) [\text{Si}_{7.73}\text{Al}_{0.27}\text{O}_{22}]$ (Table 3.1) and a corresponding $\text{Fe}/(\text{Fe}+\text{Mg})$ ratio of 33%, which is at the magnesium rich end of the cummingtonite Fe-Mg solid solution series (Deer et al., 1992). The long axes of euhedral cummingtonite grains can reach 12 mm in length.

3.15 Plagioclase

Plagioclase is dominated by the albite component (95.5 %), with a limited amount of substitution by the K-feldspar component (Table 3.1). Minor iron in the analysis is assumed to be Fe^{3+} replacing Al in the structure. The plagioclase grains are elongate in S_0/S_1 , and are either untwinned or have typical polysynthetic twinning. The grain size varies from around 0.4 to 4 mm, with the larger grains restricted to layers containing large porphyroblasts of cordierite and/or garnet.

3.16 Biotite

Biotite forms bundles up to several centimetres long that define the domainal S_1 schistosity. Assuming that all iron is present as Fe^{2+} in octahedral Y sites, the average structural formula of biotite is $(\text{K}_{1.73}\text{Na}_{0.1}) (\text{Al}_{0.7}\text{Ti}_{0.27}\text{Fe}_{2.67}\text{Mg}_{2.5}) [\text{Si}_{5.46}\text{Al}_{2.54}\text{O}_{20}]$. The Biotite is commonly riddled with numerous inclusions (possibly zircon) surrounded by pleochroic haloes.

3.17 Quartz

Xenoblastic quartz grains have an average diameter of about 0.4 mm, and are slightly elongate in the plane of S_0/S_1 (Fig. 3.1a).

3.18 Tourmaline

Euhedral, poikiloblastic tourmaline (Fig. 3.1c) is a common minor mineral that may preserve the S_x inclusion fabric in porphyroblasts.

3.19 Petrogenesis

The paragenesis: cordierite-garnet-sillimanite-quartz-feldspar is typical of high-grade regionally metamorphosed pelitic rocks, and is of great use as an indicator of metamorphic conditions. Microprobe analyses of the above minerals were processed using the THERMOCALC geo-thermometer/barometer (Powell and Holland, 1988). Assuming a temperature of 750°C, the above assemblage gives an average pressure of 5.1 ± 0.4 kbar for $a_{H_2O}=0.5$. Assuming nothing, the average pressure-temperature was calculated as 5.1 ± 1.0 kbar and $746 \pm 136^\circ\text{C}$.

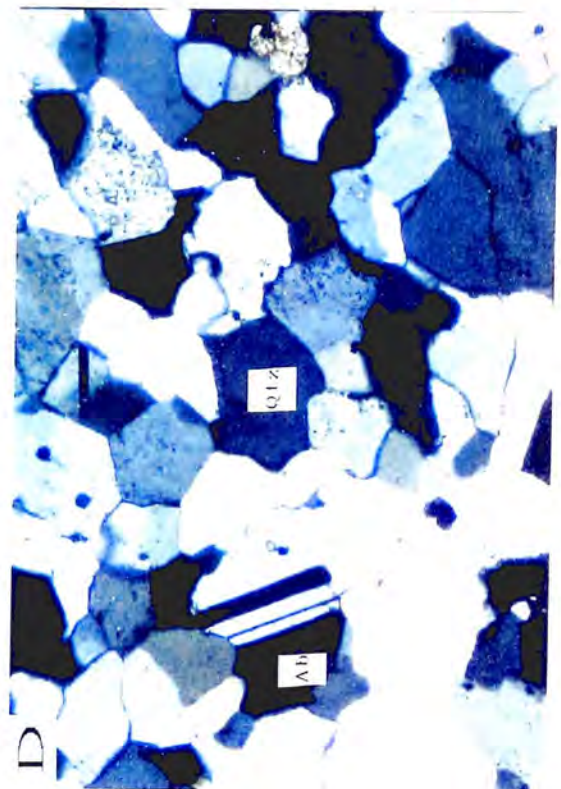
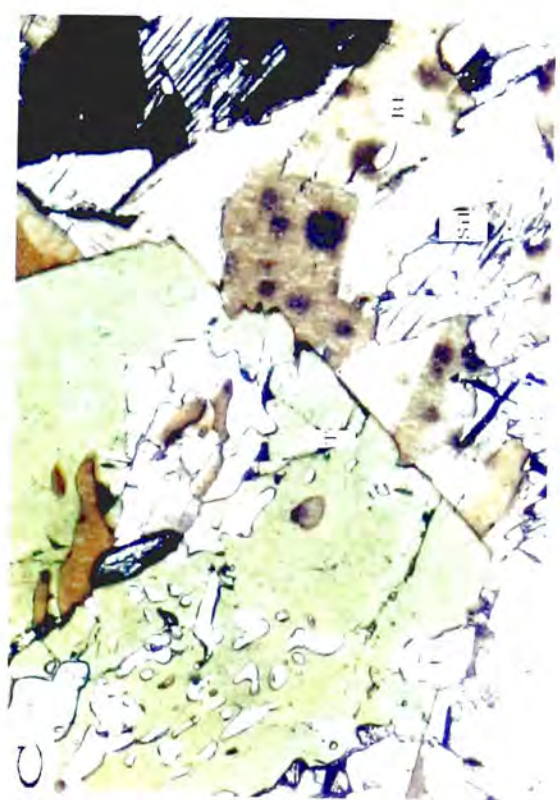
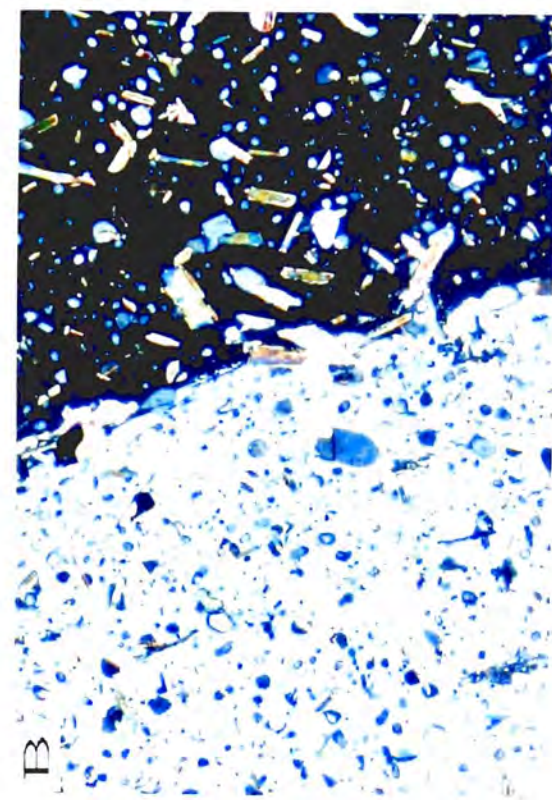
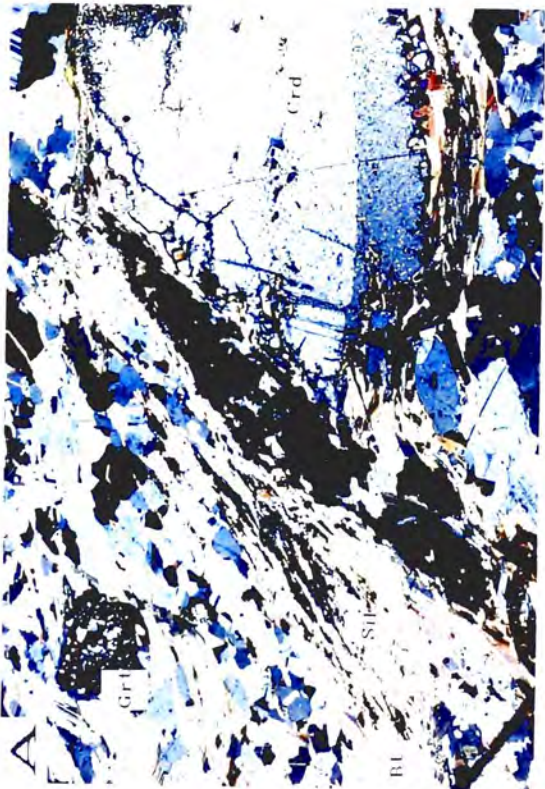
3.2 Plagioclase Quartzites

Holyland (1991) described the texture of plagioclase quartzite at the Osborne deposit as "granofelsic". However, although plagioclase quartzites are essentially equigranular, the straight grain boundaries and 120° triple junctions typical of granoblastic recrystallization textures are commonly absent, and quartz and plagioclase grains are usually slightly elongate in S_0/S_1 . This alignment is enhanced by local concentrations of biotite, the 001 surfaces of which control the grain shapes of quartz and plagioclase (e.g. Vernon, 1976).

3.21 Quartz

Quartz grains vary from about 0.15 mm to 1.4 mm, although most are around 0.3 mm in diameter (Fig. 3.1d).

- Fig. 3.1 (a)** Inclusion rich porphyroblasts of garnet and twinned cordierite in a matrix of quartz and albite, with sillimanite and biotite defining S_0/S_1 . From garnet-cordierite-sillimanite gneiss @ NQ329, 358.2 m. Base of photo=25 mm, X-polars.
- 3.1 (b)** Close up of the simple twin in poikiloblastic cordierite in fig. 3.1a. Base of photo=1.52 mm, X-polars.
- 3.1 (c)** Euhedral tourmaline surrounded by biotite with pleochroic haloes, and sillimanite. From garnet-cordierite-sillimanite gneiss @ NQ 329, 358.2 m. Base of photo=1.52 mm, plane polarized light.
- 3.1 (d)** Quartz and plagioclase (twinned and untwinned) from plagioclase quartzite @ HQ59, 196.5 m. Base of photo=1.52 mm, X-polars.



3.22 Plagioclase

Plagioclase is dominated by the albite component (94.2 %), with a limited amount of substitution by K-feldspar (Table 3.1). The plagioclase grains are similar in size to those of quartz and are commonly untwinned, which makes the identification of the two minerals difficult in thin section (Fig. 3.1d).

3.23 Biotite

Variable amounts of microscopic and mesoscopic biotite define the pervasive S_1 fabric. Assuming that all iron is present as Fe^{2+} in octahedral Y sites, the average structural formula is $(K_{1.92}Na_{0.03})(Al_{0.65}Ti_{0.26}Fe_{2.23}Mg_{2.62})[Si_{5.36}Al_{2.64}O_{20}]$, which is similar to the composition of biotite in the garnet-cordierite-sillimanite gneiss.

3.24 Corundum

Euhedral porphyroblasts of corundum, up to 15 mm in diameter, commonly have multiple lamellar growth twins and partings parallel to both the unit pinacoid $\{0001\}$ and rhombohedron $\{10\bar{1}1\}$ (Fig. 3.2a). Corundum closely approximates the ideal Al_2O_3 composition, with minor amounts of iron (assumed to be Fe^{3+}), titanium and chromium (Table 3.1). Exsolved Fe-Ti oxides commonly form thin alternating lamellae within the corundum grains (Fig. 3.2b). Corundum porphyroblasts that contain iron-rich inclusions are surrounded by a biotite-free halo that can extend several mm from the porphyroblast margin. The corundum is commonly retrogressed to muscovite, especially along partings and grain boundaries. Where not retrogressed, the porphyroblast margins commonly form symplectic intergrowths with albite.

3.25 Sillimanite

Sillimanite is essentially pure Al_2SiO_5 , with a limited amount of iron present in the crystal structure (Table 3.1). It defines S_1 , and forms bundles of "fibrolite", as well as individual needles. Both varieties are commonly retrogressed to muscovite.

3.26 Magnetite and Pyrite

Fine-grained magnetite and pyrite are ubiquitous accessory minerals, occurring both as diffuse specks and as magnetite-rich, bedding-parallel bands with quartz and plagioclase in the layered biotite-plagioclase-quartz unit.

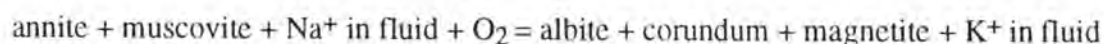
3.27 Petrogenesis

LAMINATED ALBITE-BIOTITE HORIZONS

The unusual corundum and sillimanite bearing albite-biotite horizons of the Osborne deposit are similar to descriptions of stratiform peraluminous rocks in South Africa and Zimbabwe. Willner et al. (1990) described sillimanite and sillimanite-corundum rocks intercalated with metapelites of the Mid-Proterozoic Bushmanland Sequence, South Africa. Hall (1923) and de Villiers (1976) described stratiform lenses of corundum and sillimanite-bearing mica schist from the Transvaal, where corundum occurs as euhedral crystals mantled by white sodic plagioclase, and Grubb (1986) described conformable lenses of corundum, fuschite and andalusite bearing granulite from the Concession corundum deposit in Zimbabwe.

The lateral continuity and narrow strata-bound nature of the above rocks and the main laminated albite-biotite horizon at the Osborne deposit suggest a mode of origin involving a pre-metamorphic surface enrichment of aluminium. Alumina enrichment can be caused by hydrothermal alteration; or by the dehydration and metamorphism of Al-rich regolith (e.g. bauxites).

Bauxites have been recognized with increasing frequency in Precambrian rocks in recent years. They range from unmetamorphosed and sericitic shales, through andalusite and sillimanite schists, to kyanite schists, and to massive corundum deposits in high-grade gneisses (Reimer, 1986). However, many corundum-bearing rocks that were once thought to represent metamorphosed bauxites or other Al-rich sediments have been reinterpreted as being the products of post-volcanic, pre-metamorphic hydrothermal alteration—e.g. Schreyer et al. (1981), Reimer (1986), Willner et al. (1990). Bauxites contain 45 wt. % or more of alumina (Retallack, 1990), which is more than twice the 21.15 wt. % average for corundum-bearing layers at Osborne (Table 2.2, Chapter 2). Furthermore, the main corundum bearing biotite-albite horizon is sandwiched between the upper and lower BIFs (Appendix 1), suggesting it is of submarine origin, rather than the product of subaerial weathering. The preservation of delicate bedding planes during bauxitization also seems unlikely. A plausible alternative to the "bauxite hypothesis" is that precursor rocks underwent alteration by volcanic exhalations prior to metamorphism. A possible corundum-forming reaction is:



PLAGIOCLASE QUARTZITES

Apart from bedding, pervasive metamorphic recrystallization has obliterated any primary sedimentary or volcanoclastic textures that may have existed in the plagioclase quartzites, making the identification of precursor rocks extremely difficult. Using the bulk-rock composition of a typical plagioclase quartzite (Table 2.2, Chapter 2), variation diagrams have been used to identify possible protoliths, although strictly speaking such diagrams may not be suitable for metamorphosed rocks, as the alkalis may have been mobilized. Assuming there has been no sodic alteration of the plagioclase quartzites, the abundance of albite suggests a volcanic rather than a sedimentary precursor. If a volcanic precursor is assumed, the plagioclase quartzite in Table 2.2 plots in the trachyte field using the total alkalis versus silica (TAS) diagram of Le Maitre et al. (1989). Using trace-element discrimination diagrams from Winchester and Floyd (1977) the plagioclase quartzite plots as a trachyandesite (Nb/Y vs Zr/TiO_2), as a trachyte (Nb/Y vs SiO_2) and near the trachyandesite field using Zr/TiO_2 vs SiO_2 .

If a sedimentary precursor is assumed, the plagioclase quartzite in Table 2.2 plots as a greywacke, based on the plot $\log(\text{Na}_2\text{O/K}_2\text{O})$ vs $\log(\text{SiO}_2/\text{Al}_2\text{O}_3)$ of Pettijohn et al. (1972), or as an iron rich-shale, using the $\log(\text{Fe}_2\text{O}_3/\text{K}_2\text{O})$ vs $\log(\text{SiO}_2/\text{Al}_2\text{O}_3)$ classification scheme of Herron (1988).

Lenses of pure white quartzite within the plagioclase-quartzite unit probably represent metamorphosed quartz sandstones or psammites, with biotite-rich interbeds the equivalent of more silty or pelitic interbeds.

3.3 Banded Iron Formation—Oxide Facies

3.31 Magnetite

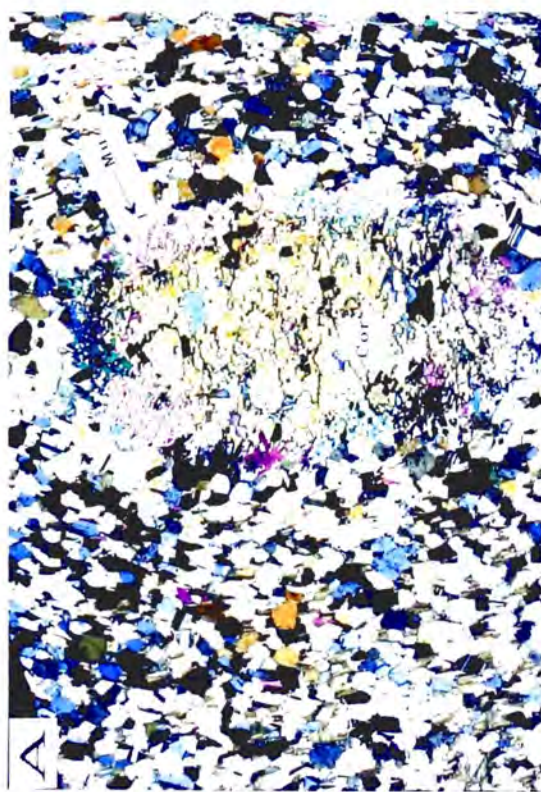
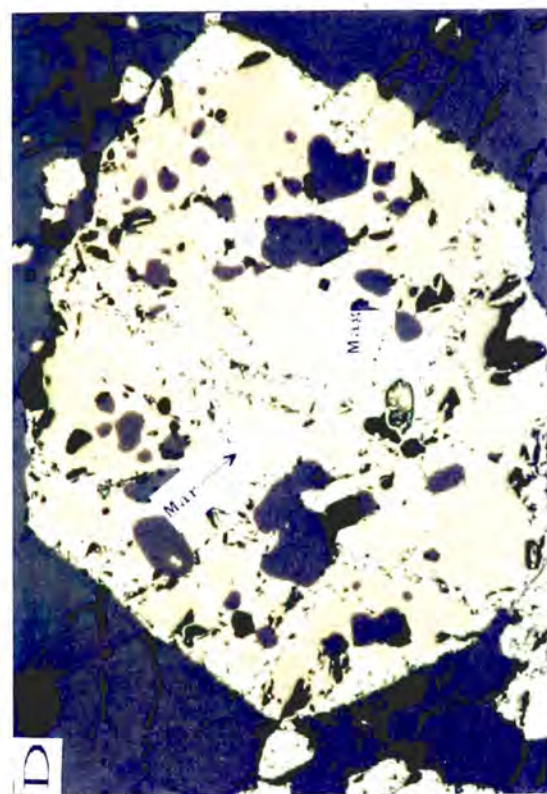
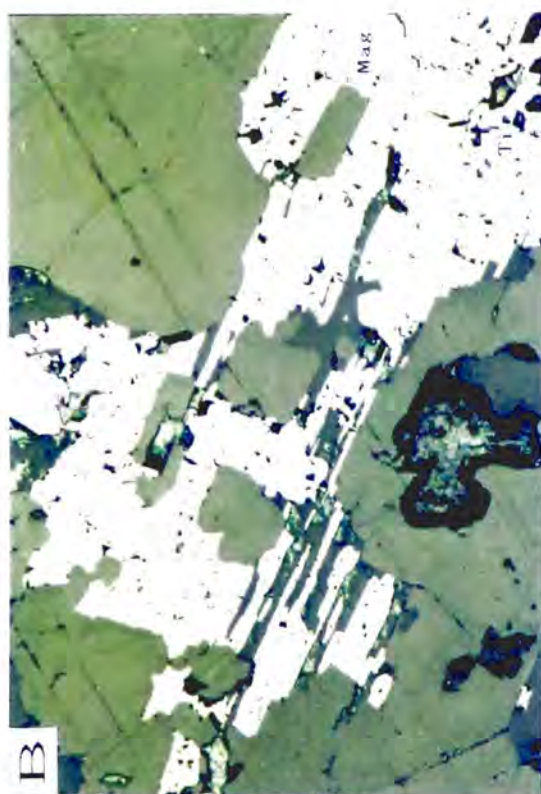
There is a considerable variation in magnetite grain size between BIF laminations, ranging from an average minimum of approximately 0.01 mm to an average maximum of approximately 2.5 mm, with grains over 5 mm common (Fig. 3.2c). The grain size depends on the original distribution of nucleating sites—layers that were originally fine-grained remained relatively fine-grained during recrystallization, whereas layers that were coarse-grained remained so (e.g. Vernon 1976). The magnetite in the BIFs is octahedral, yielding triangular, square or rhombic sections. The grains are usually slightly rounded, and moderately elongate in S_0/S_1 . Cumingtonite needles influence grain shape in the cumingtonite-quartz-magnetite schist, in which magnetite, quartz and plagioclase form tabular grains that are elongate in S_0/S_1 . Oxidation of near-surface magnetite has resulted in a triangular network of hematite lamellae ("martite") that follow octahedral cleavage planes (Fig. 3.2d). A similar texture is locally produced by the partial oxidation of the *ülvöspinel* component in titanomagnetite. A number of polished thin sections were etched with fuming HBr, HCl and H₂SO₄ to test for twinning and growth zoning. However, no internal structures were observed in the samples tested.

Recrystallization during metamorphism has produced magnetically isotropic magnetite in the Osborne BIF units, unlike the unmetamorphosed Hamersley BIF, which has a magnetic anisotropy parallel to bedding (Logan, 1995).

3.32 Quartz

The grain size of co-existing quartz and magnetite is directly proportional, quartz ranging in diameter from about 0.10 mm to 2.50 mm. Quartz rich mesobands containing numerous small grains of dispersed magnetite are much finer-grained than quartz-only mesobands. Quartz forms subhedral aggregates moderately elongate in S_0/S_1 , or granoblastic grains with straight boundaries and 120° triple-junctions. Undulose extinction is common.

- Fig. 3.2** (a) Corundum porphyroblast partially retrogressed to muscovite. From laminated biotite-albite±corundum±sillimanite marker horizon @ HQ19, 209.0 m. Base of photo=22 mm, X-polars.
- 3.2 (b) Magnetite with skeletal Ti-exsolution textures, from within a corundum porphyroblast. From laminated biotite-albite±corundum±sillimanite marker horizon @ HQ170, 101.8 m. Base of photo=0.76 mm, reflected light.
- 3.2 (c) Magnetite grain-size variations between individual layers of delicately laminated, oxide facies BIF. From HQ170, 69.3 m. Base of photo=22 mm, plane polarized light.
- 3.2 (d) Incipient martitisation in magnetite. From oxidized BIF @ NQ183, 42.44 m. Base of photo=0.76 mm, reflected light.
- Davis et al. (1968) suggested that during the oxidation of magnetite, ferrous iron diffuses through the grain structure to internal surfaces where, by reaction with oxygen, it forms hematite on or between octahedral parting planes to produce the characteristic "trellis texture".



3.33 Apatite

It is rare for apatite to be absent from any thin section of cummingtonite schist, banded quartz-magnetite-cummingtonite schist or BIF. It is usually present as small disseminated grains, but also as virtually monomineralic micron-scale bands that probably represent an original sedimentary accumulation. The apatite forms six-sided crystals that are tabular in longitudinal section and lie in the plane of S_0/S_1 .

3.34 Plagioclase

Albite is the dominant silicate in some mesobands of minor BIF lenses. Thin bands of virtually pure albite are locally interbedded with mesobands of magnetite and quartz (Fig. 2.1d, Chapter 2).

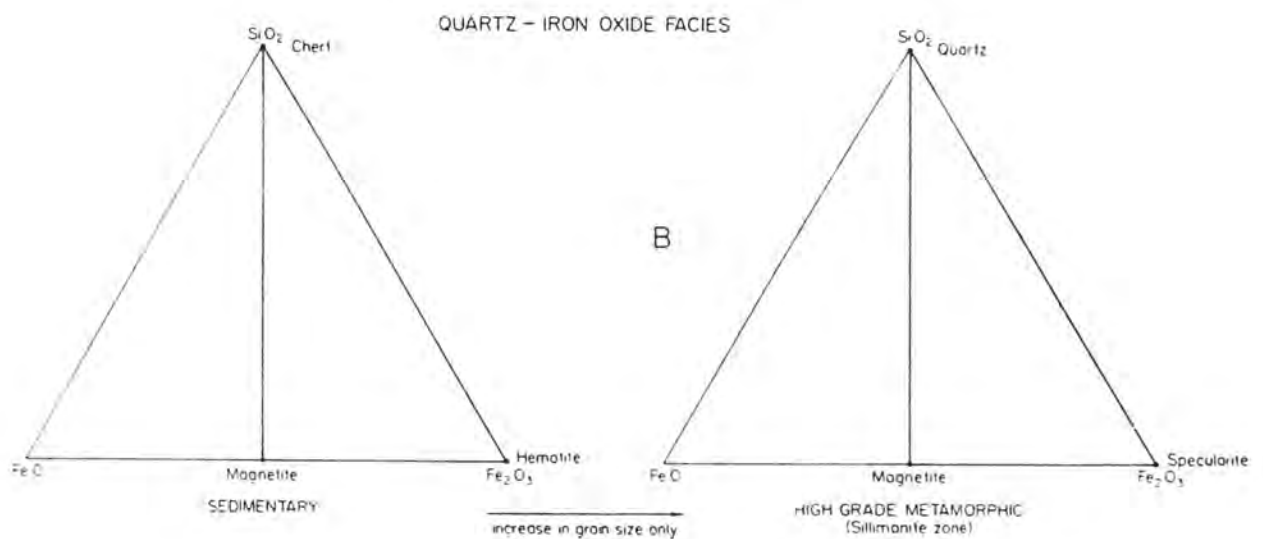


Fig. 3.3. Diagram illustrating the stability of oxide facies BIF, from diagenesis through to high grade (sillimanite zone) metamorphism. From Klein, 1973 (figure 5).

3.35 Petrogenesis

As described by James (1954), the primary oxide facies of sedimentary iron-formations consists of a finely laminated mixture of magnetite and/or hematite, chert, jasper or quartz, and possibly some hydrous iron silicates (Chapter 5). During metamorphism, recrystallization of the chert and iron oxides takes place, accompanied by an increase in grain size. According to Klein (1973), in BIFs of the chlorite zone, the average grain size of quartz is less than 0.10 mm, in the garnet to staurolite zones it ranges from 0.10 to 0.20 mm, and in the sillimanite zone it becomes greater than 0.20 mm. As previously noted, recrystallized quartz grains can reach 2.5 mm in the BIF units at Osborne, which is consistent with metamorphism under sillimanite zone conditions. Although such recrystallization textures are common, the simple chemical composition of oxide facies iron-formations means that reactions between constituent minerals are virtually absent (Fig. 3.3). The bulk-rock chemical composition of the Osborne BIF units is dominated by iron and silica, alumina and the alkalis (Na_2O and K_2O) generally constitute less than 0.5 wt.% (Table 2.3, Chapter 2). Thus, aluminium-bearing silicates are absent, apart from minor local concentrations of hornblende or albite. Such simple compositions are typical of sedimentary BIFs, and explain why the assemblage quartz-magnetite is persistent from diagenesis to upper granulite facies without reaction (e.g. Klein, 1973; Stanton, 1976; Floran and Papike, 1978; Hall, 1985; Zhu et al., 1988; Dymek and Klein, 1988; Laajoki and Devaraju, 1989). Hence the rhythmic banding of oxide facies BIF units at Osborne probably represents the original bedding of the primary iron-rich sediment. The primary sediment may have been deposited as a very fine-grained crystalline precipitate, along with minor cryptocrystalline fluorapatite (Chapter 5), with subsequent metamorphism simply recrystallizing and coarsening the original material.

Mesobands of albite, magnetite and quartz may have formed as a result of decomposition reactions involving riebeckite ($\text{Na}_2\text{Fe}_3^{2+}\text{Fe}_2^{3+}[\text{Si}_8\text{O}_{22}](\text{OH})_2$) and stilpnomelane, although the alumina budget has not been evaluated. The best known occurrences of riebeckite and the fibrous variety crocidolite are from the Hamersley Iron Formation, where they form conformable bands of diagenetic origin, interbedded with thin layers of chert, magnetite and stilpnomelane (Trendall and Blockley, 1970). Another simpler possibility is that albite-rich mesobands originally contained a component of volcanic ash. To the author's knowledge, albite-rich mesobands in metamorphosed BIFs have not previously been described.

3.4 Banded Iron Formation—Silicate Facies

Acicular cummingtonite forms mm-scale bands with quartz and magnetite in banded quartz-cummingtonite-magnetite schist, and with quartz and albite in cummingtonite schist. Massive cummingtonite also forms discontinuous metre-scale lenses within BIF units.

3.4.1 Banded Quartz-Cummingtonite-Magnetite Schist

The maximum extinction angle of cummingtonite in the banded quartz-cummingtonite-magnetite schist is about 21° in longitudinal section. Grain length varies from less than 0.01 mm to about 2 mm, with fibrous clusters of grains exceeding this. Cummingtonite fibres influence textural relationships in much the same way as fibrous sillimanite described by Vernon and Flood (1977). Grain boundaries of plagioclase and quartz meet [001] zone faces of cummingtonite at approximately 90° , or are attached to the corners of elongate cummingtonite grains (Fig. 3.4a).

3.42 Cummingtonite Schist

The average composition of cummingtonite from the cummingtonite schist is presented in Table 3.1, calculated on the basis of 23 oxygen atoms. The typical molecular formula is $(\text{Ca}_{0.04}\text{Mg}_{5.48}\text{Fe}_{1.48})[\text{Si}_{7.94}\text{Al}_{0.05}\text{O}_{22}]$, which has only minor replacement of Si by Al. The M4 site contains predominantly Mg and Fe cations, with minor Ca replacement. The A site is vacant. On the 15 cation basis, Si per formula unit averages 7.94. Members of the cummingtonite series with more than 70% $\text{Mg}_7\text{Si}_8\text{O}_{22}$ are called "magnesiocummingtonites", while "cummingtonite" is used to describe minerals containing between 30 and 70 per cent $\text{Fe}_7\text{Si}_8\text{O}_{22}$ (Deer et al., 1992). Assuming all iron present is Fe^{2+} , the ratio $\text{Fe}^{2+}/(\text{Fe}^{2+}+\text{Mg})$ averages 0.21. Cummingtonites in the cummingtonite schist are classified as "magnesiocummingtonites" as they contain 21% $\text{Fe}_7\text{Si}_8\text{O}_{22}$.

Parallel aggregates of prismatic cummingtonite crystals define S_0/S_1 . Amphiboles are the least plastic of all common rock forming minerals (Shelley, 1993), which explains why cummingtonite grains have been broken rather than folded around S_2 hinge lines (Fig. 3.4b).

3.43 Hornblende

Green hornblende of composition $(\text{Na}_{0.2}\text{Ca}_{1.81})(\text{Mg}_{3.28}\text{Fe}^{2+}_{1.96}\text{Al}_{0.67})[\text{Si}_6\text{Al}_8\text{O}_{22}]$ is a rare component of BIF units. Where encountered, hornblende forms minor, mm-scale, bedding-parallel layers.

3.44 Petrogenesis

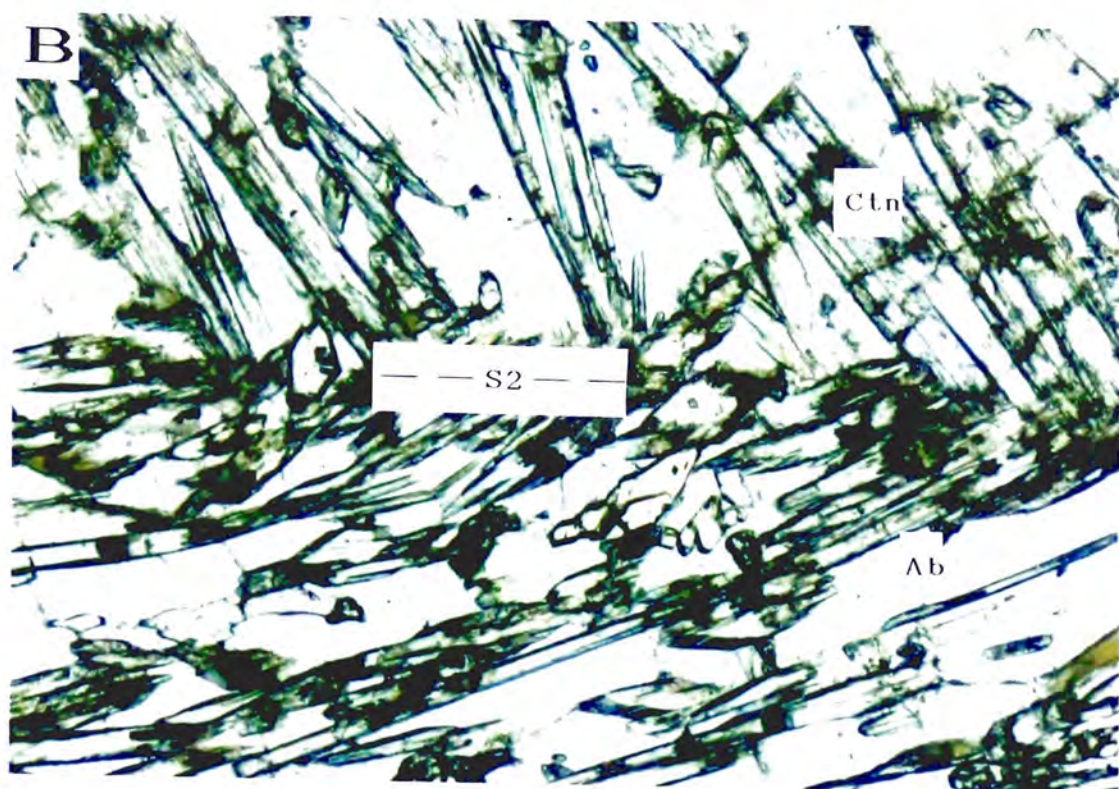
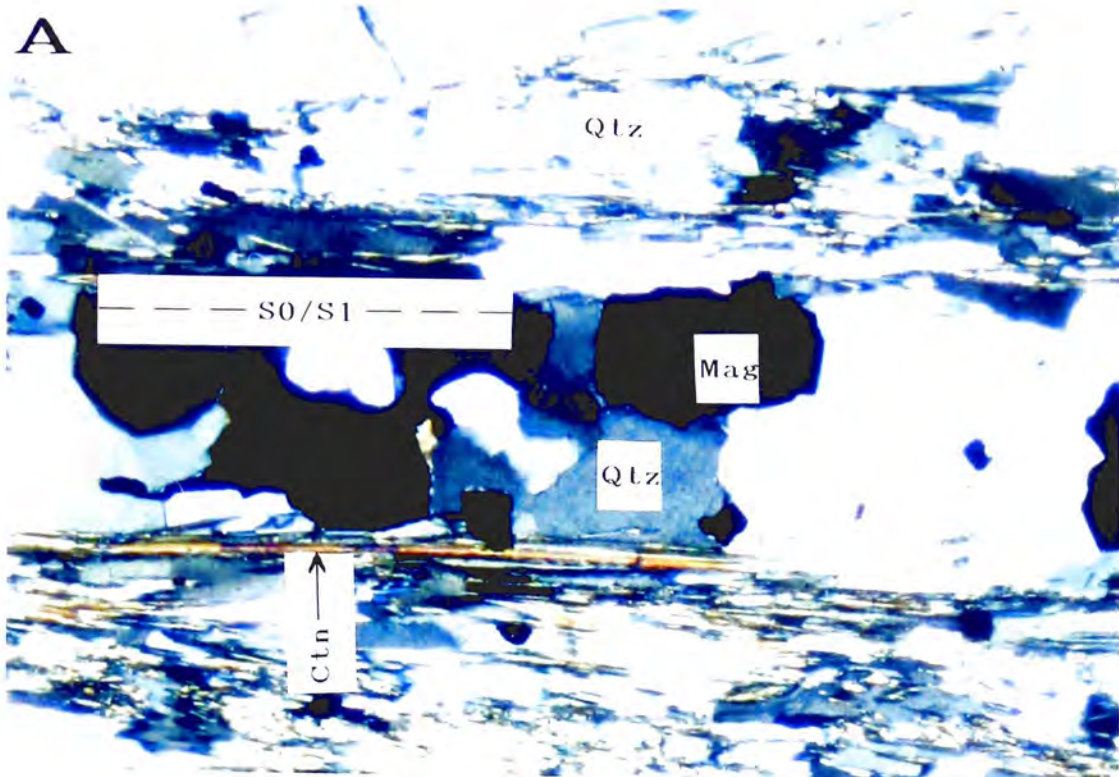
Although no direct evidence of precursor minerals or textures are available, it is probable that cummingtonite in the cummingtonite schist and banded quartz-cummingtonite-magnetite schist formed as a result of the metamorphism of a mixture of hydrous Fe-silicates and/or carbonates. The primary silicate facies iron-formation of James (1954) consists of a complex mixture of iron silicates (such as minnesotaite, stilpnomelane and greenalite), carbonates (siderite, calcite and members of the dolomite-ankerite series), quartz and magnetite (Chapter 5). Quartz-silicate minerals are commonly interbanded with oxide facies horizons.

Previous investigations of metamorphosed BIFs suggest that members of the cummingtonite-grunerite series can form via dehydration and decomposition reactions involving minnesotaite, stilpnomelane, minnesotaite + magnetite, minnesotaite + siderite + quartz, siderite + quartz + H₂O, ankerite + quartz + H₂O and greenalite + quartz (e.g. Kranck, 1961; Chakraborty and Taron, 1968; French, 1968; Klein, 1973; Floran and Papike, 1978; Gole, 1979; Klein, 1982; Melnik, 1982; Zhu et al., 1988).

The first occurrence of grunerite in BIF of northern Michigan was correlated by James (1955) with the garnet and staurolite zones of pelitic schists, implying pressures between 2 and 5 kbar and a temperature range of 450 to 500° C (Winkler, 1979). Klein (1978) noted the first occurrence of Mg-Fe clinoamphiboles at the onset of the biotite zone for iron-formations in the south-central part of the Labrador Trough. Chakraborty and Taron (1968) inferred a temperature of metamorphism of 850° ± 50° for quartz-cummingtonite-grunerite-magnetite BIF from Orissa, India. The transition from the stilpnomelane-minnesotatite zone to the grunerite zone, inferred by Haase (1981) in the Negaunee Iron Formation of northern Michigan, is close to the biotite isograd as mapped by James (1955).

Thus it appears that Mg-Fe clinoamphiboles in metamorphosed BIFs are stable from the biotite isograd, through to the garnet and staurolite isograds of pelitic schists. The relative stability fields of various minerals found in metamorphosed iron-formations are illustrated in figure 3.5.

- Fig. 3.4 (a)** Finely interbedded cummingtonite-quartz and magnetite-quartz layers from the banded quartz-cummingtonite-magnetite schist @ HQ92, 124.4 m. Note how the cummingtonite influences the shapes of adjacent quartz grains. Base of photo=1.52 mm, X-polars.
- 3.4 (b)** Cummingtonites broken around S_2 hinge line. From the cummingtonite schist @ NQ173, 226.7 m. Base of photo=1.52 mm, plane polarized light.



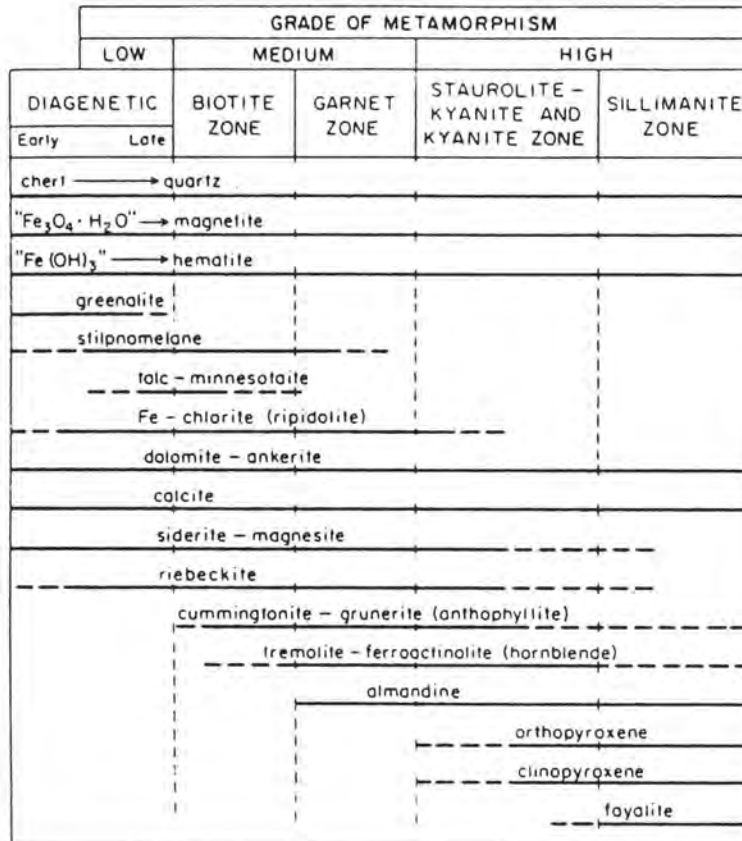


Fig. 3.5. Relative stability fields of minerals in metamorphosed BIF, as a function of metamorphic zones. From Klein, 1982 (figure 45).

Chapter 4

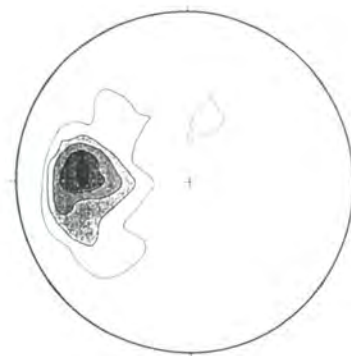
Structural Geology of the Osborne Deposit

Introduction

The Osborne mine sequence has undergone four phases of folding, an episode of brecciation and alteration, retrograde shearing, jointing and veining. I have tentatively correlated various structural features with previously described deformation and metamorphic events in the Cloncurry-Selwyn zone, mainly after Beardsmore et al. (1988) and Williams and Blake (1993).

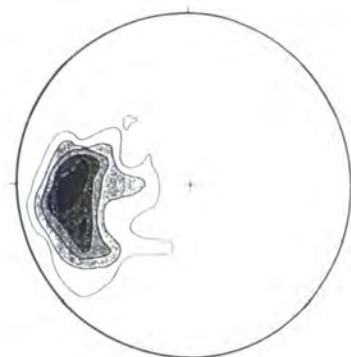
The mine sequence is covered by up to 35 m of horizontal Mesozoic cover; so measurement of geological structures relies on the use of oriented diamond drill core. The orientation is indicated by a line drawn along what was the bottom side of the core when it was in an inclined drill hole. The attitude of planar elements (e.g. S_0 , S_1) can be calculated using a stereonet. The calculation is a two-stage process. First, the attitude of the plane is measured with respect to the long axis of the core as if the core were vertical. The core axis is then rotated to its original position, using the bearing and plunge of the drill hole. Unless otherwise stated, the structures referred to in this thesis are related to the Osborne mine grid (Osborne grid north = 312.5°MN , 318.5°AMGN).

The structural analysis of the deposit was hampered by the following problems. Shear zones are usually fractured and broken, so that reliable measurement of shear surfaces is generally not possible; deeper holes are usually vertical or near-vertical and are not oriented; folds with wave lengths greater than a few 10's of centimetres are difficult if not impossible to detect at core scale; and the east-west orientation of all but a few angled drill holes results in poor representation of any east-west striking features. Oriented drill core is unsuitable for measuring the plunge and bearing of lineations (e.g. in amphibolites) and is also slower and less accurate than direct measurement of outcrop. Despite these problems, the large number of drill holes (over 400 to date) has enabled sufficient collection of data to construct a three dimensional diagram (Fig. 4.1) and a series of cross-sections through the deposit (Appendix 1). A more complete structural picture of Osborne will emerge when three dimensional exposures are available from mining development, scheduled to begin by the end of 1994.



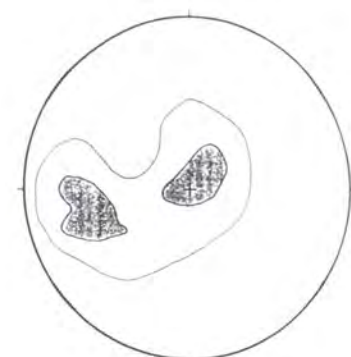
50

Av Orientation: 107°/21°/E



51

Av Orientation: 102°/15°/E



Joints

Av Orientation: 1159°/34°/E

Av Orientation: 121°/12°/E

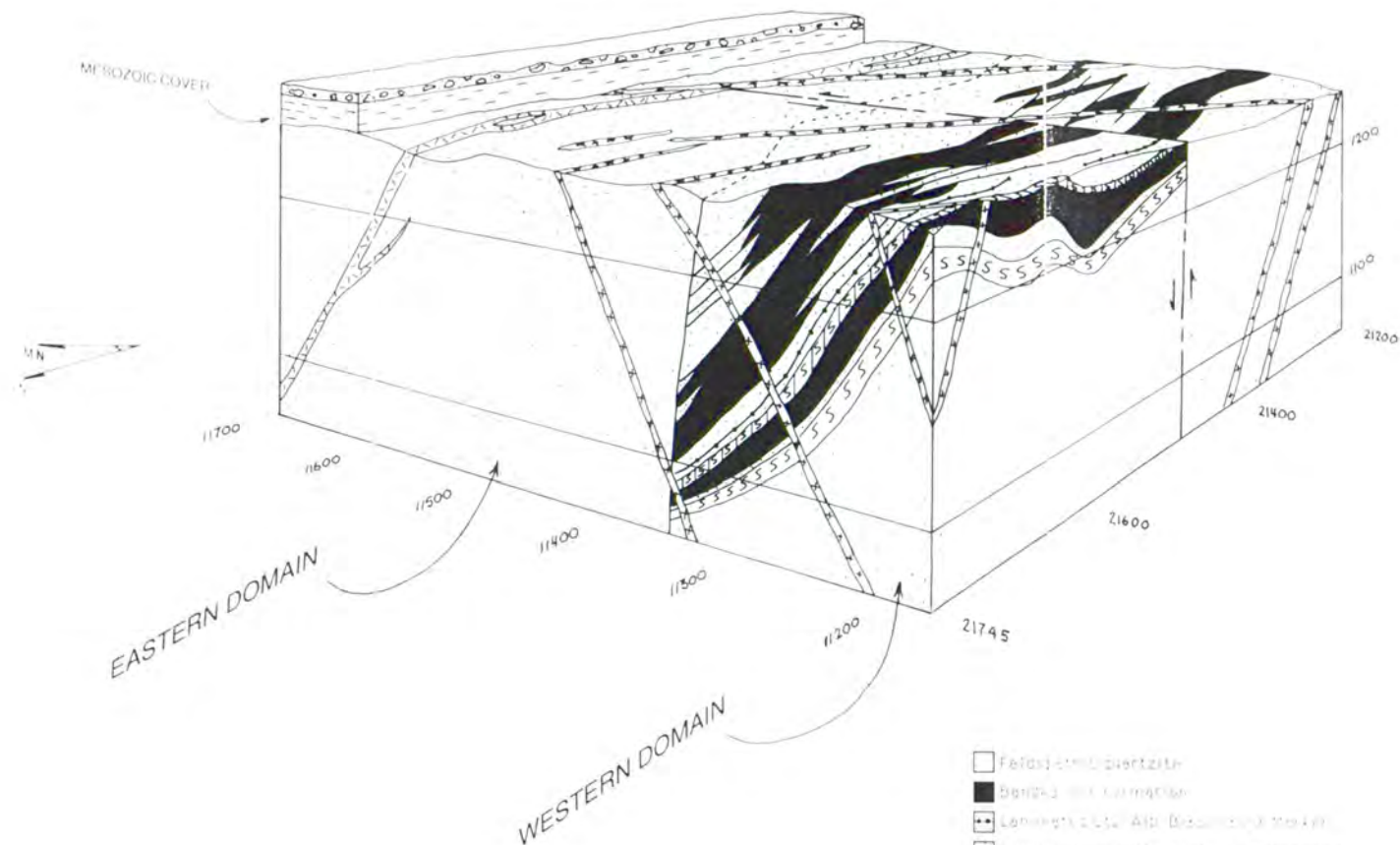


Fig. 4.1. Block diagram of the Osborne deposit, showing major rock types and structural elements. The diagram is drawn in two point perspective from the cross sections in Appendix 1.

4.1 Previous Structural Interpretations

Evidence presented in this investigation contrasts with previous structural interpretations by company geologists and consultancy firms, made mostly without the benefit of the large number of drill holes available for this study. Davidson et al. (1989) interpreted the Upper and Lower BIF units as limbs of a synformal fold. However there is no stratigraphic repetition on either side of the supposed hinge surface, and extensive drilling since their study has failed to find any evidence of a fold closure (Appendix 1).

Because lithological contacts and S_0 is nearly everywhere virtually parallel to a pervasive S_1 (Fig. 4.1), it has been suggested (e.g. Adshead, 1995) that compositional layering in drill core formed as a result of transposition, and does not represent original bedding. However, parallelism of foliation and layering alone is not diagnostic of transposition. Evidence against the transposition hypothesis includes the lack of repetition or segmentation of marker horizons, the persistence of folded layering (S_0) with locally developed S_1 axial planar foliation, and the gross orientation of the Osborne mine sequence, which is approximately parallel to the mean $183^\circ/43^\circ/\text{E}$ orientation of bedding (Fig. 4.1). In transposed areas elsewhere, the predominant orientation of bedding is approximately parallel to the axial planar schistosity and inclined to the enveloping surface of the various beds (Fig. 4.2).

Early cross sections constructed by Placer geologists show the upper ironstone as a single, variably dipping body that chaotically branches, lenses and anastomoses around enclaves of plagioclase-quartzite. Cross sections presented in this thesis (Appendix 1) show the upper ironstone as a bedding parallel unit that is cut and displaced by numerous retrograde shear zones that were not drawn on the earlier sections. The earlier interpretation may have contributed to the belief of many company geologists that BIFs at Osborne represents a granite-sourced metasomatic accumulation of magnetite.

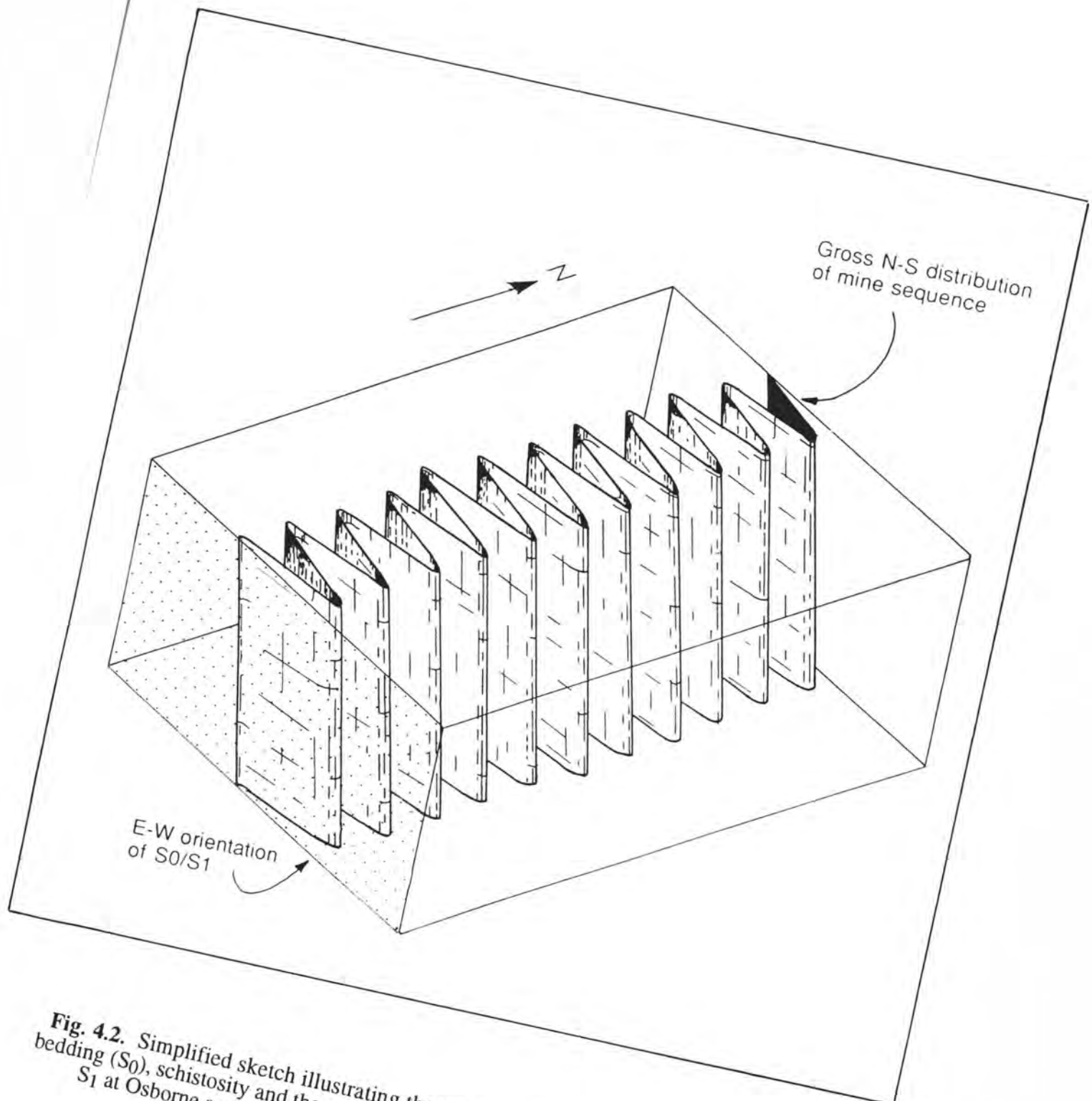


Fig. 4.2. Simplified sketch illustrating the relationship between transposed bedding (S₀), schistosity and the enveloping surface in a hypothetical area. Bedding and S₁ at Osborne are parallel to the gross distribution of the mine sequence units.

A north-south trending discontinuity that bisects the deposit into eastern and western domains was recognized by company geologists and termed the "Awesome Fault". Each domain is characterized by distinctive lithologies and styles of alteration. "Fault" may be a misnomer, as it has yet to be intersected by drilling. The "Awesome Fault" is cut by, and hence predates, alteration, mineralisation, pegmatites, amphibolites, and possibly regional metamorphism, as there is no change in metamorphic grade across the discontinuity.

The origin of the BIF units and associated Cu-Au mineralisation has been the subject of controversy since the Osborne orebody was discovered. One school of thought holds that the mineralisation and BIFs are syn-sedimentary (e.g. Davidson et al., 1989), whereas others believe that both mineralisation and BIFs are related to metasomatic alteration and emplacement of the Williams Batholith (e.g. Adshead, 1995). Evidence presented in this thesis indicates that the BIF units are the deformed and metamorphosed equivalents of sedimentary iron formations, that have subsequently undergone epigenetic alteration and Cu-Au mineralisation (Chapter 7).

4.2 Bedding (S_0)

The average orientation of S_0 is $183^\circ/43^\circ/\text{E}$ (Fig. 4.1). S_0 is characterized by compositional layering—in BIFs by alternating centimetre-, millimetre- and micron-scale laminations rich in quartz or magnetite, in layered biotite-albite quartzites by interbedded quartzofeldspathic layers and thin (from 1 to 10 cm) micaceous layers, and in garnet-cordierite-sillimanite gneiss by alternating layers of relatively mafic or felsic material.

4.3 Structures Related to Ductile Deformation

Small structures present in drill core have been divided into three groups (Fig. 4.3). Recognition of each group depends primarily on the relationship between foliation and S_0 . The shapes of folds in profile are of limited use in distinguishing between fold groups, as variations in fold shapes primarily reflect contrasts in composition, layer thickness and ductility contrasts between layers during deformation. All phases of ductile deformation pre-date alteration and economic mineralisation. Table 4.1 summarizes the deformation history of the Osborne deposit. Deformation structures in the mine sequence are tentatively correlated with regional structures, on the basis of fold- and fault-styles, timing, alteration assemblages and metamorphic grade.

4.31 Inclusion Fabrics Related to D_x

The earliest recognizable deformation event is labelled " D_x " in view of its uncertain age and extent. D_x locally produced straight inclusion trails (S_x) in some porphyroblasts of garnet, cordierite and tourmaline (Fig. 4.4a). S_x is sharply discordant with the external domainal schistosity (S_1), and consist of fine grains of preferentially aligned biotite, quartz and plagioclase.

4.32 Folds Related to D_1

D_1 produced a pervasive bedding parallel schistosity (S_1) that is the dominant tectonic fabric in the Osborne host rock sequence. D_1 is labelled to conform with the nomenclature of other workers (e.g. Williams and Blake, 1993) who described a regional bedding-parallel schistosity (S_1) that developed in the Cloncurry-Selwyn zone during the 1620-1550 Ma Isan Orogeny.

Borradaile et al. (1982) defined three types of schistosity: (a) *Domainal schistosity*, characterized by domains of sub parallel layer silicates that anastomose around lenticular grains composed of other minerals; (b) *Continuous schistosity Type 1*, characterized by a strong preferred orientation of mica grains and no mesoscopic lenticular microlithons (microlithons may be visible under the microscope); (c) *Continuous schistosity Type 2*, characterized by layer silicates and flattened/stretched grains that are distributed evenly throughout the rock.

Deformation Event	Resulting fabric	Tectonic Surface	Average Orientation	Inferred Age (Ma)
Basin formation, diagenesis, extension and dyke emplacement	Bedding and banding	S0	183°/43°/E	1870-1760 (Blake and Stewart, 1992)
			Amphibolite Dykes 195°/60°/E	
Dx	Straight inclusion trails in porphyroblasts	Sx	Approx. 90° to S1	
D1 (ductile compression) <i>Peak metamorphism</i> 749°C, 5.1 kbar	Penetrative bedding parallel foliation, Group 1 folds, amphibolite lineation	S1 L1	169°/50°/E	Isan Orogeny 1595 (Perkins 1994)
D2 (ductile compression)	Folding of S0/S1 to produce rounded symmetrical Group 2 folds			Isan Orogeny 1550 (Page and Bell, 1986)
D3 (ductile compression)	Folding of S0/S1 to produce Group 3 kink folds with axial planar foliation	S2	229°/70-80°/NW-SE	
Granite intrusion	Pegmatite swarms, brecciation, metasomatic alteration and mineralisation		Breccia Lenses sub-parallel to S0/S1 Pegmatite Sheets 033°/70°/W	1500 (Blake and Stewart, 1992)
Shearing <i>Greenschist Facies</i>	Retrograde Shear Zones (mostly normal)		Shears sub-parallel to S0/S1	
Unloading	Conjugate joint set Veins	J1	169°/54°/E	
		J2	318°/14°/SW	
		V1	151°/44°/NE	

Table 4.1. Structural and metamorphic history of the Osborne mine.

S_1 is defined in the Osborne host rock sequence by: (a) Domainal schistosity in the garnet-cordierite-sillimanite gneiss, with biotite, sillimanite and cummingtonite wrapping around lenticular porphyroblasts of cordierite and garnet; (b) Continuous schistosity type 1 in plagioclase quartzites and cummingtonite bearing units, defined by the alignment of biotite, sillimanite and cummingtonite, and by a moderate elongation of quartz and feldspar (Fig. 4.4b); (c) Continuous schistosity type 2 in BIF units, defined by moderately stretched and flattened grains of quartz and magnetite.

The mean orientation of S_1 ($169^\circ/50^\circ/E$, Fig. 4.1) is parallel to the axial surfaces of small, locally developed, asymmetrical Group 1 folds that fold bedding (Fig. 4.3a). Changes in the thickness of S_0 around Group 1 folds (Fig. 4.3a) suggests a deformation mechanism involving plastic flow. D_1 was accompanied by peak metamorphic conditions (5.1 kbar, $746^\circ C$, Chapter 3) and growth of metamorphic mineral assemblages defining S_1 .

The large first order folds responsible for S_1 at Osborne are not observable at drill-core scale. However, elsewhere in the Cloncurry-Selwyn zone, D_1 produced crustal scale, tight to isoclinal nappes and thrusts, and a penetrative S_1 that is almost everywhere parallel to S_0 (Loosveld, 1987, 1992; Williams and Blake, 1993).

Amphibolites have a lineation (L_1) defined by the dimensional preferred orientation of green and brown hornblende (Fig. 4.4c). Although L_1 appears to lie in the plane of S_1 , its orientation could not be measured due to the difficulty in accurately measuring linear fabrics in drill core.

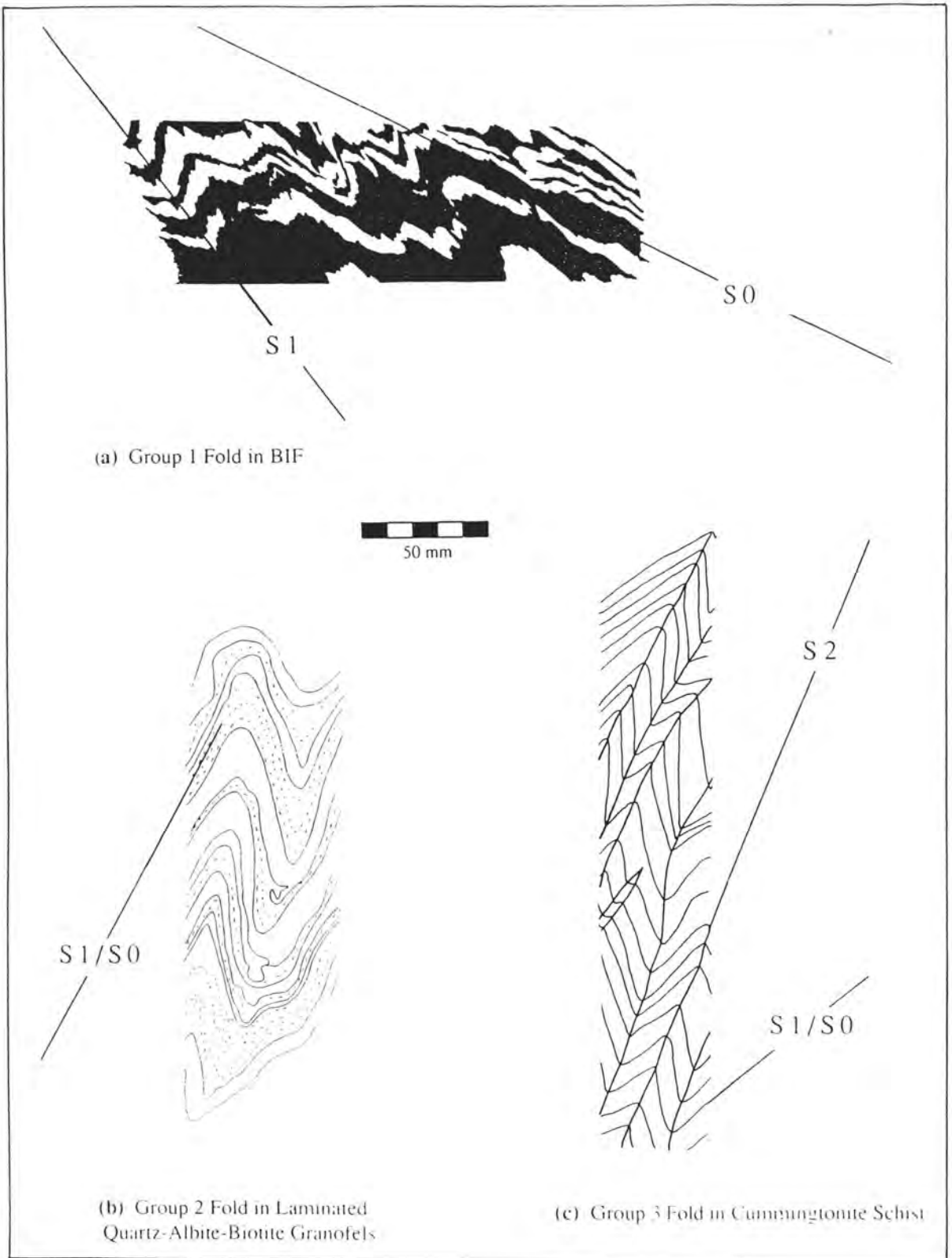
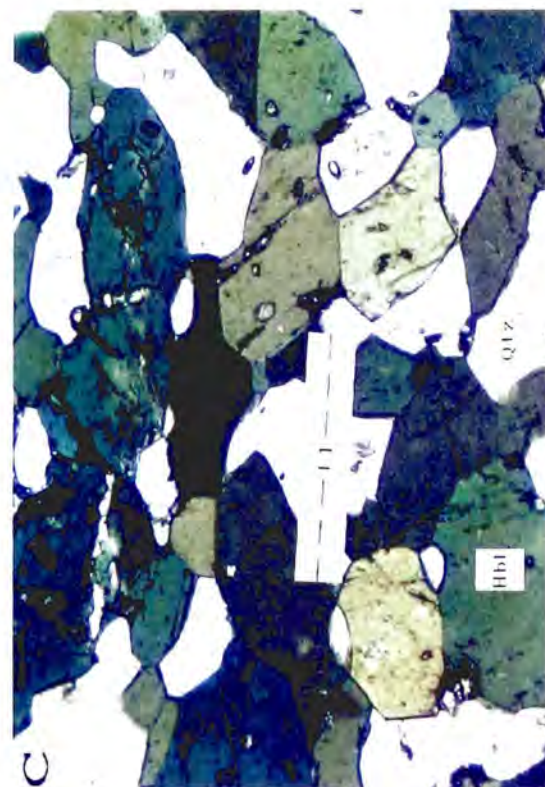
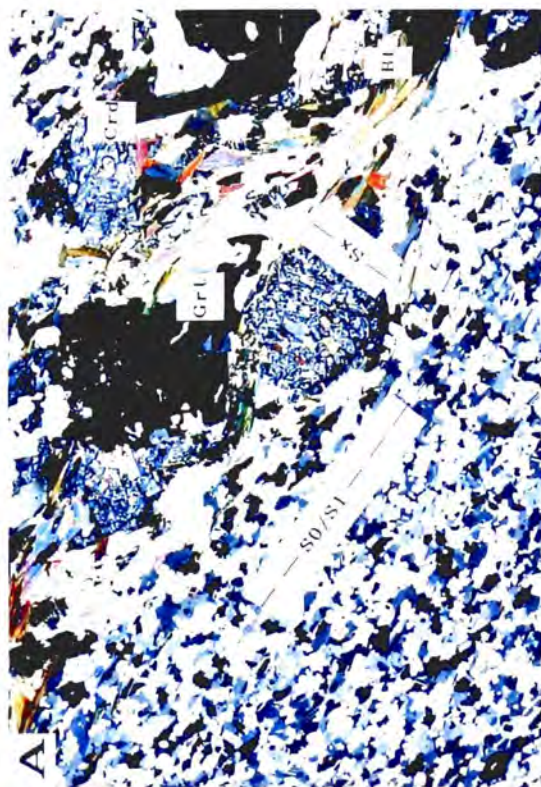


Fig. 4.3. Profile planes of small folds that formed as a result of D_1 (Group 1), D_2 (Group 2) and D_3 (Group 3).

- Fig. 4.4 (a)** Rarely preserved S_x inclusion fabric in poikiloblastic cordierite. S_x lies at approximately 90° to the external bedding-parallel schistosity (S_1). From garnet-cordierite-sillimanite gneiss @ NQ329, 299.4 m. Base of photo=22 mm, X-polars.
- 4.4 (b)** S_1 in layered biotite-albite-quartzite, defined by the preferred orientation of biotite and the moderate elongation of quartz and feldspar. From NQ81 @ 254.8 m. Base of photo=12mm, plane polarized light.
- 4.4 (c)** Lineation (L_1) in amphibolite, defined by the preferred orientation of hornblende and quartz. From NQ 314 @ 488.0 m. Base of photo=1.52 mm, plane polarized light.
- 4.4 (d)** S_2 axial surface in Group 3 kink band. From cummingtonite schist @ NQ173 @ 226.7 m. Base of photo=22 mm, X-polars.



4.33 Folds Related to D₂

Minor Group 2 folds (Fig. 4.3b) that refold S₀ and S₁ resulted from compression during D₂ (Table 4.1). Group 2 folds are commonly rounded and symmetrical in profile, with only slight changes in layer thickness around closures, suggesting a folding mechanism that involved flexural slip due to ductility contrast between micaceous and quartzofeldspathic layers. It is impossible to correlate deformation and metamorphism during D₂, as an axial surface foliation is absent or only very poorly developed in Group 2 folds (Fig. 4.3b). Elsewhere in the Cloncurry-Selwyn zone, D₂ produced upright to steeply inclined, generally tight, polyharmonic folds with amplitudes up to at least several kilometres (Williams and Blake, 1993).

4.34 Folds Related to D₃

D₃ produced sets of near parallel, curvi-planar, Group 3 kink bands (Fig. 4.3c). In profile, the kink bands have an average interlimb angle of 62° and are symmetrical (±5°) around S₂ axial surfaces. Study of thin sections show that S₂ kink boundaries are narrow regions of acute flexure of S₀/S₁, where cummingtonite grains have snapped, separating planar or near planar segments of foliation on opposite sides of the boundary (Fig. 4.4d). The kink bands die out along their length by tapering to a point as their amplitudes diminish. Group 3 folds are restricted to well foliated cummingtonite schists and highly micaceous lenses, as a pre-existing well developed foliation is essential for the formation of kink folds.

S₂ kink boundaries strike between 222° and 233° and dip steeply to the NW or SE. However, because of a lack of oriented drill core, only seven measurements of S₂ were made, mostly from one drill hole. D₃ (mine sequence) probably correlates with post-D₃ (regional) deformation, which produced localized chevron folds and kink banding elsewhere in the Cloncurry-Selwyn zone (Beardsmore et al., 1988; Williams and Blake, 1993).

- Fig. 4.5 (a)** Gradation from unbrecciated, barren BIF (A), to brecciated BIF with minor pyrite and chalcopyrite (B), to massive silicic alteration ("silica flooding") with abundant pyrite and chalcopyrite (C). From BIF @ NQ315, 625.3–631.7 m, scale bar=10 cm.
- 4.5 (b)** Close up view of banded and rotated clasts from brecciated BIF in zone (B), Fig. 4.5a. Scale bar=5 cm.



4.4 Structures Related to Brittle-Ductile Deformation

4.41 Brecciation and Economic Mineralisation

Cu—Au minerals in the Western Domain are restricted to grossly conformable lenses of brecciated BIF. The highest grade ore-bearing breccias occur in the upper BIF, especially in the vicinity of lithologic contacts. Smaller amounts of brecciation and Au-Cu minerals occur in the lower BIF, and iron-poor units are generally barren (Appendix 1).

The main alteration style in the Western Domain is termed "silica flooding" by Placer geologists, and is characterized by zones of replacement by massive grey or pale grey quartz ("silicic alteration"), coarse-grained magnetite and very fine-grained disseminated magnetite, pyrite and chalcopyrite (zone C, Fig. 4.5a). A second style of alteration is characterized by rotated clasts of BIF in a matrix of coarse-grained, granular to massive magnetite, pyrite and chalcopyrite (zone B, Fig. 4.5a). The two styles of alteration are usually closely associated, suggesting that they are genetically related. Both styles transgress and hence post date bedding, amphibolites, pegmatites and all recognized deformation fabrics (S_x , S_1 , S_2) in metasedimentary units.

Epigenetic sulphide grains within ore-bearing breccias are commonly weakly deformed sub parallel to S_0/S_1 , suggesting that their formation was simultaneous with brecciation. Elongate clasts of plagioclase-quartzite in a matrix of secondary magnetite without sulphides have also been observed.

4.42 Shear Zones

Narrow retrograde shear zones, oriented approximately $178^\circ/50^\circ/E$, are sub-parallel to lithological contacts, S_0 and S_1 (Appendix 1). Characteristic features include slickenlines, retrograde chlorite and "sericite", and mesoscopic and microscopic areas of high strain that anastomose around relatively undeformed fragments of wall rock. Shear sense indicators (porphyroclast tails, folded layering and deformed plagioclase) are commonly unusable, as the shear zones are usually fractured and cannot be reliably oriented.

Movement sense was mostly determined using the relative displacement of shear bounded BIF lenses, indicating normal movement along the majority of shears (Appendix 1). The net movement was non-rotational, as S_0 and S_1 maintain constant orientation across shear zones.

Thin section studies reveal that areas of high strain consist of variably retrogressed biotite (Fig. 4.6a) that wraps around the grain boundaries of flattened and deformed quartz, plagioclase and microscopic lenses of crush breccia, with areas of low strain preserved as granofelsic enclaves of wall rock.

Shearing has resulted in bent growth twins, deformation twinning, pronounced undulose extinction, and micro-faulting and displacement of individual plagioclase grains (Figs 4.6b, 4.6c). Microscopic shear sense is dependant on the original orientation of grains relative to the shear surface, and may be sympathetic or antithetic to the overall sense of shear.

Two phases of shearing and faulting are recognized. The first and most widely developed phase took place under greenschist facies conditions, resulting in a dominantly normal sense of movement, ductile/brittle deformation features (sigmoidal foliation, S-C planes), and the partial breakdown of biotite to chlorite and "sericite". The second phase involved localized brittle fracture of earlier shear surfaces, providing openings for fluid flow and the subsequent precipitation of carbonates, minor sulphides and apatite, and oxidation of magnetite to hematite (Fig. 4.6d). Both stages postdate alteration and the formation of Cu-Au bearing sulphides, and strongly influence the distribution of ore bodies. Recognition and careful mapping of shear zones will be essential for optimum ore recovery, once mining commences.

4.5 Structures Related to Brittle Deformation

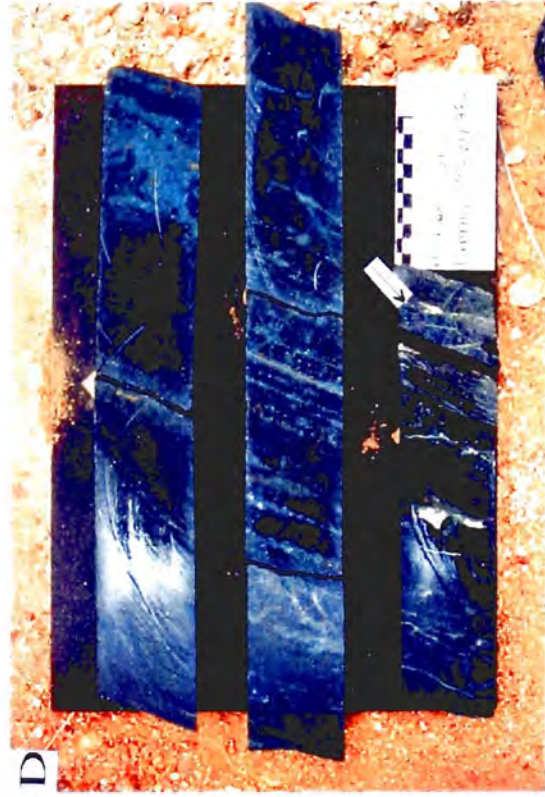
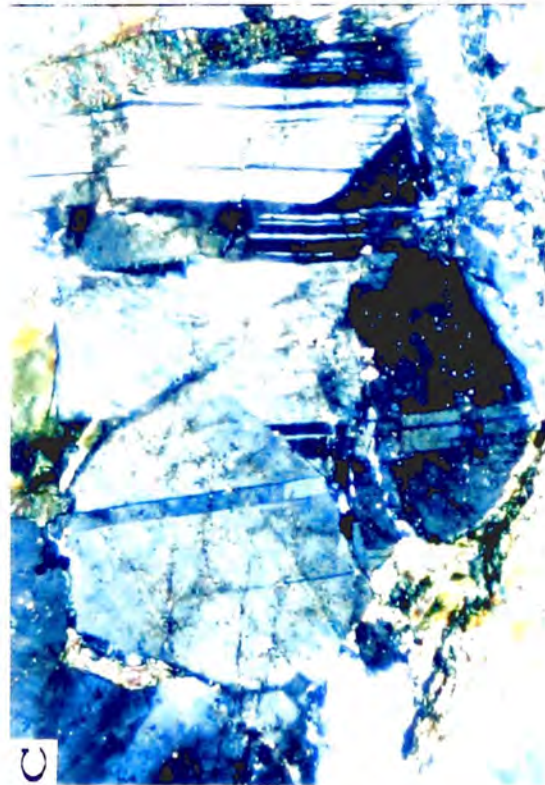
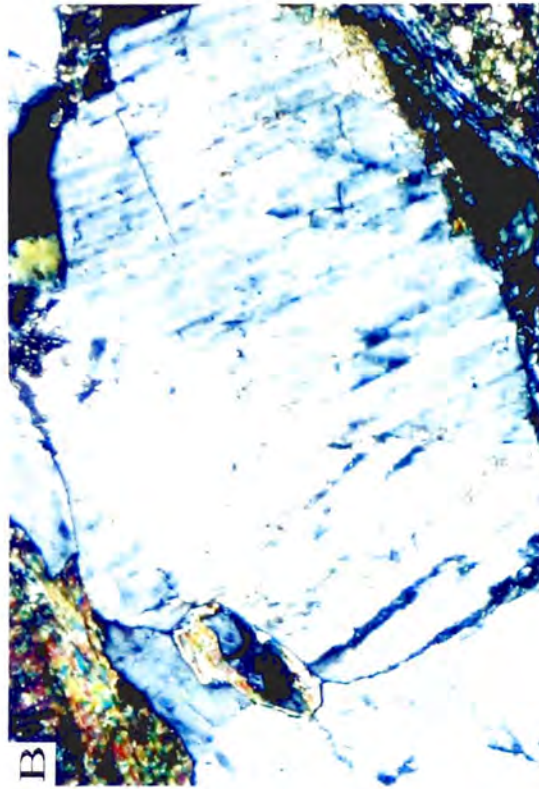
4.51 Joints

Two sets of joints, labelled J_1 and J_2 , form a joint system with an average dihedral angle of 65° (Fig. 4.1). The dominant set, J_1 , is oriented $169^\circ/54^\circ/\text{E}$. Less numerous J_2 joints strike $318^\circ/14^\circ/\text{SW}$. Joints are most common in and around BIF units, where the joint frequency ranges from 0 to 6 per metre.

4.52 Veins

J_1 joints are commonly coated with carbonate (calcite, dolomite, siderite) and uneconomic amounts of sulphide (pyrite, chalcopyrite) vein minerals. Taken together, barren and vein coated J_1 joints far outnumber J_2 joints. The virtual absence of vein minerals in J_2 joints indicates either that J_2 post-dates J_1 , or that the stress regime kept the J_2 joint set closed to vein forming fluid circulation. Centimetre-scale alteration haloes around veins usually consist of hematite and red apatite in BIFs and "sericite" and red apatite in quartzofeldspathic units. Examination of alteration around veins in thin section shows that "sericite" forms delicately radiating rosettes that must post-date deformation.

- Fig. 4.6** (a) Biotite partially retrogressed to chlorite, from within a retrograde shear zone. Base of photo=1.52 mm, plane polarized light.
- 4.6 (b) Glide surface in plagioclase grain, from within a retrograde shear zone. Base of photo=1.52 mm, X-polars.
- 4.6 (c) Highly deformed plagioclase grain, from within a retrograde shear zone. Base of photo=1.52 mm, X-polars.
- 4.6 (d) Hematite, red apatite and carbonate around fractured shear zone (arrow) in BIF. From HQ62 @ 211.3–212.48 m, scale bar=10 cm.



Chapter 5

An Overview of Ironstones and Precambrian Iron-Formations

Introduction

This chapter summarizes the characteristics, nomenclature, origins, and distribution of Au-Cu sulphides in both metasedimentary and metasomatic iron rich bodies, from Broken Hill, Tennant Creek, South Australia, Western Australia, the United States, Canada, Zimbabwe, Sweden, Chile and the former USSR.

5.1 Definition of Terms

The terms *iron formation*, *ironstone* and *banded iron formation* are widely used by geologists, though not always consistently. James (1954) defined *iron formation* as "a chemical sediment, typically thin-bedded or laminated, containing 15% or more iron of sedimentary origin, commonly but not necessarily containing layers of chert". *Banded iron-formation* (BIF) has a more restricted meaning than iron-formation. It is generally accepted that the term refers to "thinly layered or laminated rock in which chert (or its metamorphic equivalent) alternates with layers that are composed mainly of iron minerals" (James, 1983). The iron minerals may include magnetite, hematite, silicates or carbonates, usually intergrown to some degree with chert or quartz. Both terms are used in this thesis and include rocks poor in iron oxides, such as siderite-rich and iron silicate-rich metasediments. Although many geologists consider that the term *ironstone* refers to a ferruginous gossan, in this thesis and in the Cloncurry-Selwyn zone in general, *ironstone* is used to describe any massive, brecciated or banded iron-rich rock not of sedimentary origin.

5.2 Classification of Banded Iron Formations (BIFs)

Two general schemes of classification are used to subdivide BIFs: (1) a classification using the dominant iron mineral present, based on the facies concept of James (1954); or (2) a classification first proposed by Gross (1965), based on geologic association.

5.21 Classification According to Facies

Early workers (e.g. Harder, 1919; Teodorovich, 1947) recognized that, due to its divalence, iron is capable of forming a variety of minerals in response to particular environmental conditions. The chemical relationships between these iron-bearing assemblages (Fig. 5.1) was assessed by Krumbein and Garrels (1952), and led James (1954) to classify iron-formations by depositional-environmental facies: oxide, silicate, carbonate and sulphide. James recognized that relatively high-energy, shallow-water environments are strongly oxidizing and are characterized by hematite stability and magnetite metastability, whereas low-energy, deep-water environments are poorly oxygenated and characterized by siderite and pyrite stability (Fig. 5.2).

OXIDE FACIES

The *magnetite subfacies* is the most common type of BIF, and consists of cm-scale ("mesoband") to micron-scale ("microband") laminations of magnetite and quartz, chert or jasper. Trendall (1983) demonstrated that microbands in the Brockman Iron-formation are laterally continuous for many kilometres. Iron silicates, siderite and riebeckite are common constituents of oxide facies BIFs, either as dispersed grains or as discrete layers (James, 1992). The minerals and association of the magnetite subfacies suggests weakly oxidizing to moderately reducing conditions.

The *hematite subfacies* consists of wavy to irregularly banded layers of hematite and quartz, chert or jasper. The layers are commonly oolitic, with transitions into contemporaneous breccia or even iron-rich conglomerate—all features indicative of accumulation in a shallow-water, high-energy environment. Diagenetic magnetite and carbonate minerals are common in small amounts (James, 1992).

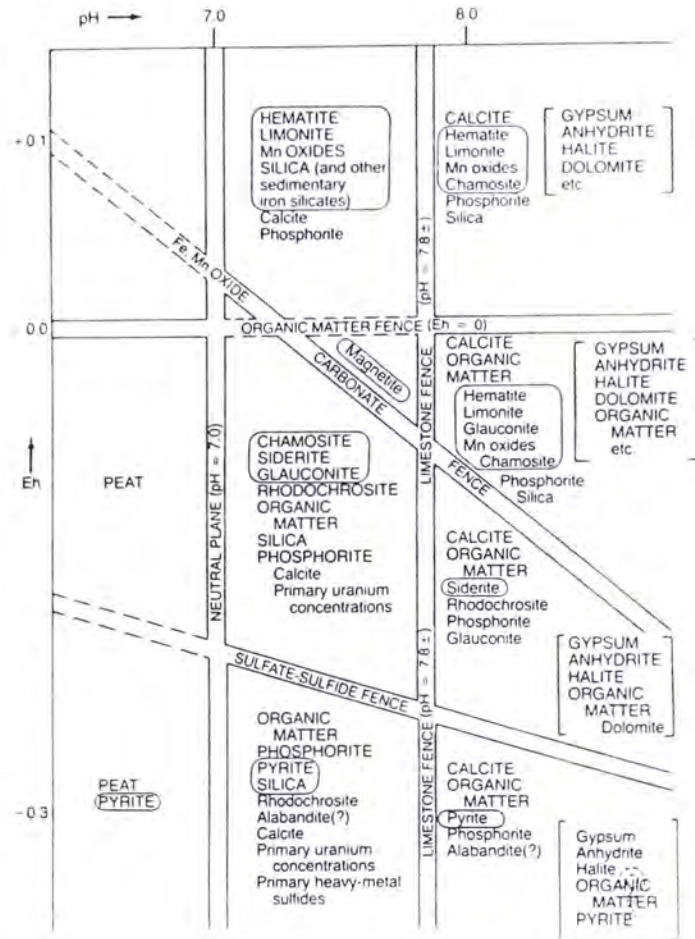


Fig. 5.1. Fence diagram showing Eh-pH stability fields for sediment formation under normal seawater conditions (from Krumbein and Garrels, 1952).

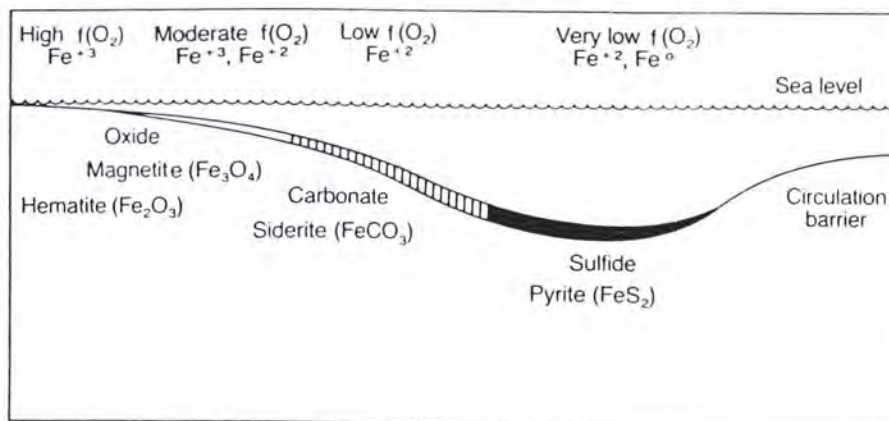


Fig. 5.2. Depositional zones of iron-rich precipitates in a hypothetical basin. From James, 1954 (figure 3).

SILICATE FACIES

Silicate facies iron-formations are characterized by abundant hydrous ferrous silicates, such as minnesotatite, greenalite and stilpnomelane, with smaller amounts of chlorite, chamosite, magnetite and carbonate minerals (Guilbert and Park, 1986). According to James (1992), most silicate-rich horizons probably reflect the introduction of fine volcanic ash from a distant source.

CARBONATE FACIES

Where uncontaminated by detrital grains, the *carbonate facies* consists almost entirely of interlayered siderite or iron-rich ankerite, and chert. Interbedded transitions from carbonate iron-formation into oxide facies and/or silicate facies iron-formation are recognized in many districts (e.g. James et al., 1968; Beukes, 1973). The carbonate facies formed in environments in which the oxygen concentration was high enough to destroy most organic material, but not high enough to permit ferric compounds to form (Guilbert and Park, 1986).

SULPHIDE FACIES

Sulphide facies rocks are typically black, carbonaceous, fine-grained pyrite-bearing slates or shales that occur either alone or as minor constituents of oxide facies BIFs. The sulphide facies formed under stagnant, oxygen-poor conditions, and is the least abundant facies-type (James, 1992).

5.22 Classification According to Geological Association

The classification of BIFs by geological association was first introduced by Gross (1965), who recognized two principal types of iron-formation, Lake Superior and Algoman, based on the characteristics of their depositional basins and their associated rock-types. In contrast to the facies scheme of classification, which is applicable from unit scale down to the scale of individual microbands, the type classification applies to the stratigraphic unit as a whole.

Oxide, silicate and carbonate facies are common to both Lake Superior- and Algoma-type BIFs (Gross, 1980). The Proterozoic Lake Superior-type iron-formations were deposited with quartzite, black shale and dolomite in near-shore continental shelf environments (Gross, 1980). According to Schissel and Aro (1992), most of the major basins with Lake Superior-type BIFs were formed in a trailing margin tectonic setting.

Whereas Lake Superior-type iron-formations are found only in the Precambrian, Algoma-type iron-formations are found in rocks of all ages, and are associated with greywackes and volcanoclastic rocks, along volcanic arcs, rift zones and deep-seated fault and fracture systems. Multiple facies iron-formation develops proximal to volcanic vents that are the source of iron and silica, whereas oxide facies BIF forms distal to the vents, and is deposited with greywacke and turbiditic sediments (Gross, 1980). The comparative features of Superior- and Algoma-type iron-formations are presented in Table 1.

5.3 The Origin of Lake Superior-Type BIFs

Early debate on the origin of BIFs centred on what is now termed Superior-type BIF. Opinions on its origin fell into two divisions; either the iron and silica originated from submarine volcanism, or they were derived from the weathering of nearby land masses, with subsequent deposition as banded sediments in water—probably in response to seasonal variations (e.g. Baarghorn and Tyler, 1965; Eugster and I-Ming, 1973). Holland (1973) found serious weaknesses in both hypotheses, including the enormous volume of crust (about 10^6 km^3 —Trendall and Blockley, 1970) that would have to be eroded, the lack of a mechanism that could explain the total separation of chemical sediment and clastic load, and the absence of volcanism in stable Superior-type basins. Holland (1973) proposed that Superior-type BIFs resulted from the upwelling of cold, deep seawater, saturated in Fe^{2+} and Ca^{2+} , onto a warm continental shelf—a theory that has gained widespread acceptance in the last two decades.

5.4 The Origin of Algoma-Type BIFs

The iron and silica in Algoman BIF is generally thought to have originated from spatially and temporally associated submarine volcanic vents (e.g. Trendall, 1965, 1983; Gross, 1980). Volcanic emissions may augment already high levels of iron and silica in seawater, providing enough excess to trigger precipitation (James, 1992).

	Superior	Algoma
Depositional environment	Anorogenic "miogeosynclinal"-stable shelf, marginal basins, generally nonvolcanic	Orogenic, "eugeosynclinal"-submarine volcanic greenstone belts
Associated strata	Quartzite, dolomite, black shale; iron-formation generally low in sequence	Volcanogenic rocks, graywacke; iron-formation irregularly distributed
Dimensions	Commonly 100 m or more thick; laterally continuous for tens to hundreds of kilometers	Lenticular, meters to tens of meters thick; rarely continuous for more than a few tens of kilometers
Age	Mostly early Proterozoic (1900 m.y. – 2500 m.y.)	Majority are Archean, particularly late Archean, but some are as young as Paleozoic
Facies	All facies represented, order of abundance: oxide – carbonate – silicate – sulfide	All facies represented, but hematitic oxide facies rare
Examples	Sokomon Iron-formation, Labrador (Gross and Zajac, 1983); Kuruman and Penge Iron-formations, Transvaal, Supergroup, South Africa (Beukes, 1983)	Helen Iron-formation, Michipicoten district, Ontario (Goodwin, 1973); Late Proterozoic iron-formations of Eastern Desert, Egypt (Sims and James, 1984)

Table 5.1. Comparative features of Superior- and Algoma-types of iron-formation. From James, 1992 (table 11.6).

5.5 The Origin of "Ironstones"

A number of authors (e.g. Laing, 1993; Williams and Blake, 1993) have suggested that many if not all of the "ironstones" in the Cloncurry-Selwyn zone (e.g. Osborne, Selwyn, Maronan) are structurally induced metasomatic replacement bodies, comparable to the giant Olympic Dam and Kiruna-type ore bodies, and metasomatic ironstones from the Tennant Creek Block.

The term *metasomatism* was defined by Lindgren (1933) as "the process of practically simultaneous capillary solution and deposition by which a new mineral of partly or wholly differing chemical composition may grow in the body of an old mineral or mineral aggregate". Thus metasomatism meant literally "change of body" or replacement. In more recent literature, and in this thesis, *metasomatism* infers a change in bulk chemical composition of rocks as a direct result of hydrothermal solutions of igneous or metamorphic origin, even though no temperature restrictions were originally implied.

The origin of ironstones has been argued for many years. Lindgren and Ross (1916) described magnetite skarn deposits at Diaquiri, Cuba. The skarns were found within diorite stocks, magnetite replacing limestone xenoliths and the diorite itself. Magnetite skarns replacing thinly interbedded sequences of limestones, volcanic rocks and tuff were described by Sangster (1969) in British Columbia, and by Sokolov and Grigor'ev (1977) in the Urals, western Siberia, where they form conformable bodies several kilometres in strike length. As did others before him, Frietsch (1978) concluded that Kiruna-type iron deposits are intrusive-magmatic. He argued that intrusion of the iron ores as magmas was accompanied by metasomatic alteration of the host rocks and the formation of skarn minerals, including actinolite, diopside, andradite, biotite, chlorite and epidote.

The Tennant Creek gold field contains approximately 650 massive to crudely banded, irregularly shaped metasomatic ironstone bodies (Le Messurier et al., 1990). The ironstones have colloform textures, including rhythmically alternating botryoidal, concretionary, spheroidal, mamillary and reniform aggregates of magnetite, hematite, chlorite and quartz. The colloform textures were destroyed by flow banding generated in the margins of the ironstones during deformation (Main et al., 1990). The ironstones form strongly to moderately transgressive bodies (Wedekind et al., 1989; Wedekind and Love, 1990) that are surrounded by alteration haloes of low-grade, chloritized metasediments (Fig. 5.3). The intensity of chloritization increases from the margin of the unaltered metasediments towards the ironstone bodies (Nguyen et al., 1989).

Many authors (e.g. Large, 1975) have suggested that the Tennant Creek ironstones formed by metasomatic replacement of Proterozoic Warramunga Group metasediments. Edwards et al. (1990) argued that the geometry of the ironstones suggests a fault or shear emplacement mechanism, and Rattenbury (1992) concluded that ironstone formation has occurred where cleavage or fault fluid conduits have intersected a relatively oxidized hematite shale horizon in the stratigraphy, commonly within fold hinges.

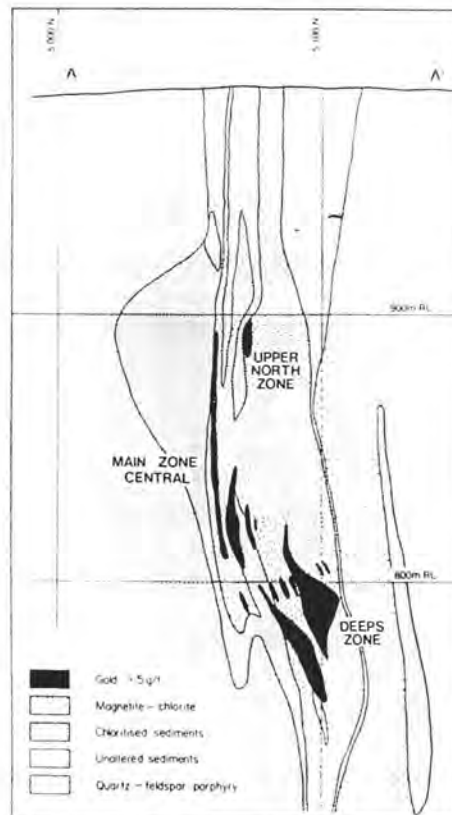


Fig. 5.3. Cross section of the White Devil ore-body, Tennant Creek, showing magnetite ironstone surrounded by a chloritic alteration halo.
From Edwards et al., 1990 (figure 4).

A detailed study of ironstones from the Olympic Dam Cu-U-Au-Ag deposit, South Australia, the Wernecke Mountain breccias, Yukon, the Kiruna district, Sweden and the southeast Missouri iron ore district by Hitzman et al. (1992) suggested that these and other similar ore deposits constitute a new association, which they termed "Proterozoic iron oxide (Cu-U-Au-REE) deposits". These ore bodies are found within early- to mid-Proterozoic host rocks in extensional tectonic environments, and inferred to have formed primarily by shallow-level metasomatic processes related to deep-seated magmatism. Many of the ore bodies occur within silicic to intermediate anorogenic igneous rocks, although the host rocks may also be sedimentary. They are dominated by either hematite or magnetite zones, with abundant CO_3 , Ba, P or F minerals and anomalous to potentially economic concentrations of REEs, which form strongly discordant veins and breccias, or massive concordant bodies. The host-rock alteration of Proterozoic iron oxide (Cu-U-Au-REE) deposits is usually intense, and shows a general transition from sodic alteration at deeper levels (albite-rich) to potassic alteration at intermediate levels (potassium feldspar + "sericite"), to "sericitic" and silicic alteration in the uppermost portion of the system ("sericite" + quartz), with intense localized Fe-metasomatism.

Hitzman et al. (1992) suggested that the Great Bear magmatic zone of northwest Canada, the Bayan Obo district of China, and possibly the Redbank breccia pipes of the Northern Territory may also belong to the Proterozoic iron oxide (Cu-U-Au-REE) class of deposits.

Concentrations of virtually pure magnetite-hematite and minor apatite at the Laco Sur iron ore deposit in northern Chile have been interpreted as shallow intrusions, or as "lava flows" (Park, 1959, 1972; Henriques and Martin, 1978). However, the significant amounts of titanium usually found in igneous melts are absent at Laco (Morris, 1985), and the presence of scapolite (Ruiz-Fuller, 1964—quoted from Park, 1972) is suggestive of evaporitic rather than igneous environments.

Other examples of magnetite deposits that have been inferred to be magmatic include the Kachkanar and Gusevogorsk deposits from the old USSR (Sokolov and Grigor'ev, 1977). These ores supposedly represent zones of late-stage segregation of a basic magma, with magnetite localized mainly in the pyroxenite or hornblendite-pyroxenite and gabbroic facies of differentiated intrusions. Language difficulties prevent full justice being given to numerous accounts of metasomatic and igneous ironstones published in Russian language journals.

5.6 BIF as Host to Base Metal Sulphides

In a detailed investigation of the minerals and field relationships between BIFs and the Broken Hill ore body, Richards (1966) suggested that both the BIFs and the Ag-Pb-Zn sulphide ores represent metamorphosed chemical sediments. Based on Richards' work, Stanton (1972, 1976) concluded that the BIFs and the sulphide lode were derived from submarine exhalative fluids, with the sulphide ores a result of intense sea floor hydrothermal activity, and the BIF units a result of a later, dying phase.

The exploration value of BIFs were appreciated once it was realized that many stratiform base metal ore bodies are either components or close associates of BIF units, and their strong magnetic signature could be used as an indicator of stratiform base metal deposits. Goodwin (1965, 1973) noted that BIFs contain time-stratigraphic horizons that can be used as mapping and correlation aids in highly deformed and metamorphosed terrains. Examples of the BIF-base metal association include Broken Hill, New South Wales (e.g. King and Thompson, 1953; Richards, 1966; Stanton, 1976); Aggeneys-Gamsberg, Namaqualand (e.g. Rozendaal and Stumpfl, 1984) and Bathurst, New Brunswick (e.g. Stanton, 1959; McAllister, 1960; Bhatia, 1981).

Various types of silicate facies and mixed silicate-oxide facies BIFs are associated with stratiform Ag-Pb-Zn ores in the Cloncurry-Selwyn zone, including Cannington (Skrzeczynski, 1993), Pegmont (Locsei, 1977; Stanton and Vaughan, 1979; Orridge, 1980; Vaughan, 1980; Taylor and Scott, 1982; Vaughan and Stanton, 1986; Newbery, 1991), Fairmile (Taylor and Scott, 1982; Vaughan, 1980) and Maronan (Williams and Blake, 1993; Randell, 1993).

5.7 BIF as Host to Au-Cu Sulphides

BIFs are an important host rock to Au-Cu minerals in the Archaean Yilgarn Block, Western Australia, where BIF-hosted deposits account for about 15% of gold deposits, and nearly 5% of total gold production.(Groves et al., 1990). Important BIF-hosted, gold-producing areas include the Paddy's flat zone and the Mount Magnet district.

BIF-hosted gold deposits in the Paddy's flat zone, including the Prohibition, Red Spider, Fenian West and Golden Bar deposits, are characterized by intense brecciation and sulphidation of BIF units related to N and NNW-trending reverse faults (Hickman and Watkins, 1988—quoted from Newton, 1991).

Significant BIF-hosted gold deposits in the Mount Magnet district include the Brownhill, Evening Star, Poverty Flats, Saturn, Wheel of Fortune, Water Tank Hill, Eclipse, Hill 60, Galtee More, Saint George, and Hill 50 deposits (Thompson et al., 1990). BIFs in the Mount Magnet district consist of chemically precipitated laminations of quartz, iron oxides and carbonates that have been subjected to various degrees of metamorphism (Philips et al., 1984). Gold occurs in parallel fracture sets within BIF (locally termed "Boogardie breaks"), as sheetlike to irregular pods, or as large cylindrical ore shoots (Thompson et al., 1990).

Other BIF-hosted ore bodies of the Yilgarn Block include the Copperhead ore body, where gold distribution is controlled by intense fracturing in folded oxide facies BIF (Carter and Grayson, 1990), and the Nevoria gold deposit, which consists of crosscutting, gold-bearing veins localized by shears and fold hinges in metamorphosed oxide facies (quartz + magnetite) and silicate facies (quartz + cummingtonite-grunerite) BIFs (Cullen et al., 1990).

Thirteen percent of total recorded gold production in Zimbabwe can be attributed to 126 BIF-hosted deposits (Fisher and Foster, 1991). Current major gold producers include the Golden Kopje, Elvington and Vubachikwe mines. The distribution of gold-sulphide minerals at the Vubachikwe and Golden Kopje mines is controlled by brittle deformation structures in oxide facies BIFs, whereas the Elvington deposit is characterized by auriferous, silicified shear zones that cut oxide facies BIF units (Fisher and Foster, 1991).

BIF-hosted gold deposits have been reviewed in detail in other terrains, dominantly the Archaean greenstone belts of Canada (e.g. Fyon et al., 1983; McDonald, 1983; Gibbins et al., 1991) and South Africa (e.g. Pretorius et al., 1986; Potgeiter and De Villiers, 1988).

The origin of gold in BIF-hosted gold deposits has been a controversial topic, the level of controversy declining over the last five years. Three proposed models involve (i) syngenetic (exhalative) processes; (ii) syngensis and later remobilization; and (iii) epigenetic (metasomatic) processes. Based on analogies with volcanogenic massive sulphide (VMS) deposits, several authors have suggested that BIF-hosted gold is syngenetic (e.g. Ridler, 1970; Hutchinson et al., 1971; Fripp, 1976; Saager et al., 1987; Davidson et al., 1988; Gibbins et al., 1991). The concept of remobilisation of sulphides was later invoked to explain the strong structural control obvious in many deposits. Numerous other authors have applied criteria erected by Philips et al. (1984) and Groves et al. (1987) to argue for an epigenetic model, and the present consensus on the subject, in Western Australia at least, strongly favours an epigenetic origin.

The epigenetic versus syngenetic debate has been lively in the Cloncurry–Selwyn zone in recent years. Based largely on a study of the ironstone-hosted Selwyn gold-copper ore body, Davidson et al. (1989) argued that the "ironstones" and gold-copper sulphides are of submarine exhalative origin, and that high-grade ore pockets formed during later deformation and remobilization into dilatant sites such as boudin necks. Other authors have examined the Selwyn deposit and suggested that both the gold-copper sulphides and a large component of the ironstones themselves were introduced via metasomatic fluids during deformation (e.g. Switzer et al., 1988). A similar conclusion was reached by Adshead (1995) in a study of the zoning and alteration of the Osborne ore body. However, evidence presented in this thesis (Chapters 2, 3 and 8) indicates that the laminated quartz-magnetite rocks at the Osborne deposit represent metamorphosed oxide facies BIF, with a later, post-deformational overprint of epigenetic sulphide minerals.

Chapter 6

Massive Hematite Bodies North-North-East of the Osborne Deposit—Examples of Metasomatic Ironstones

This chapter describes massive hematite ironstones located approximately 80 km NNE of the Osborne deposit (Fig. 1.3, Chapter 1), at GR VB405332 on the Duchess 1:250 000 map sheet. The purpose of this chapter is to compare the metasedimentary oxide facies BIF units at the Osborne deposit with ironstones that formed as a result of metasomatism. Several days were spent preparing a detailed map of the ironstones, which crop out in low-grade quartz-muscovite metasediments of the Proterozoic Stavely Formation, near the contact with the Kuridala Formation. Mapping was undertaken at 1:500 scale using a 20 m² grid, and subsequently reduced to 1:925 scale (Fig. 6.1).

The mapped area contains two main hematite bodies and five smaller hematite lenses. The more westerly ironstone consists of a sub-rectangular "lobe", 58 m in diameter, that joins two narrow, north-south striking "spines" (Fig. 6.1). The "lobe" consists of brecciated hematite-quartz (Fig. 6.2a), whereas the "spines" consist of massive hematite, and have a steep easterly-dipping foliation (S_1) at their extremities (Fig. 6.2b). The brecciated "lobe" contains a circular inclusion of poorly cemented porous sandstone, roughly 2 m in diameter (Fig. 6.2c). In detail, the rim of the sandstone inclusion is irregular, and interfingered by hematite.

The ironstone to the east has a maximum diameter of 45 m, consists of massive hematite, and has a well developed, steeply dipping foliation (S_1) along its eastern margin, which forms an elongate "spine" (Fig. 1). The five smaller hematite lenses do not contain quartz, and are either massive or strongly foliated.

The contacts between the ironstones and the surrounding hematite-poor country rocks are commonly transgressive, ironstones passing abruptly along strike into mylonitic polymictic conglomerates (Figs 6.2d, 6.3a and 6.3b) or quartz-muscovite metasediments. The country rocks have a well developed, bedding-parallel schistosity (S_1) that dips between 70° and 80° to the east. "Copper bush" is common around the flanks of the ironstones and along the banks of an E-W trending creek bed that crosses the map area. "Copper bush" is a well known biological indicator of anomalous copper levels in soils of the Cloncurry-Selwyn zone.

Blake et al. (1983, 1984) described quartz-hematite ironstones similar to those in the mapped area, outcropping in the Double Crossing Metamorphics, Mitakoodi Quartzite, Answer Slate, Stavely Formation, Agate Downs Siltstone and Kuridala Formation, and in screens of country rock within intrusions of metadolerite and Gin Creek Granite. Drilling has shown that the ironstones continue at depth, and that hematite grades to down to magnetite (White, 1957), suggesting that the ironstones aren't simply the products of surface weathering.

The ironstones in the mapped area are unlike sedimentary BIFs, as they are irregularly shaped, non-laminated bodies that commonly transgress bedding in the surrounding metasediments. They are also locally interbedded with deformed pebble-bearing polymictic conglomerates, which are indicative of high-energy, near-shore or fluvial environments (Friedman and Sanders, 1978), whereas sedimentary iron-formations are thought to have formed in low-energy depositional environments (Chapter 5). White (1957) suggested that ironstones in the Cloncurry-Selwyn zone are granite-related skarns that formed by replacement of calcareous rocks. However, there are no skarn minerals in the mapped area, and no evidence that the original rock was calcareous.

Blake et al. (1983) noted that non-laminated, replacive ironstones in the Cloncurry-Selwyn zone occur at various stratigraphic levels and in several different rock types, are developed preferentially in fold hinges, and pass abruptly along strike into non-hematitic rocks. They concluded that the ironstones are the result of granite-derived iron-rich metasomatic solutions, which passed through loosely cemented detrital sediments, dissolving such minerals as feldspar, calcite and mica, and depositing magnetite, quartz and traces of gold and copper. A similar epigenetic origin is envisaged by the author for the ironstones in the map area, although further study is required to prove the genetic relationship between the ironstones and granite.

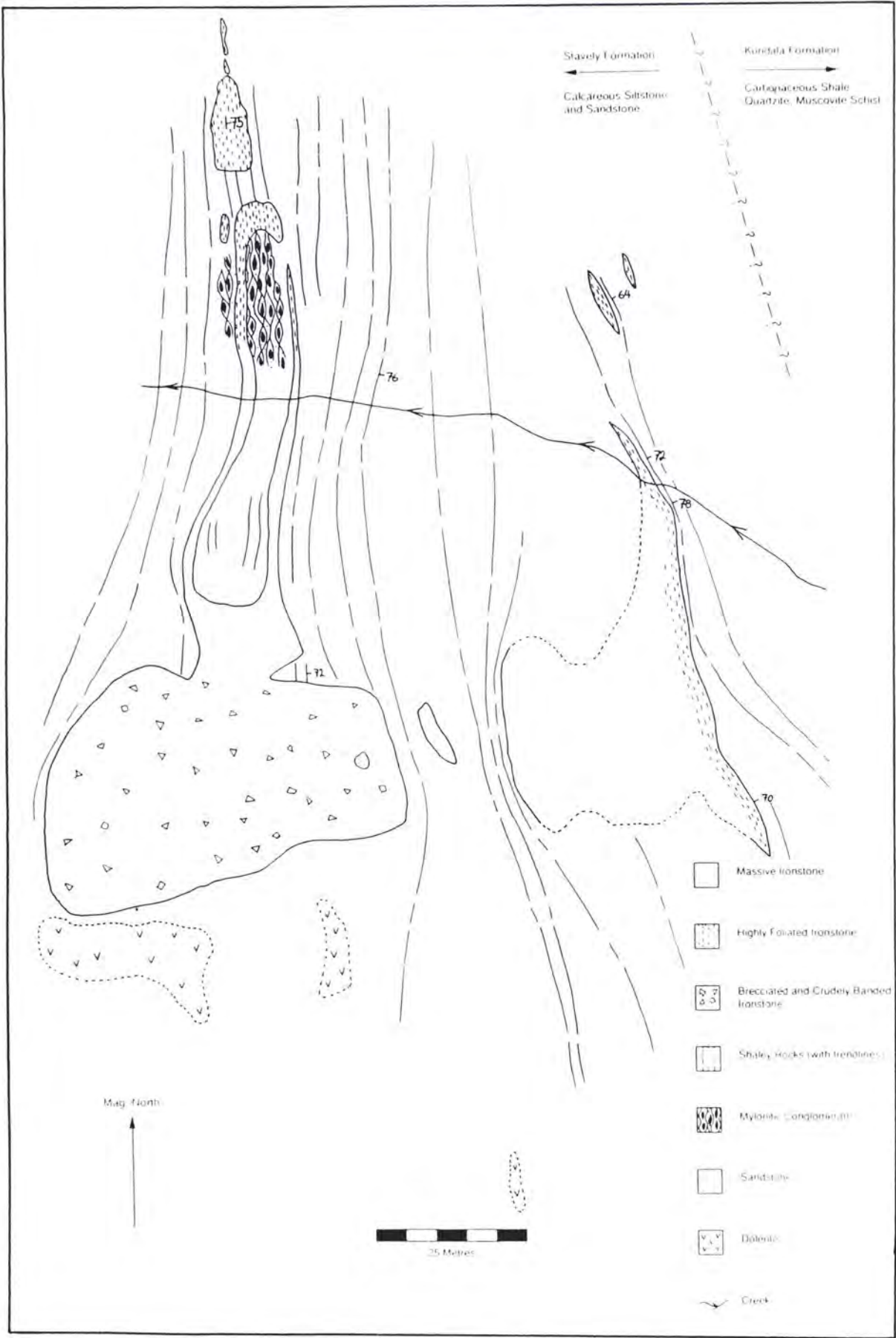
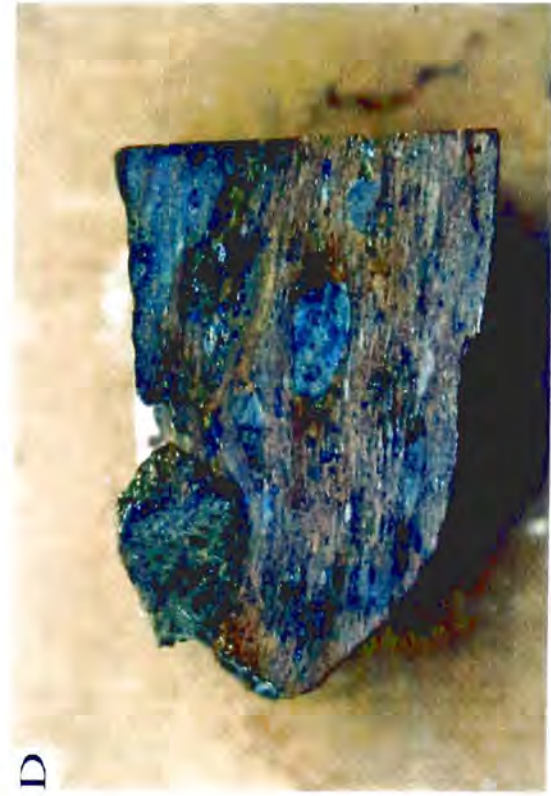
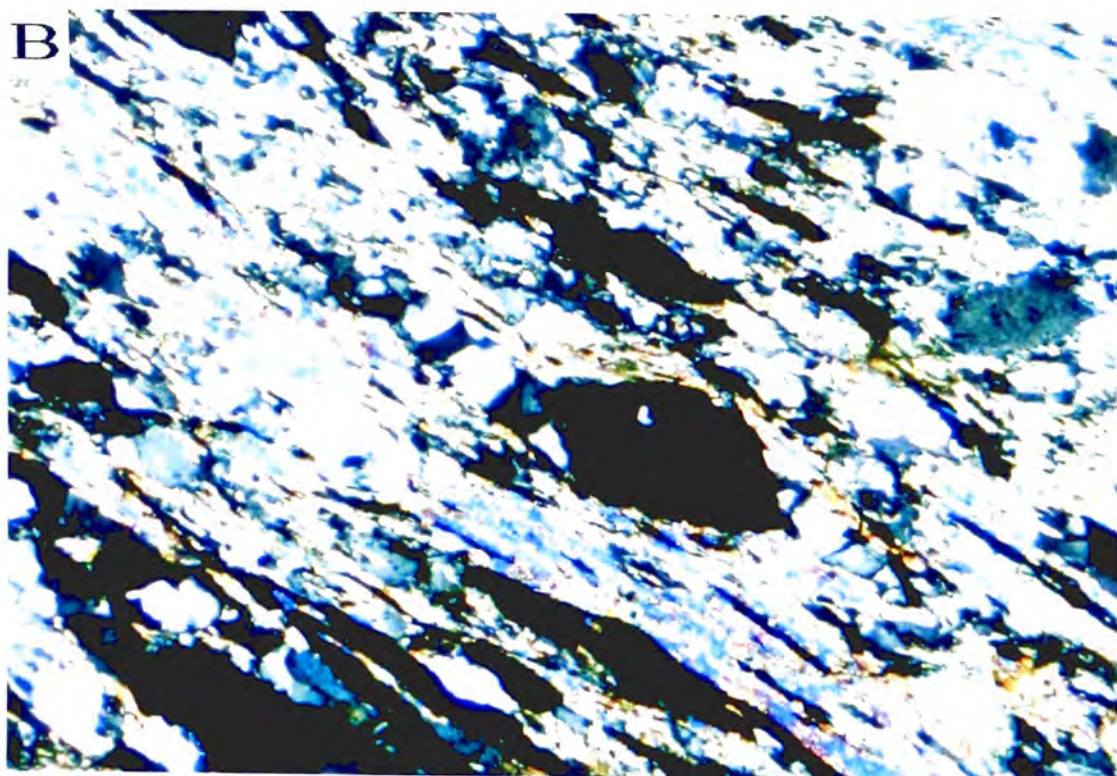
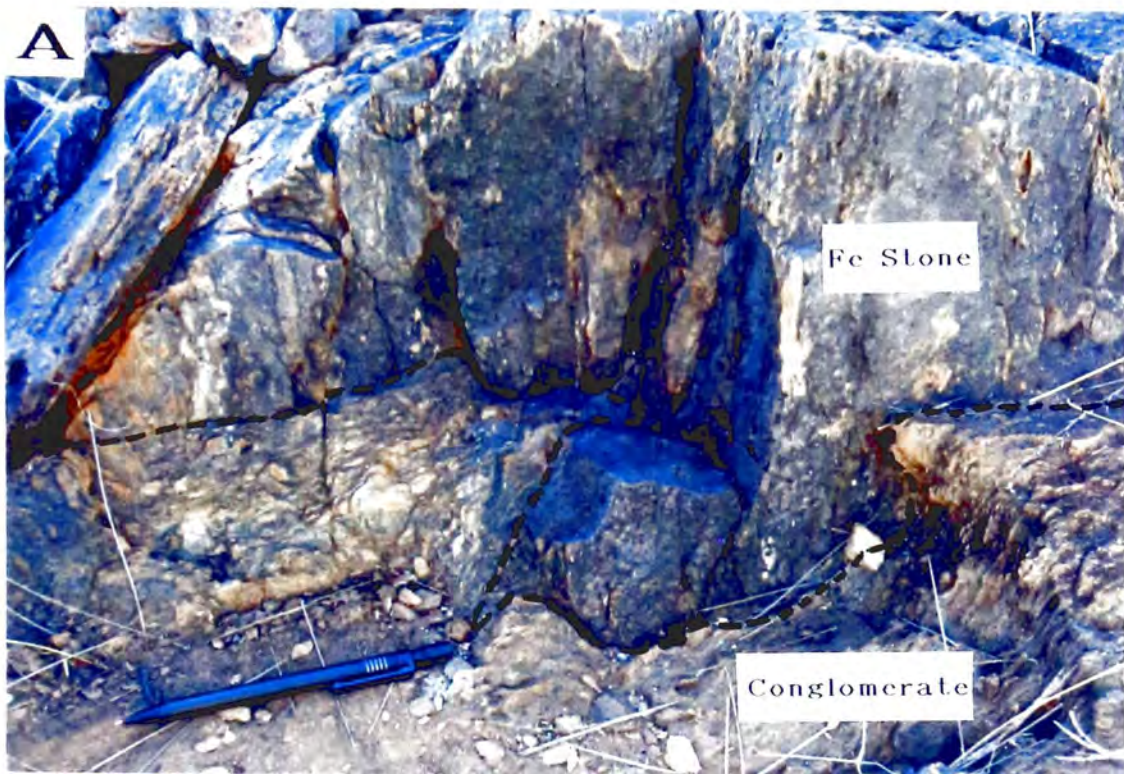


Fig.6.1. 1:925 scale outcrop map of hematite ironstones 80 km NNE of Osborne.

- Fig. 6.2 (a)** Brecciated quartz-hematite ironstone, from the main brecciated "lobe" in Fig. 6.1. Pencil for scale.
- 6.2 (b)** Hematite "spine" viewed from the south, showing steeply dipping foliation (S_1) and cross-cutting, boudinaged quartz vein. Hammer for scale.
- 6.2 (c)** Porous sandstone inclusion from within brecciated lobe. Hammer for scale.
- 6.2 (d)** Close up of deformed, pebble-bearing, polymictic conglomerate from Fig. 6.3a, showing moderately developed mylonitic fabric.



- Fig. 6.3 (a)** Irregular contact between foliated hematite ironstone and deformed polymictic conglomerate. Pencil for scale.
- 6.3 (b)** Photomicrograph of low grade quartz-muscovite metasedimentary rock ("shaley rocks" in Fig. 6.1), showing hematite, muscovite and ribbon quartz aligned in S_1 . Base of photo=1.52 mm, X-polars.



Chapter 7

Synthesis

Introduction

This chapter incorporates a summary of the Osborne mine geology, a discussion of the origin of the BIF units, and speculations on future exploration for BIF-hosted economic mineral deposits in the Cloncurry-Selwyn zone.

7.1 Geological Summary

Three broad lithological groups were recognized by Placer geologists within the Proterozoic Osborne host-rock sequence: garnet-cordierite-sillimanite layered gneisses, plagioclase quartzites, and banded iron-formations (locally termed "ironstones"). The three groups have a combined thickness of at least 400 m, and were interpreted by Adshead (1995) as belonging to the Mount Norna Quartzite, the middle unit of the Soldiers Cap Group. In this thesis, the host rock sequence is subdivided into seven conformable units on the basis of mineral assemblages and textures (Chapters 2 and 3). Although sedimentary bedding is preserved, much of the early history of the host-rock sequence has been obscured by recrystallization during deformation and metamorphism. Thus the petrogenesis (Chapter 3) is largely inferred from mineralogy and geochemistry.

The rocks preserve evidence of amphibolite-facies metamorphism, four phases of deformation (D_x - D_3), and later metasomatic alteration involving economic minerals (Chapter 4). Evidence for the first deformation, labelled " D_x " because of its uncertain age and extent, is restricted to straight inclusion trails (S_x) within some porphyroblasts of garnet, cordierite and tourmaline. The second deformation event, labelled " D_1 " to conform with the nomenclature used by other workers in the Cloncurry-Selwyn zone (e.g. Williams and Blake, 1993), is inferred to have taken place around 1595 Ma ago during the Isan Orogeny. D_1 resulted in a lineation in amphibolites (L_1), and a widespread bedding-parallel foliation (S_1) in metasediments, which is also parallel to the axial surfaces of small asymmetrical Group 1 folds (Chapter 4). Peak metamorphic mineral assemblages that developed during D_1 include garnet-cordierite-sillimanite in metapelitic gneisses, which suggest metamorphic conditions of $T=749^\circ\text{C}$ and $P=5.1\text{ kbar}$ (Chapter 3). Refolding of S_0 and S_1 during D_2 resulted in the localized development of small symmetrical Group 2 folds, and D_3 produced sets of near-parallel Group 3 kink bands with curvi-planar S_2 axial surfaces (Chapter 4).

Brecciated BIF hosts the majority of Au-Cu and other late replacement minerals. Brecciation is most intensely developed near contacts between BIFs and quartzofeldspathic units, and formed as a result of strain incompatibility during post D₃ brittle deformation. Replacement minerals, including coarse-grained "sugary" magnetite, pale grey to clear quartz, pyrite, and Cu-Au sulphides, are present as breccia-fill in grossly conformable but locally transgressive lenses that locally cross-cut and hence post date bedding, amphibolites, pegmatites and all recognized deformation fabrics (S_x, S₁, S₂). Alteration minerals are commonly only weakly deformed, suggesting that they post-date the 1620-1550 Ma Isan Orogeny.

Narrow retrograde shear zones displace and thus postdate all metasedimentary units, pegmatites, amphibolites and ore-bearing breccias. The relative displacements of marker units suggest that the net movement along the majority of shears was normal and non-rotational.

7.2 The Origin of the BIF Units

Several authors have suggested that iron-rich rocks in the Cloncurry-Selwyn zone are structurally controlled metasomatic replacement bodies, associated with the emplacement of the Williams Batholith (e.g. Switzer et al., 1988; Morrison, 1991; Etheridge and Henley, 1993; Laing, 1993; Williams and Blake, 1993; Adshead, 1995).

Evidence used in support of a metasomatic/structural origin for BIF units at Osborne include the irregular shape and apparently transgressive nature of the upper BIF, the high concentrations of iron oxides in the Osborne BIFs (~65 Wt % Fe₂O₃ total) compared with typical Algoma- or Lake Superior-type BIFs (~45 Wt % Fe₂O₃ total), the absence of iron-rich garnets, pyroxenes or amphiboles typical of some types of metasedimentary iron-formations, and the inferred proximity of the Williams Batholith (e.g. Morrison, 1991; Etheridge and Henley, 1993; Adshead, 1995).

However, evidence presented in this thesis suggests that narrow retrograde shear zones have produced tectonic repetition, attenuation, and abrupt variations in thickness of the originally planar upper BIF (Chapters 2 and 4). This interpretation contrasts with early Placer cross sections that show the upper BIF as a discontinuous body that branches and anastomoses around blocks of plagioclase quartzite. The highly disrupted upper BIF contrasts with the well bedded, stratiform lower BIF that is relatively unaffected by shearing (Chapter 2). The lower BIF has a virtually uniform thickness and a strike length greater than several kilometres.

Geochemically the Osborne BIFs have similarities with the exhalative Lahn-Dill type ore deposits that consist of more than 80 wt.% iron oxide (e.g. Davidson et al., 1989; Quade, 1976). The Lahn-Dill ores are atypical variants of volcanogenic Algoman iron-formations that overlie basic volcanic rocks in the European Paleozoic. On the other hand, the Osborne BIFs are chemically distinct from the metasomatic iron oxide (Cu-U-Au-REE) class of deposits (Hitzman et al., 1992) that contain abundant CO_3 , Ba, P or F minerals and anomalous to economic concentrations of REEs.

The Osborne BIFs are dominated by iron and silica, alumina and the alkalis (Na_2O and K_2O) generally constitute less than 0.5 wt.% (Chapter 2). This explains why the assemblage quartz-magnetite is persistent in oxide facies BIFs from diagenesis to upper granulite facies without reaction, and why iron-rich silicates (pyroxenes, amphiboles or garnets) are unable to form during metamorphism (e.g. Klein, 1973).

The numerous westerly-dipping pegmatite sheets (Appendix 1) that cross-cut the Osborne deposit suggest proximity to a granite. However, the Williams Batholith is precluded as a source of iron and silica, as the Osborne BIFs were deformed several times prior to intrusion of the undeformed 1500 Ma old Williams Batholith, and pegmatites cross-cut all metasedimentary units, including the BIFs.

The upper and lower BIF units consist solely of interbanded quartz and magnetite. They show no evidence of the intense host-rock alteration halo that typically surrounds metasomatic ironstones (e.g. Kiruna, Olympic Dam, Tennant Creek), and there is no evidence of the upward passage of the immense amount of iron-rich metasomatic fluids that would have passed through the surrounding quartzo-feldspathic rocks.

Positive evidence suggesting that the Osborne BIFs are metamorphosed sediments includes the alternating cm-, mm- and micron-scale laminations of quartz-magnetite (oxide facies) and quartz-magnetite-cummingtonite (silicate facies), which are typical of sedimentary layering in metasedimentary iron formations (Chapters 3 and 5). This compositional layering is parallel to bedding and lithological contacts in all mine sequence units, and there is no textural evidence to suggest that banding is a result of formerly coarser-grained minerals or breccia fragments being sheared to form a tectonic quartz-magnetite foliation.

BIFs are stratigraphically restricted to the Soldiers Cap Group, which is the only unit to contain BIFs in the entire 50 000 km² Mount Isa Inlier. If BIFs in the Cloncurry-Selwyn zone are metasomatic replacement bodies, it would be reasonable to expect some occurrences in units adjacent to the Soldiers Cap Group, such as the Mary Kathleen or upper Malbon Groups (Chapter 1). The fact that no such occurrences have been documented suggests that BIFs within the Soldiers Cap Group may represent the same depositional event.

The laminated, stratiform BIFs at Osborne are unrelated to the massive, transgressive hematite ironstones mapped 80 km to the NNE (Chapter 6). I consider that these hematite ironstones are of metasomatic origin, because they (1) occur at various stratigraphic levels and in several different rock types, including pebble-bearing conglomerate, (2) pass abruptly along strike into non-hematitic rocks, (3) commonly cross-cut bedding and (4) contain large fragments of country rock.

7.3 Controls on Economic Minerals

According to Phillips et al. (1984), BIFs are suitable host rocks for gold mineralisation, as (1) they are competent relative to most surrounding rock units and are therefore susceptible to hydraulic fracturing, and (2) they contain sufficient iron for the oxidation of sulfur (S^{-2}) to form pyrite (S^{-1}), providing the driving force to reduce auroous complexes to gold metal.

Copper and gold sulphide minerals have a strong spatial relationship to pyrite and lenses of brecciated BIF at Osborne, which indicates that both chemical and structural controls were active during the formation of economic minerals. S_0 , S_1 , ore- and breccia-lenses, shear zones, and the majority of joints and veins are all virtually parallel in the upper BIF (Chapter 4), suggesting that the economic replacement bodies lie within a zone of repeated failure parallel to the structural grain.

Dilation resulting from strain incompatibility between units is a common feature of many BIF-hosted gold deposits in Western Australia (e.g. Hronsky et al., 1990; Thompson et al., 1990; Carter and Grayson, 1990) Tennant Creek (e.g. Wall, 1991; Yates and Robinson, 1990) and Zimbabwe (e.g. Tsomondo, 1988, Saager et al., 1987; Fisher and Foster, 1991).

Epigenetic sulphide grains within ore-bearing breccias are commonly weakly deformed sub parallel to S_0/S_1 (Chapter 4), suggesting that their formation was simultaneous with brecciation. Hydrodynamic considerations (e.g. Kerrich and Allison, 1978) also suggest that brecciation must have been active during sulphidation, as only continuing deformation can maintain porosity and permeability by successive fracturing events. Once deformation ceases, rock permeability drops rapidly as the fracture network becomes clogged by the precipitation of alteration minerals in fractures and voids.

7.4 Future Exploration

One of the reasons that BIFs are favourable strata for Au-Cu minerals is that they are competent relative to most surrounding rock units, and are therefore susceptible to brecciation as a result of strain incompatibility with the surrounding rocks during deformation. Such competency contrasts might also exist within non-BIF units that have contrasting rheological properties with the enclosing rocks (e.g. amphibolite in mica schist), providing a possible locus for Au-Cu bearing fluid flow.

Small oxide facies BIFs that crop out in metamorphosed and multiply deformed Proterozoic rocks to the north of Osborne can be used as mapping and stratigraphic correlation aids during exploration, as they are resistant to erosion and constitute time-stratigraphic markers (Figs 7.1a and 7.1b).

Oxide and silicate facies BIFs are genetically related facies variants of submarine volcanism (e.g. Stanton, 1976). Since virtually all the stratiform Ag-Pb-Zn deposits in the Cloncurry-Selwyn zone are either components or close associates of silicate facies and mixed silicate-oxide facies BIF (Table 1.2), the possibility exists that the oxide facies BIF units at Osborne represent the lateral facies equivalent of Ag-Pb-Zn bearing silicate facies BIF. The possibility of stratiform base metal sulphides is especially promising towards the south of the Osborne deposit, where both upper and lower BIFs can be traced as a magnetic anomaly for 20 km beneath Mesozoic cover, and drill chips contain specks of pyrite and anomalously high levels of zinc.

Fig. 7.1 (a) and (b) Small oxide facies BIFs outcropping in Proterozoic metasediments of the Mount Norna Quartzite, several kilometres north of the Osborne deposit. 7.1b should be viewed looking along strike, towards the cap of the pen.



References

- Adshead, N.A., 1995. Geology, alteration and paragenesis of the Osborne Cu-Au deposit, Cloncurry District, NW Queensland. PhD thesis, James Cook University, Townsville (unpublished)
- Anonymous, 1993. Osborne Annual Report. Internal Company Report, Placer Pacific Ltd. (unpublished).
- Baarghorn, E.S. and Tyler, S.A., 1965. Microorganisms from the Gunflint chert. *Science*, **147**, 563-577.
- Beardsmore, T.J. , Newbery, S.P. and Laing, W.P., 1988. The Maronan Supergroup: An inferred early volcanosedimentary rift sequence in the Mount Isa Inlier, and its implications for ensialic rifting in the middle Proterozoic of northwest Queensland. *Precambrian Research*, **40/41**, 487-507.
- Bell, T.H., 1983. Thrusting and duplex formation at Mount Isa. *Nature*, **304**, 493-497.
- Beukes, N.J., 1973. Precambrian iron-formations in Southern Africa. *Econ Geol.*, **68**, 960-1004.
- Bhatia, D.M.S., 1981. Role of iron formation in the exploration of massive sulphide deposits. Paper presented to AIME annual meeting, Chicago, 1981, 11.
- Blake, D.H., 1987. Geology of the Mount Isa Inlier and environs, Queensland and Northern Territory: *Australian Bureau of Mineral Resources Bull.* **225**, 83.

- Blake, D.H., Jaques, A.L. and Donchak, P.J.T., 1983. Selwyn Region, Queensland. *Bur. Min. Resour., Geol. Geophys.* 1:100 000 map commentary.
- Blake, D.H., Bultitude, T.F., Donchak, P.J.T., Wyborn, L.A.I and Hone, I.G., 1984. Geology of the Duchess-Urandangi Region, Mount Isa Inlier, Queensland. *Australian Bureau of Mineral Resources Bull.*, **219**, 96.
- Blake, D.H. and Stewart, A.J., 1988. Block and possible terrane boundaries in the Mount Isa Inlier. *BMR Research Newsletter*, **9**, 2-3.
- Blake, D.H., Etheridge, M.A., Page, R.W., Stewart, A.J., Williams, P.R. and Wyborn, L.A.I., 1990. Mount Isa Inlier—Regional Geology and Mineralisation. In: *Geology of the Mineral Deposits of Australia and Papua New Guinea* (ed. Hughes, F.E.). The Australian Institute of Mining and Metallurgy, Melbourne, pp. 915-925.
- Blake, D.H. and Stewart, A.J., 1992. Stratigraphic and tectonic framework, Mount Isa Inlier. In: *Detailed Studies of the Mount Isa Inlier* (eds. Stewart, A.J. and Blake, D.H.). AGSO Bulletin **243**, pp. 1-11.
- Borradaile, G.C., Bayly, M.B. and Powell, C.McA. (eds.), 1982. Atlas of Deformational and Metamorphic Rock Fabrics. Springer-Verlag, New York, pp. 551.
- Carter, D.N. and Grayson, M.I., 1990. Copperhead gold deposit, Bullfinch. In: *Geology of the Mineral Deposits of Australia and Papua New Guinea* (ed. Hughes, F.E.). The Australian Institute of Mining and Metallurgy, Melbourne, pp. 283-285.
- Carter, E.K., Brooks, J.H. and Walker, K.H., 1961. The Precambrian Mineral Belt of northwestern Queensland. *Australian Bureau of Mineral Resources Bull.*, **51**, 344pp.

- Chakraborty, K.L. and Taron, P.B., 1968. Thermal metamorphism of the Banded Iron Formation of Orissa, India. *Geol. Soc. Amer. Bull.*, 363-373.
- Cullen, I., Jones, M. and Baxter, J.L., 1990. Neveoria gold deposits. In: *Geology of the Mineral Deposits of Australia and Papua New Guinea* (ed. Hughes, F.E.). The Australian Institute of Mining and Metallurgy, Melbourne, pp. 301-305.
- Davidson, G.J., Large, R., Kary, G., and Osborne, R. 1989. The deformed iron-formation-hosted Starra and Trough Tank mineralization: a new association from the Proterozoic of Mount Isa, Australia. In: *The Geology of Gold Deposits: The Perspective in 1988* (eds. Keays, R.R., Ramsay, W.R.H. and Groves, D.I). Economic Geology Monograph 6, the Economic Geology Publishing Company, El Paso TX., pp. 135-150.
- Davis, B.L., Rapp Jr., G. and Walawender, M.J., 1968. Fabric and structural characteristics of the martitization process. *Am. J. Sci.*, **266**, 482-496.
- Deer, W.A., Howie, R.A. and Zussman, J., 1992. An introduction to the rock forming minerals. *Longman Scientific and Technical*.
- Derrick, G.M., 1991. Field Conference, Mt Isa Inlier. *Geological Society of Australia, Queensland Division*, Brisbane, 139.
- Derrick, G.M., Wilson, I.H. and Hill, R.M., 1976. Revision of stratigraphic nomenclature in the Precambrian of northwestern Queensland V: Soldiers Cap Group. *Queensland Government Mining Journal*, **77**, 601-604.

- Derrick, G.M., Wilson, I.H. and Hill, R.M., 1977. Revision of stratigraphic nomenclature in the Precambrian of northwestern Queensland VI: Mary Kathleen Group: *Queensland Government Mining Journal*, **78**, 15-23.
- Donchak, P.J.T., Blake, D.H., Noon, T.A., and Jaques, A.L., 1983. 1:100 000 geological map commentary Kuridala region, Queensland. *Australian Bureau of Mineral Resources* 32p.
- Dunnet, D., 1976. Some aspects of the Panantartic cratonic margin in Australia. *Philos. Trans. London, Ser. A*, **280**, 651-654.
- Dymek, R.F. and Klein, C., 1988. Chemistry, petrology and origin of banded iron formation lithologies from the 3800 Ma Isua supracrustal belt, West Greenland. *Precambrian Research*, **39**, 247-302.
- Edwards, G.C., Booth, S.A. and Cozens, G.J., 1990. White Devil gold deposit. In: *Geology of the Mineral Deposits of Australia and Papua New Guinea* (ed. Hughes, F.E.). The Australian Institute of Mining and Metallurgy, Melbourne, pp. 849-855.
- Etheridge, M.A. and Henley, R.W., 1993. Structural controls on ironstones and Cu-Au mineralisation at Osborne and environs. Internal Company Report, Placer Pacific Ltd. (unpublished).
- Eugester, H and Chou, I-Ming, 1973. The depositional environments of Precambrian banded iron-formations. *Econ. Geol.*, **68**, 1144-1168.
- Fisher, N.J. and Foster, R.P., 1991. Deformation, fluid-flow and gold precipitation in iron-formation, Zimbabwe. In: *Brazil Gold'91*, (ed. Ladeira, E.A.), Balkema, Rotterdam, pp. 367-373.

- Floran, R.J. and Papike, J.J., 1978. Mineralogy and petrology of the Gunflint Iron formation, Minnesota-Ontario: correlation of compositional and assemblage variations at low to moderate grade. *J. Petrol.*, **19**, 215-288.
- French, B.M., 1968. Progressive contact metamorphism of the Biwabik Iron Formation, Mesabi Range, Minnesota. *Minnesota Geol. Surv. Bull.* **45**.
- Friedman, G.M. and Sanders, J.E., 1978. Principles of Sedimentology. *John Wiley and Sons, Canada*.
- Frietsch, R., 1978. On the magmatic origin of iron ores of the Kiruna type. *Econ. Geol.*, **73**, 478-485.
- Fripp, R.E.P., 1976. Gold metallogeny in the Archaean of Rhodesia. In: *The early history of the earth* (ed. Windley, B.F.). Wiley, London, pp. 455-466.
- Fyon, J.A., Crocket, J.H. and Schwartz, H.P., 1983. The Carshaw and Malga iron-formation-hosted gold deposits of the Timmins area. In: *The geology of gold in Ontario* (ed. Colvine, A.C.). *Ontario Geological Survey, Miscellaneous paper* **110**, pp. 98-110.
- Gibbins, W.A., Padgham, W.A., Atkinson, D., Brophy, J.A. and Gault, C.D., 1991. The Central Iron Formation Zone, Slave Structural Province, Northwest Territories, Canada—A gold-rich Archean metallotect. In: *Brazil Gold'91*, (ed. Ladeira, E.A.), Balkema, Rotterdam, pp. 159-165.
- Glikson, A.Y., 1972. Structural setting and origin of Proterozoic calc-silicate megabreccias, Cloncurry region, northwestern Queensland. *Journal of the Geological Society of Australia*, **19**, 53-63.

- Glikson, A.Y., Derrick, G.M., Wilson, I.H. and Hill, R.M., 1976. Tectonic evolution and crustal setting of the middle Proterozoic Leichhardt River Fault Trough, Mount Isa region, northwestern Queensland. *BMR Jour. Aust. Geol. Geophys.*, **1**, 115-129.
- Gole, M.J., 1979. Metamorphosed Banded Iron-Formation in the Archaean Yilgarn Block, Western Australia. PhD. Thesis, University of Western Australia, Nedlands (unpublished).
- Goodwin, 1965. Mineralised volcanic complexes in the Porcupine Kirkland Lake-Noranda region, Canada. *Econ. Geol.*, **60**, 955-971.
- Goodwin, 1973. Archean iron formations and tectonic basins of the Canadian Shield. *Econ. Geol.*, **68**, 915-934.
- Gross, G.A., 1965. Geology of iron deposits in Canada. General geology and evaluation of iron deposits. *Geol. Surv. Can., Econ. Geol.*, **22**, 1: 181 pp.
- Gross, G.A., 1980. A classification of iron formations based on depositional environments. *Can. Mineral.*, **18**, 215-222.
- Groves, D.I., Phillips, G.N., Falconer, L.J., Houston, S.M., Ho, S.E., Browning, P., Dahl, N. and McNaughton, N.J., 1987. Evidence for an epigenetic origin for BIF-hosted gold deposits in greenstone belts of the Yilgarn block, Western Australia. In: *Recent advances in understanding Precambrian gold deposits* (eds. Ho, S.E. and Groves, D.I.). Geology Department and University Extension, University of Western Australia, Publication **11**, pp. 167-179.

- Groves, D.I., Knox-Robinson, C.M., Ho, S.E. and Rock, N.M.S., 1990. An overview of Archaean lode-gold deposits. In: *Gold deposits of the Archaean Yilgarn Block, Western Australia: Nature, Genesis and exploration guides*, (eds. Ho, S.E., Groves, D.I. and Bennet, J.M.). Geology Department (Key Centre) and University Extension, The University of Western Australia, Publication **20**: pp. 2-18.
- Grubb, P.L.C., 1986. Paragenesis of the Concession Corundum Deposit in Zimbabwe. In: *Mineral Parageneses*, (eds. Craig, J.R., Hagni, R.D., Kiesl, W., Lange, I.M., Petrovskaya, N.V., Shadlum, T.N., Ubudasa, G. and Augustithis, S.S.) Theophratus Publications S.A. Athens.
- Guilbert, J.M. and Park Jr, C.F., 1986. The geology of ore deposits. W.H. Freeman and Co., N.Y.
- Haase, C.S. 1981. Metamorphic petrology of the Negaunee Iron Formation, Marquette district, Northern Michigan: Mineralogy, metamorphic reactions and phase equilibria. *Econ. Geol.*, **77**, 60-81.
- Hall, A.L., 1923. On the marundites and allied corundum-bearing rocks on the Leysdorf District of the Eastern Transvaal. *Trans. geol. Soc. S. Afr.*, **24**, 43-67.
- Hall, R.P., 1985. Mg-Fe-Mn distribution in amphiboles, pyroxenes, and garnets and implications for conditions of metamorphism of high-grade early Archaean iron-formation, southern West Greenland. *Mineral. Mag.*, **49**, 117-128.
- Harder, E.C., 1919. Iron depositing bacteria and their geologic relations. *U.S. Geol. Surv. Prof. Pap.*, **113**, 89.

- Henriquez, F. and Martin, R.F., 1978. Crystal-growth textures in magnetite flows and feeder dykes, El Laco, Chile. *Can. Mineral.*, **16**, 581-589.
- Herron, M.M., 1988. Geochemical classification of terrigenous sands and shales from core or log data. *Jour. Sed. Petrol.*, **58**, 820-829.
- Hickman, A.H. and Watkins, K.P., 1988. Gold mineralisation in the Murchison Province, Western Australia. *Bicentennial Gold '88, Extended Abstracts Oral Programme. Geol. Soc. Australia*, **122**, 23-25.
- Hill, E.J., 1987. Refolded folds, Eastern Mary Kathleen Fold Belt, northwest Queensland. Poster, International Conference on the Deformation of Crustal Rocks, Mount Buffalo. *Geol. Soc. Aust.*, Abstr. no. **19**, 25.
- Hitzman, M.W., Naomi, O. and Einaudi, M., 1992. Geological characteristics and tectonic setting of Proterozoic iron oxide (Cu-U-Au-REE) deposits. *Precambrian Research*, **58**, 241-287.
- Holcombe, R.J., Pearson, P.J. and Oliver, N.H.S., 1987. The Mary Kathleen Fold Belt, northwest Queensland: geometry and timing of deformation. Abstr., International Conference on Deformation of Crustal Rocks, Mount Buffalo. *Geol. Soc. Aust.*, Abstr. No. **19**, 35-36.
- Holcombe, R.J., Pearson, P.J. and Oliver, N.H.S., 1991. Geometry of a middle Proterozoic extensional decollement in northeastern Australia. *Tectonophysics*, **191**, 255-274.
- Holland, H.D., 1973. The Oceans: A possible source of iron in iron-formations. *Econ. Geol.*, **68**, 1169-1172.

- Holyland, P., 1991. Paragenesis and Alteration in the Osborne Deposit, Queensland. Internal Company Report, Placer Pacific Ltd. (unpublished).
- Hronsky, J.M.A., Cassidy, K.F., Grigson, M.W., Groves, D.I., Hagemann, S.G., Mueller, A.G., Ridley, J.R., Swarnecki, M.S. and Vearncombe, J.R., 1990. Deposit- and mine-scale structures. In: *Gold Deposits of the Archean Yilgarn Block, Western Australia* (eds. Ho, S.E., Groves, D.I. and Bennet, J.M.). University of Western Australia Publication no. **20**, pp 39-54.
- Hutchinson, R.W., Ridler, R.H. and Suffel, 1971. A model for Archean metallogeny. *Can. Inst. Min. Metall. Bull.*, **64**, 48-57.
- James, H.L., 1954. Sedimentary facies of iron-formation. *Econ. Geol.*, **49**, 235-293.
- James, H.L., 1955. Zones of regional metamorphism in the Precambrian of northern Michigan: *Geol. Soc. America Bull.*, **66**, 1455-1488.
- James, H.L., Dutton, C.E., Pettijohn, F.J. and Wier, K.L., 1968. Geology and ore deposits of the Iron River-Crystal Falls district, Iron County, Michigan. *U.S. Geol. Surv. Prof Pap.*, **570**, 134.
- James, H.L., 1983. Distribution of banded iron-formation in space and time. In: *Iron Formation: Facts and Problems* (eds. Trendall, A.F. and Morris, R.C). Elsevier, Amsterdam, pp. 471-490.
- James, H.L., 1992. Precambrian iron-formations: Nature, origin, and mineralogic evolution from sedimentation to metamorphism. In: *Diagenesis III* (eds. Wolf, K.H. and Chilingarian, G.V.). Developments in sedimentology **47**. Elsevier Science Publishers.

- Jaques, A.L., Blake, D.H. and Donchak, P.J.T., 1982. Regional Metamorphism in the Selwyn Range area, northwest Queensland. *BMR Journal of Australian Geology and Geophysics*, **7**, 181-196.
- Kary, G.L. and Harley, R.A., 1990. Selwyn Gold-Copper Deposits. In: *Geology of the Mineral Deposits of Australia and Papua New Guinea* (ed. Hughes, F.E.). The Australian Institute of Mining and Metallurgy, Melbourne, pp. 955-960.
- Kerrick, R. and Allison, I., 1978. Vein geometry and hydrodynamics during Yellowknife mineralisation. *Canadian Jour. Earth Sci.*, **15**, 1653-1660.
- King, H.F. and Thomson, B.P., 1953. The geology of the Broken Hill district. In: *Geology of Australian ore deposits* (ed. Edwards, A.B.). The Australian Institute of Mining and Metallurgy, Melbourne, pp. 533-577.
- Klein, C., 1973. Changes in mineral assemblages with metamorphism of some banded iron-formations. *Econ. Geol.*, **68**, 1075-1088.
- Klein, C., 1978. Regional metamorphism of Proterozoic iron-formation, Labrador Trough, Canada. *Amer. Mineral.*, **63**, 898-912.
- Klein, C., 1982. Amphiboles in Iron-Formations. In: *Amphiboles: Petrology and experimental phase relations* (eds. Veblen, D.R. and Ribbe, P.H.). *Reviews in mineralogy*, **9B**, 88-97.
- Kranck, S.H., 1961. A study of the phase equilibria in a metamorphic iron-formation. *J. Petrol.*, **2**, 137-184.
- Kretz, R., 1983. Symbols for rock forming minerals. *Amer. Mineral.*, **68**, 277-279.

- Krumbein, W.C. and Garrels, R.M., 1952. Origin and classification of chemical sediments in terms of pH and oxidation-reduction potentials. *J. Geol.*, **60**, 1-33.
- Laajoki, K. and Devaraju, T.C., 1989. Fe-chlorite, Grunerite, Stilpnomelane, Ankerite and Siderite occurrence in the Iron-formation of Chiknayakaanhalli Schist Belt, Karnataka. *Jour. Geol. Soc. India.*, **33**, 175-182.
- Laing, W.P., 1991. Base metal and gold mineralisation styles in the Cloncurry Terrane, Mount Isa Inlier. Base Metal Deposits Symposium, Townsville, April 1991. James Cook University Economic Geology Research Unit Contribution no. **38**, 77-88.
- Laing, W.P., 1993. Structural/metasomatic controls on ore deposits in the east Mount Isa Block: the key to tonnes and grade. Symposium on recent advances in the Mount Isa Block. *Australian Institute of Geoscientists Bulletin*, **13**, 17-24.
- Laing, W.P. and Beardsmore, T.J., 1986. Stratigraphic rationalisation of the eastern Mount Isa block, recognition of key correlations with Georgetown and Broken Hill blocks in an eastern Australian Proterozoic terrain, and their metallogenic implications. Eighth Australian Geological Convention, Adelaide. *Geol. Soc. Aust. Abstr.*, **15**, 163-164.
- Laing, W.P., Rubenach, M.J and Switzer, C.K., 1988. The Starra gold-copper deposit—syndeforational metamorphic mineralisation localised in a folded early regional zone of decollement. In: Achievements in Australian geoscience, Ninth Australian Geological Convention, Brisbane. *Geol. Soc. Aust. Abstr.*, **21**, 229.
- Large, R.R., 1975. Zonation of hydrothermal minerals at the Juno mine, Tennant Creek goldfield, Central Australia. *Econ. Geol.*, **70**, 1387-1413.

- Le Maitre, R.W., Bateman, P., Dudek, A., Keller, J., Lameyre Le Bas, M.J., Sabine, P.A., Schmid, R., Sorensen H., Streckeisen, A., Woolley, A.R. and Zanettin, B., 1989. A classification of igneous rocks and glossary of terms. Blackwell, Oxford.
- Le Messurier, P., Williams, B.T. and Blake, D.H., 1990. Tennant Creek Inlier—regional geology and mineralisation. In: *Geology of the Mineral Deposits of Australia and Papua New Guinea* (ed. Hughes, F.E.). The Australian Institute of Mining and Metallurgy, Melbourne, pp. 829-838.
- Lindgren, W., 1933. Mineral Deposits (4th Ed.). McGraw-Hill, New York, N.Y.
- Lindgren, W. and Ross, C.P., 1916. The iron deposits of Daiquire, Cuba. *Am. Inst. Min. Eng., Trans.*, **53**, 40-66.
- Locsei, J., 1977. Pegmont: a stratiform lead-zinc deposit in the Precambrian of northwestern Queensland. *Proceedings of the Australasian Institute of Mining and Metallurgy*, **262**, 25-27.
- Logan, K., 1995. Investigations into the magnetic properties and associated magnetic field of Proterozoic Ironstone hosted Cu-Au deposits. MSc Thesis, University of Sydney, Sydney (unpublished).
- Loosveld, R.J.H., 1987. A complex fold nappe within the Soldiers Cap Group, Mount Isa Inlier, Queensland, Australia. Abstr., International Conference on Deformation of Crustal Rocks, Mount Buffalo. *Geol. Soc. Aust.*, Abstr. no. **19**, 45-46.
- Loosveld, R.J.H., 1989. The Intra-cratonic evolution of the Central Eastern Mount Isa Inlier, Northwest Queensland, Australia. *Precambrian Research*, **44**, 243-276.

- Loosveld, R.J.H., 1992. Structural geology of the central Soldiers Cap Belt, Mount Isa Inlier, Australia. In: *Studies of the Mount Isa Inlier* (eds. Stewart, A.J. and Blake, D.H.). AGSO Bulletin **243**, pp. 349-359.
- Main, J.V., Nicholson, P.M. and O'Neill, W.J., 1990. K44 ironstone copper-gold deposit, Gecko Mine. In: *Geology of the Mineral Deposits of Australia and Papua New Guinea* (ed. Hughes, F.E.). The Australian Institute of Mining and Metallurgy, Melbourne, pp. 845-848 .
- Melnik, Y.P., 1982. Precambrian banded iron-formations. Elsevier Pub. Co.
- McAllister, A.L., 1960. Massive sulphide deposits in New Brunswick. *Trans. Can. Inst. Min. Metall.*, **63**, 50-60.
- McDonald, A.J., 1983. The iron formation-gold association: evidence from the Geraldton area. In: *The geology of gold in Ontario* (ed. Colvine, A.C.). *Ontario Geological Survey, Miscellaneous Paper* **110**, 75-83.
- Morris, R.C., 1985. Genesis of iron ore in banded iron-formation by supergene and supergene-metamorphic process—a conceptual model. In: *Handbook of strata-bound and stratiform ore deposits*, **13** (ed. Wolf, K.H.). Elsevier Amsterdam, pp. 73-235.
- Morrison, G.W., 1991. Paragenesis and zoning in the Osborne deposit, Queensland. Internal Company Report, Placer Pacific Ltd. (unpublished).
- Newbery, S.P., 1991. Iron formation hosted base-metal mineralisation of the Cloncurry terrane, Mount Isa Inlier. Base Metal Deposits Symposium, Townsville, April 1991. James Cook University Economic Geology Research Unit Contribution no. **38**, 89-99.

- Newton, P. Structure and genesis of gold mineralisation in the prohibition BIF-hosted deposit, Meekatharra, Western Australia. Honours thesis, The University of Western Australia, Nedlands (unpublished).
- Nguyen, P.T., Booth, S.A. Both, R.A. and James, P.R., 1989. The White Devil gold deposit, Tennant Creek, Northern Territory, Australia. In: *The Geology of Gold Deposits: The Perspective in 1988* (eds. Keays, R.R., Ramsay, W.R.H. and Groves, D.I). Economic Geology Monograph 6, the Economic Geology Publishing Company, El Paso TX., pp. 180-192.
- Nisbet, B. and Joyce, P., 1980. Squirrel Hills Zn-mineralisation, Mt Isa Belt, Qld. *Journal of Geochemical Exploration*, **12**(2/3), 259-264.
- Oliver, N.H.S., Holcombe, R.J., Hill, E.J. and Pearson, P.J., 1991. Tectonometamorphic evolution of the Mary Kathleen Fold Belt, northwest Queensland: A reflection of mantle plume processes. *Aust. Jour. Earth Sci.*, **38**, 425-455.
- Orridge, G.R., 1980. The Pegmont Pb-Zn deposit, Mt Isa belt, Qld. *Journal of Geochemical Exploration*, **12**(2/3), 256-259.
- Page, R.W., 1978. Response of U-Pb zircon and Rb-Sr total-rock and mineral systems to low-grade regional metamorphism in Proterozoic igneous rocks, Mount Isa, Australia. *Journal of the Geological society of Australia*, **25**, 141-164.
- Page, R.W., 1983. Timing of superimposed volcanism in the Proterozoic Mount Isa Inlier, Australia. *Precambrian Research*, **21**, 223-245.

- Page, R.W., 1988. Geochronology of Early to Middle Proterozoic fold belts in northern Australia: a review. *Precambrian Research*, **40/41**, 1-19.
- Page, R.W. and Bell, T.H., 1986. Isotopic and structural responses of granite to successive deformation and metamorphism. *Jour. Geol.*, **94**, 365-379.
- Park Jr, C.F., 1959. The origin of hard hematite in itabarite. *Econ. Geol.*, **54**, 573-587.
- Park Jr, C.F., 1972. The iron deposits of the Pacific Basin. *Econ Geol.*, **67**, 333-349.
- Pearson, P.J., Holcombe, R.J. and Oliver, N.H.S., 1987. The Mary Kathleen fold Belt northwest Queensland: D₁—a product of crustal extension? Abstr., International Conference on Deformation of Crustal Rocks. *Geol. Soc. Aust.*, Abstr. no. **19**, 37-38.
- Pettijohn, F.J., Potter, P.E. and Siever, R., 1972. Sand and Sandstones. Springer-Verlag, New York.
- Phillips, G.N., Groves, D.I. and Martyn, J.E., 1984. An epigenetic origin for Archean banded iron-formation-hosted gold deposits. *Econ. Geol.*, **79**, 162-171.
- Plumb, K.A. and Derrick, G.M., 1975. Geology of the Proterozoic Rocks of the Kimberly to Mount Isa Region. *Economic Geology of Australia and Papua New Guinea, 1, Metals* (ed. Knight, C.L.). The Australian Institute of Mining and Metallurgy, Melbourne, pp. 217-252.

- Plumb, K.A., Derrick, G.M. and Wilson, I.H., 1980. Precambrian geology of the McArthur River-Mount Isa region, northern Australia. In: *The Geology and Geophysics of Northeastern Australia* (eds. Henderson, R.A. and Stephenson P.J.). Geol. Soc. Aust., Queensland Div., Brisbane, pp. 71-88.
- Potgieter, G.A. and de Villiers, J.P.R., 1988. Controls of mineralisation at the Fumani gold deposit, Sutherland greenstone belt. In: *Mineral deposits of Southern Africa* (eds. Anhaeusser, C.R. and Maske, S.). Geological Society of Southern Africa, pp. 197-203.
- Powell, R. and Holland, T.J.B., 1988. An internally consistent dataset with uncertainties and correlations: 3. Applications to geobarometry, worked examples and a computer program. *Journal of Metamorphic Petrology*, **6**, 173-204.
- Pretorius, A.I., van Reenen, D.D. and Barton Jr., J.M., 1986. BIF-hosted gold mineralisation at Fumani Mine, Sutherland greenstone belt, South Africa. *South African Journal of Geology*, **91**, 429-438.
- Quade, H., 1976. Genetic problems and environmental features of volcano-sedimentary iron-ore deposits of the Lahn-Dill type. In: *Handbook of strata-bound and stratiform ore deposits* (ed. Wolfe, K.H.). New York, Elsevier, pp. 89-156.
- Ramsay, J. G., 1980. The crack-seal mechanism of rock deformation: *Nature*, **284**, 135-139.
- Randell, J., 1993. Maronan Cu-Pb-Zn-Ag-Au prospect. In: Core shack explanatory notes, AMF course 832/93 (ed. Derrick, G.). Australian Mineral Foundation, 24-28.

- Rattenbury, M.S., 1992. Stratigraphic and structural controls on ironstone mineralisation in the Tennant Creek goldfield, Northern Territory, Australia. *Aust. Jour. Earth Sci.*, **39**, 591-602.
- Reimer, T.O., 1986. Alumina-Rich Rocks from the Early Precambrian of the Kaapvaal Craton as Indicators of Paleosols and as Products of other Decompositional Reactions. *Precambrian Research*, **32**, 155-179.
- Retallack, G.J., 1990. Soils of the Past—An Introduction to Paleopedology, 342-343.
- Richards, S.M., 1966 The banded iron formations at Broken Hill, Australia, and their relationship to the lead-zinc orebodies, Parts 1 and 2. *Econ. Geol.*, **61**, 72-96; 257-274.
- Ridler, R.H., 1970. Relationship of mineralization to volcanic stratigraphy in the Kirkland-Larder area, Ontario. *Geol. Assoc. Can. Proc.*, **21**, 33-42.
- Rozendaal, A. and Stumpfl, E.F., 1984. Mineral chemistry and genesis of Gamsberg zinc deposit, South Africa. *Trans. Inst Min. Metall. (Sect. B: Appl. earth sci)*, **93**: B161-75.
- Ruiz-Fuller, C., 1965. Geologia y yacimientos metaliferos de Chile: *Instituto Invest. Geol. Chile*.
- Saager, R., Oberthur, T. and Tomschi, H., 1987. Geochemistry and mineralogy of Banded Iron Formation-hosted gold mineralization in the Gwanda Greenstone Belt, Zimbabwe. *Econ. Geol.*, **82**, 2017-2032.

- Sangster, D.F., 1969. The contact metasomatic magnetite deposits of south western British Columbia. *Can. Geol. Surv. Bull.*, **172**, 85.
- Schissel, D. and Aro, P. The major early Proterozoic sedimentary iron and manganese deposits and their tectonic setting. *Econ Geol.*, **87**, 1367-1374.
- Schreyer, W., Werding, G. and Abraham, K., 1981. Corundum-Fuchsite Rocks in Greenstone Belts of Southern Africa: Petrology, geochemistry, and Possible Origin. *Journal of Petrology*, **22**, 191-231.
- Shelley, D., 1993. Igneous and metamorphic rocks under the microscope. Classification, textures, microstructures and mineral preferred orientations. Chapman and Hall, London.
- Skrzeczynski, R., 1993. From concept to Cannington: a decade of exploration in the Eastern Succession. Symposium on Recent Advances in the Mount Isa Block. Australian Institute of Geoscientists Bulletin, **13**, 35-37.
- Sokolov, G.A. and Grigor'ev, V.M., 1977. Deposits of iron. In: *Ore Deposits of the USSR* (ed. Smirnov, V.I.). Pittman, London, pp. 7-113.
- Stanton, R.L., 1959. Mineralogical features and possible mode of emplacement of the Brunswick Mining and Smelting orebodies, Gloucester County, New Brunswick. *Can. Min. metall. Bull.*, **52**, 631-43.
- Stanton, R.L., 1972. A preliminary account of chemical relationships between sulfide lode and "banded iron formation" at Broken Hill, New South Wales. *Econ Geol.*, **67**, 1128-45.

- Stanton, R.L., 1976. Petrochemical studies of the ore environment at Broken Hill, New South Wales: 1-Constitution of 'Banded Iron Formation'. *Inst. Min. Metall. (sect. B. Appl. Earth Sci.)*, **85**: B33-46.
- Stanton, R.L. and Vaughan, J.P., 1979. Facies of ore formation: a preliminary account of the Pegmont deposit as an example of potential relations between small iron formations and stratiform sulphide ores. *Proceedings of the Australian Institute of Mining and Metallurgy*, **270**, 25-38.
- Switzer, C.K., 1987. Implications of high strain for regional structural geometry and control on gold mineralization in the Selwyn Region, northwestern Queensland. Honours thesis, James Cook University, Townsville (unpublished).
- Switzer, C.K., Laing, W.P. and Rubenach, M.J., 1988. The Proterozoic Starra Au + Cu deposit-syntectonic mineralization in a folded early regional zone of decollement. *Geol. Soc. Australia Abstr. Series*, **23**, 212-214.
- Taylor, G.F., and Scott, K.M., 1982. Evaluation of gossans in relation to lead-zinc mineralisation in the Mount Isa Inlier, Queensland. *BMR Journal of Australian Geology and Geophysics*, **7**, 159-180.
- Teodorovich, G.I., 1947. Sedimentary geochemical cycles: *Soc. Naturalistes Moscou Bull.*, **52**: Sec. Geol., 22 (1): 32-24 (Russian with English summary).
- Thompson, M.J., Watchorn, R.B., Bonwick, C.M., Frewin, M.O., Goodgame, V.R., Pyle, M.J. and MacGeehan, P.J., 1990. Gold deposits of Hill 50 gold mine at Mount Magnet. In: *Geology of the Mineral Deposits of Australia and Papua New Guinea* (ed. Hughes, F.E.). The Australian Institute of Mining and Metallurgy, Melbourne, pp. 221-241.

- Trendall, A.F., 1965. Origin of Precambrian banded iron formations, discussion. *Econ. Geol.*, **60**, 1065-1069.
- Trendall, A.F., 1983. The Hamersley Basin. In: *Iron-Formation: Facts and Problems* (eds. Trendall, A.F. and Morris, R.C.). Elsevier, Amsterdam, pp. 69-130.
- Trendall, A.F. and Blockley, J.G., 1970. The Iron Formations of the Precambrian Hamersley Group, Western Australia, with special reference to the associated crocidolite: *Western Australia Geol. Survey Bull.*, **119**, 336.
- Tsomondo, J.M., 1988. Lennox mine, Mashava Zimbabwe: a consanguineous association between quartz-gold veins in metavolcanics and quartz-pyrrhotite replacement lodes in interlayered BIF. In: *Bicentennial Gold '88. Geol. Soc. Australia*, **122**, 128-123.
- Vaughan, J.P., 1980. Relationships between base metal sulphide mineralization and metamorphosed iron rich sediments in Proterozoic strata of Northwest Queensland. PhD Thesis, University of New England, Armidale (unpublished).
- Vaughan, J.P. and Stanton, R.L., 1986. Sedimentary and metamorphic factors in the development of the Pegmont stratiform Pb-Zn deposit, Queensland, Australia. *Trans. Inst. Min. Metall. (Sect. B: Appl. earth sci)*, **95**, 94-121.
- Vernon, R.H., 1976. *Metamorphic Processes*. Allen and Unwin, London.
- Vernon, R.H. and Flood, R.H., 1977. Interpretation of metamorphic assemblages containing fibrolitic sillimanite. *Contrib. Min. Petrol.*, **59**, 227-235.

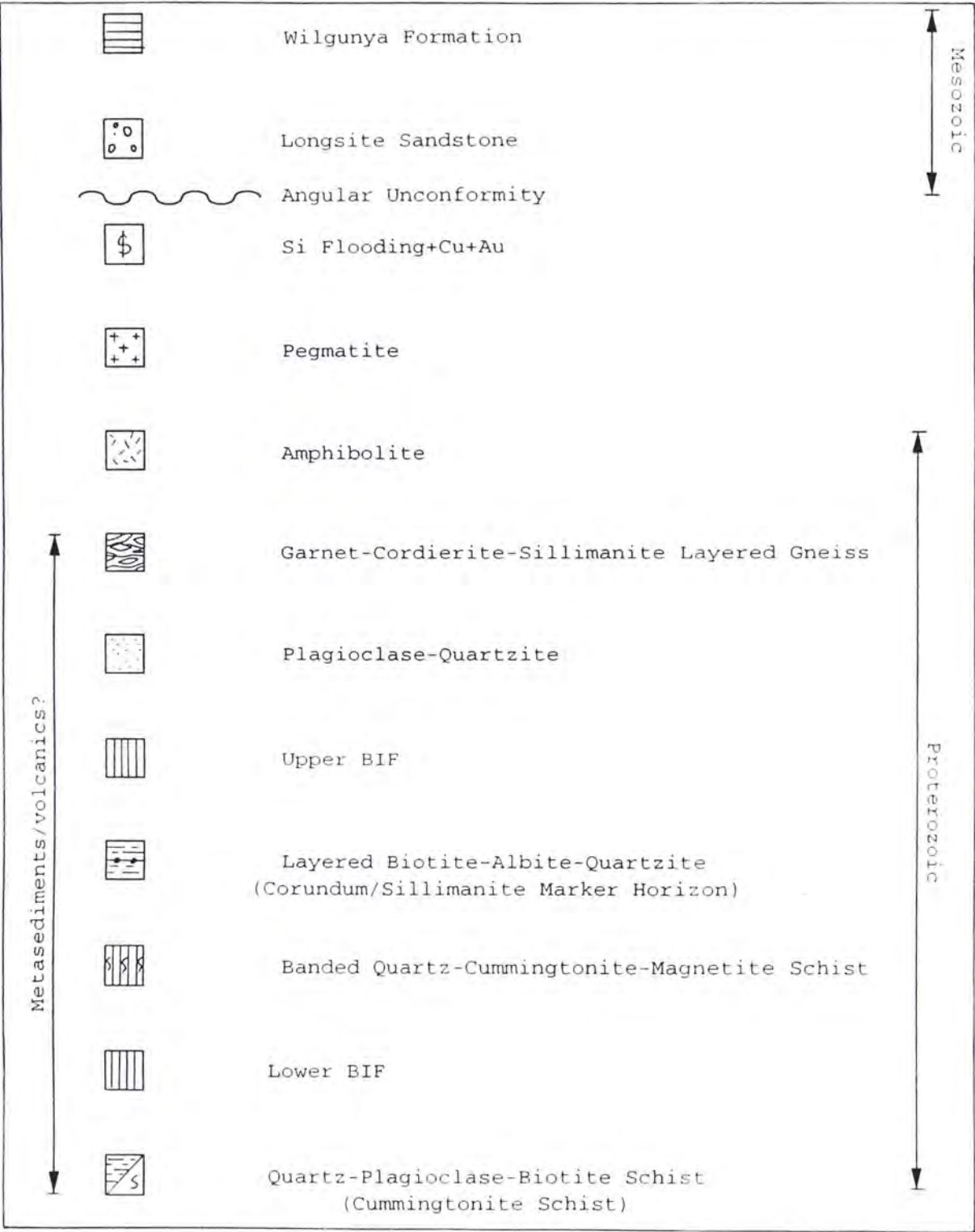
- de Villiers, S.B., 1976. Non metallic minerals, corundum. In: *Mineral Resources of Southern Africa, 5th edition* (ed. Coetzee, C.B.), pp. 341-345.
- Wall, V.J., 1991. The ironstone-related copper-gold (U, REE) ore association. University of Queensland Seminar abstr., Brisbane.
- Wedekind, M.R., Large, R.R., and Williams, B.T., 1989. Controls on high-grade gold mineralization at Tennant Creek, Northern Territory, Australia. In: *The Geology of Gold Deposits: The Perspective in 1988* (eds. Keays, R.R., Ramsay, W.R.H. and Groves, D.I). Economic Geology Monograph **6**, the Economic Geology Publishing Company, El Paso TX., pp. 168-179.
- Wedekind, M.R. and Love, R.J., 1990. Warrego gold-copper-bismuth deposit. In: *Geology of the Mineral Deposits of Australia and Papua New Guinea* (ed. Hughes, F.E.). The Australian Institute of Mining and Metallurgy, Melbourne, pp. 839-843.
- Wellman, P., 1992. Structure of the Mount Isa region inferred from gravity and magnetic anomalies. In: *Detailed Studies of the Mount Isa Inlier* (eds. Stewart, A.J. and Blake, D.H.). AGSO Bulletin **243**, pp. 15-27.
- White, W.C., 1957. The geology of the Selwyn area of north Queensland. Bureau of Mineral Resources, Australia, Record 1957/94 (amended 1963, unpublished).
- Williams, P.J. and Blake, K.L., 1993. Alteration in the Cloncurry district. James Cook University Economic Geology Research Unit Contribution no. **49**.

- Williams, P.J. and Heinemann, M., 1991. The Maramungee zinc skarn: Implications for base metal exploration in the Cloncurry Metamorphic Terrain. Base Metal Deposits Symposium, Townsville, April 1991. James Cook University Economic Geology Research Unit Contribution no. **38**, 89-99.
- Willner, A., Schreyer, W. and Moore, J.M., 1990. Peraluminous metamorphic rocks from the Namaqualand Metamorphic Complex (South Africa): Geochemical evidence for an exhalation-related, sedimentary origin in a Mid-Proterozoic rift system. *Chemical Geology*, **81**, 221-240.
- Wilson, I.H., 1978. Volcanism on a Proterozoic continental margin in northwestern Queensland. *Precambrian Research*, **7**, 205-235.
- Winchester, J.A. and Floyd, P.A., 1976. Geochemical discrimination of different magma series and their differentiation products using immobile elements. *Chemical Geology*, **20**, 325-343.
- Winkler, H.G.F., 1979. Petrogenesis of Metamorphic Rocks, 5th ed. Springer-Verlag, N.Y., pp. 348.
- Wyborn, L.A.I. and Blake, D.H., 1982. Reassessment of the tectonic setting of the Mount Isa Inlier in the light of new field, petrographic and geochemical data (abstract), *B.M.R. J. Aust. Geol. Geophys.*, **7**, 143.
- Wyborn, L.A.I., Page, R.W., and McCulloch, M.T., 1988. Petrology, geochronology and isotope geochemistry of the post-1820 Ma granites of the Mount Isa Inlier: mechanisms for the generation of Proterozoic anorogenic granites. *Precambrian Research*, **40/41**, 509-541.

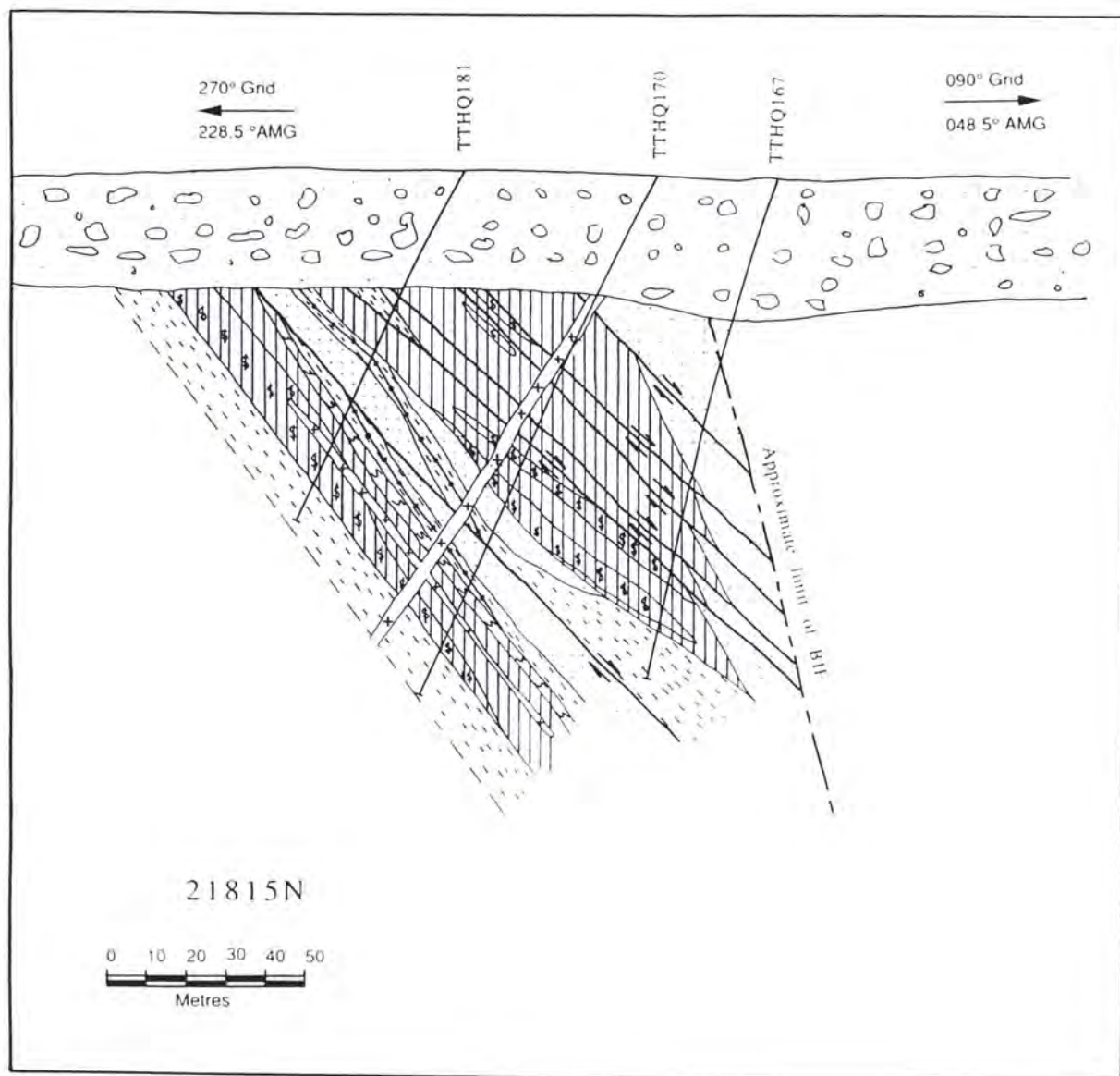
- Yates, K.R. and Robinson, P., 1990. Nobles Nob gold deposit. In: *Geology of the Mineral Deposits of Australia and Papua New Guinea* (ed. Hughes, F.E.). The Australian Institute of Mining and Metallurgy, Melbourne, pp. 861-865.
- Zhu, J., Zhang, F., Xu, K., 1988. Depositional environment and metamorphism of early Proterozoic iron-formation in the Luliangshan region, Shanxi Province, China. *Precambrian Research*, **39**, 39-50.

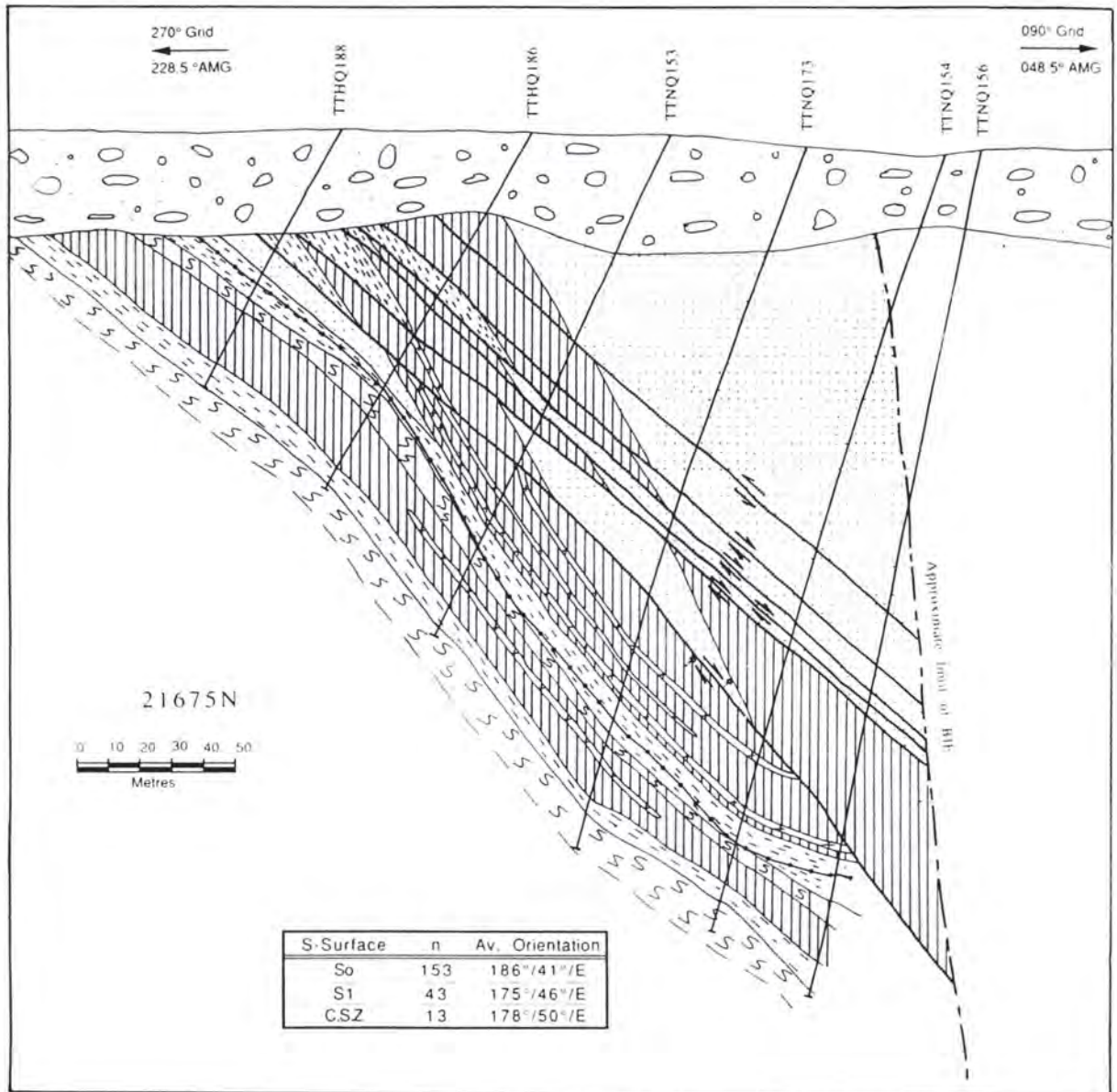
Appendix 1

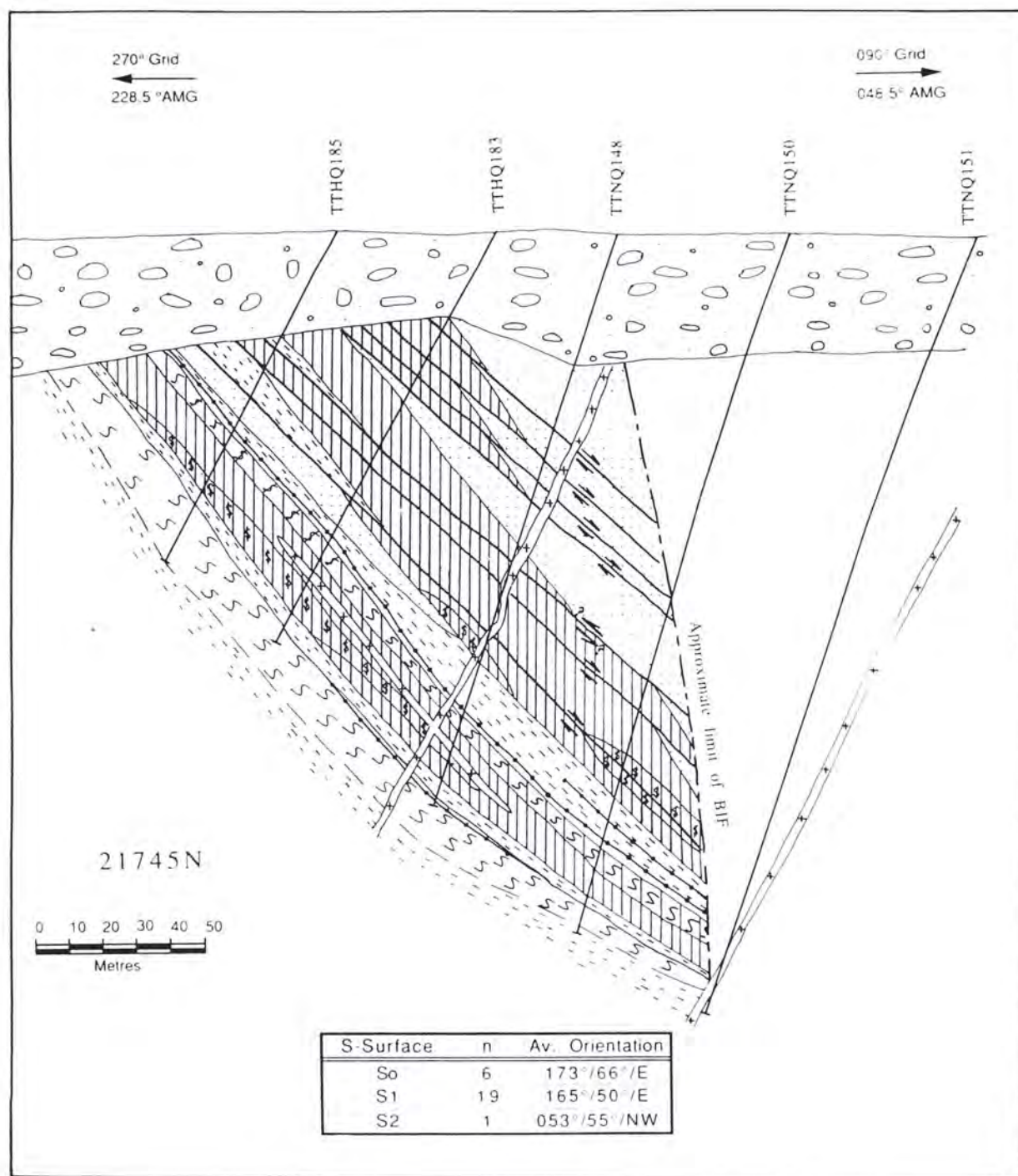
Geological Cross Sections

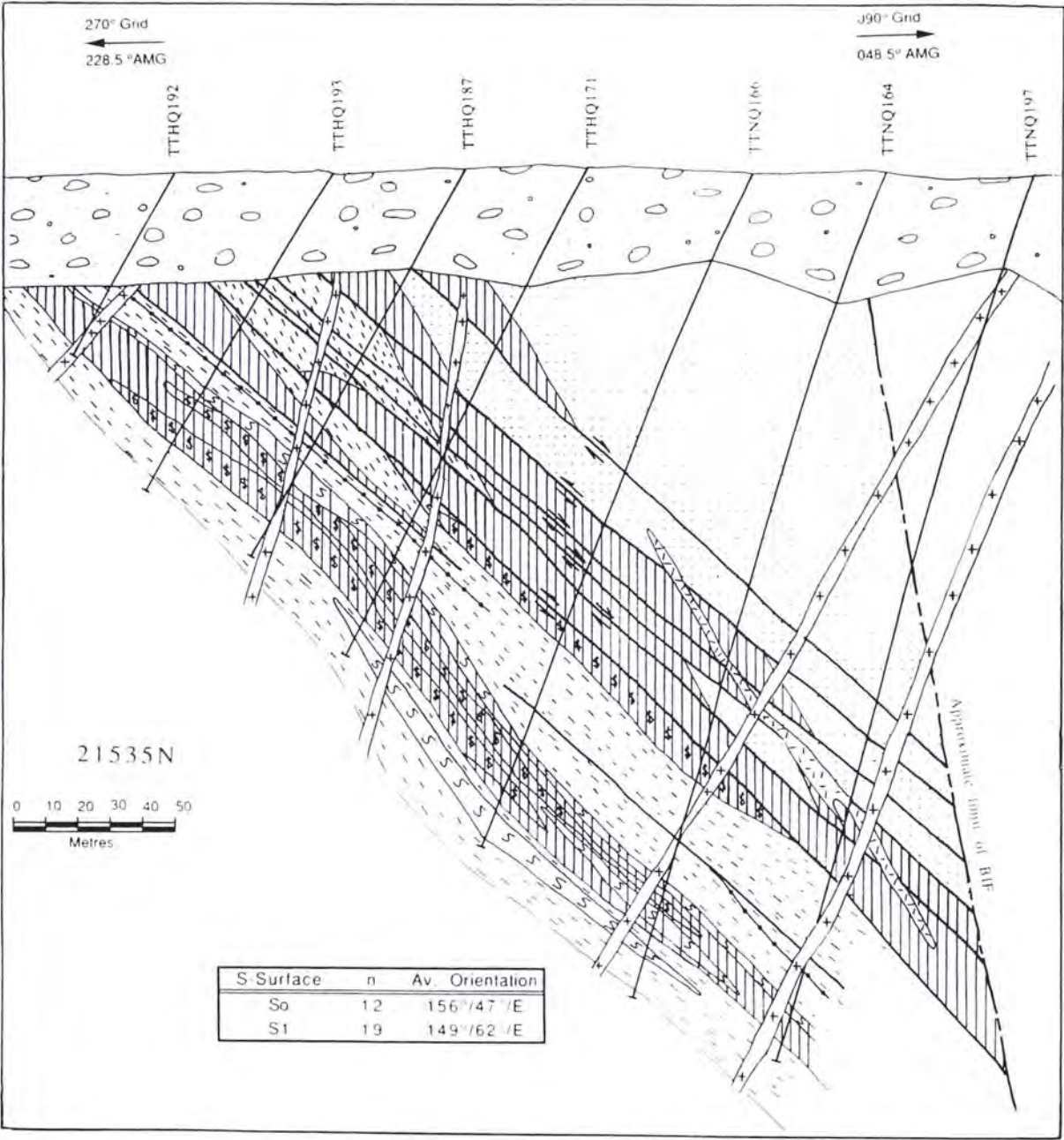


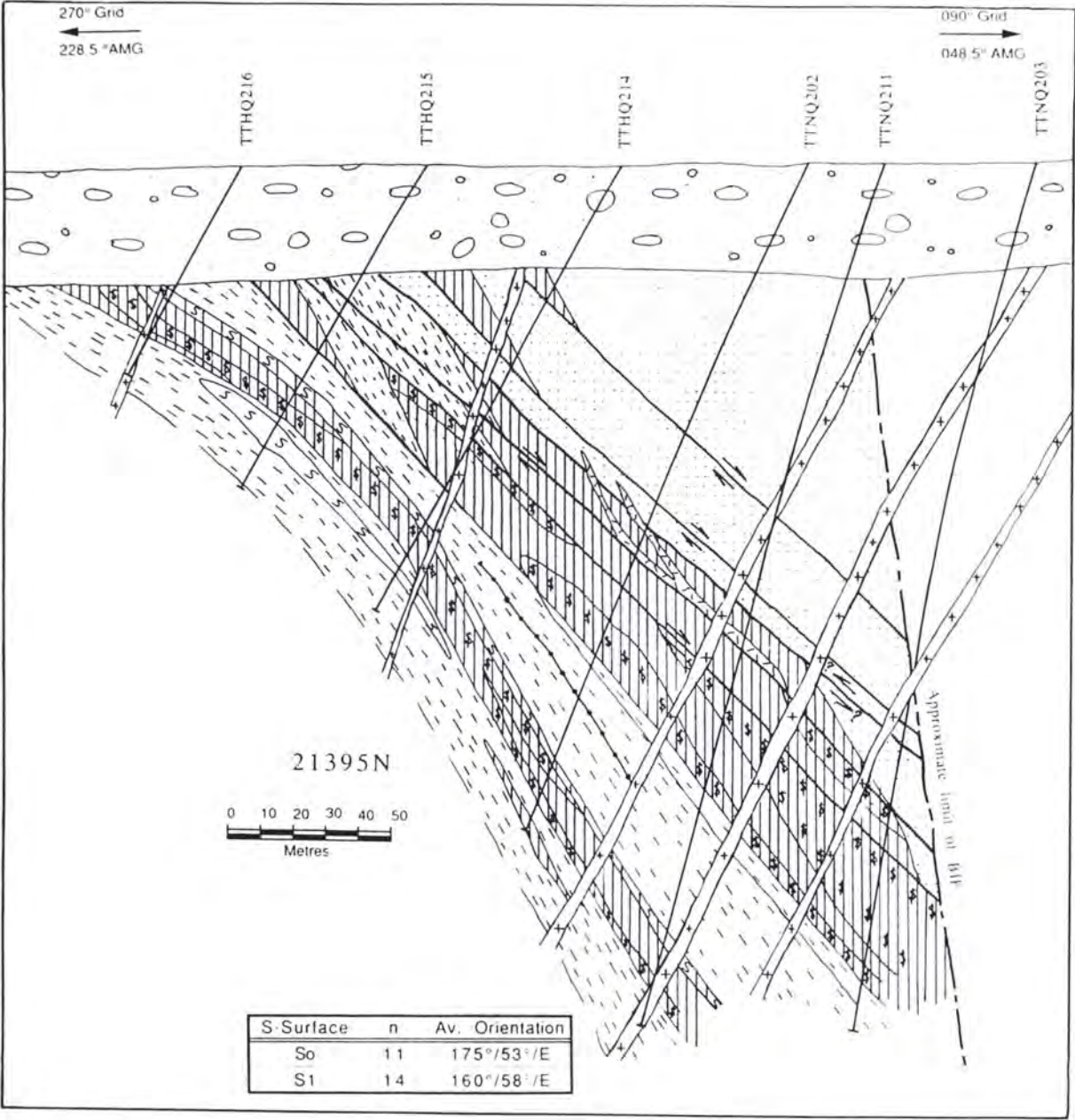
Stratigraphy of the Osborne mine

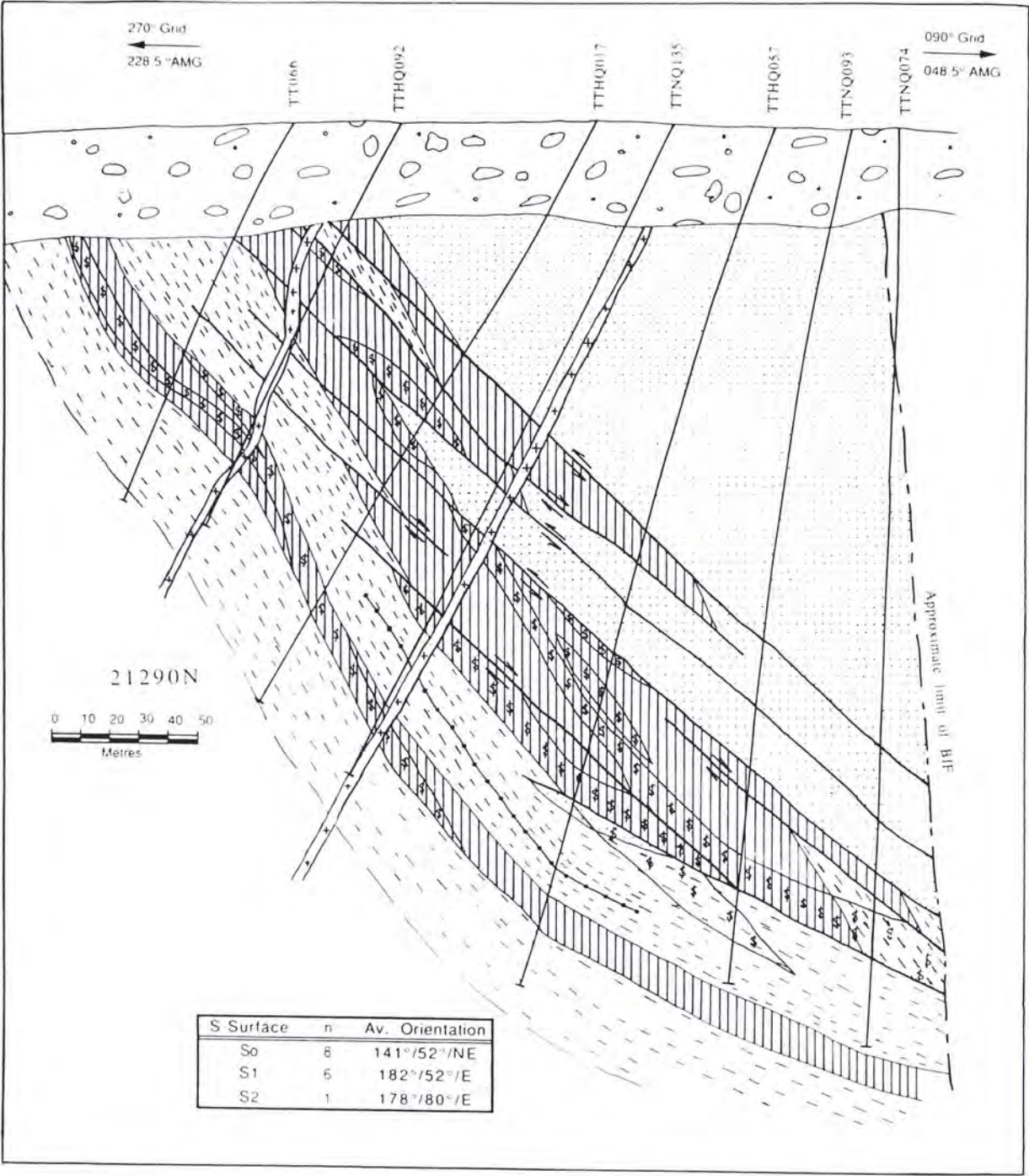












Detection Limits For Trace Elements Analysed By XRF

Element	Lowest level of detection (ppm)
Ga	4
Nb	1
Pb	3
Rb	1
Sr	2
Th	2
U	3
Y	2
Zr	2
Ba	8
V	4
Cr	3
Ni	2
Cu	1
Zn	2

Samples were crushed in a TEMA tungsten-carbide mill. Major elements SiO_2 , Al_2O_3 , Fe_2O_3 etc. were determined by X-Ray Fluorescence (XRF) using a Siemens SRS-1. Trace elements were determined by X-Ray Diffraction (XRD) using a Siemens Type F Diffractometer. H_2O and CO_2 were analysed using a Leco induction furnace, with Magnesium perchlorate (H_2O) and Lecosorb (CO_2) collectors. Analyses were carried out by Ms Carol Lawson at the School Of Earth Sciences, Macquarie University

Detection Limits For Elements Analysed By Electron Microprobe

Element	Lowest level of detection (wt%)
SiO_2	0.06
TiO_2	0.05
Al_2O_3	0.08
FeO	0.07
MnO	0.08
MgO	0.03
CaO	0.04
Na_2O	0.03
K_2O	0.03
NiO	0.11

Minerals were analysed using a Cameca SX50 Electron Microprobe. Analyses were carried out by Dr Norm Pearson at the School Of Earth Sciences, Macquarie University.